The Pennsylvania State University

The Graduate School

College of Earth and Mineral Sciences

FLEXIBLE NETWORK TOPOLOGIES AND THE SMART GRID IN ELECTRIC POWER SYSTEMS

A Dissertation in

Energy and Mineral Engineering

by

Clayton P. Barrows

Submitted in Partial Fulfillment
of the Requirements
for the Degree of

Doctor of Philosophy

May 2013

The dissertation of Clayton P. Barrows was reviewed and approved* by the following:

Seth A. Blumsack
Assistant Professor of Energy Policy and Economics
Dissertation Adviser
Chair of Committee

Andrew Kleit
Professor of Energy and Environmental Economics

Luis F. Ayala H.
Associate Professor of Petroleum and Natural Gas Engineering

Réka Albert
Professor of Physics
Professor of Biology

Paul D. Hines
Assistant Professor of Electrical Engineering
University of Vermont

R. Larry Grayson
Professor of Energy and Mineral Engineering
Graduate Program Officer of Energy and Mineral Engineering

*Signatures are on file in the Graduate School.

Abstract

Recently, the demands placed on the electrical transmission system have increased disproportionally relative to the investments made in the system. As a result, the system has become increasingly constrained, hindering the ability of the transmission system to facilitate competition among generators. New transmission can fix this problem, but is difficult to construct due to political, environment and financial concerns. Topological reconfigurations of the transmission system could improve the efficiency of power system operations and represents a particularly valuable application of the smart grid. However, in practice the topology reconfiguration problem is difficult to solve.

Reconfiguration of the transmission network can be accomplished through topology optimization. The act of temporarily removing transmission lines from service, known as "transmission switching", can relieve transmission congestion and enable the re-dispatch of lower cost generators. Optimal Transmission Switching (OTS) co-optimizes the generator dispatch and the network topology and has been shown to minimize costs when applied to test systems. When considering every line in the network as switchable, the problem scales such that $2^{\#\text{-}lines}$ distinct network topologies must be considered. Real systems often contain tens of thousands of transmission lines. The size and complexity of OTS has limited optimal solutions to small test systems and linearized DC power flow models.

A Marginal Analysis of OTS investigates the predictors of the probability with which each transmission line is optimally switched and the contribution of each line to cost savings. The analysis leads to two conclusions. First, the majority of cost savings can be achieved through switching a small subset of lines. And second, the effects of transmission switching are relatively localized. These conclusions lead to the development of two strategies to reduce the computational complexity of the OTS problem. Network partitioning methods are used to

generate sub-networks where the OTS problem can be solved in parallel and then aggregated to form a complete system solution. Additionally, a candidate switchable line screen based on the Line Outage Distribution Factors is presented to identify a superset of switchable lines.

Thus far in the evolution of transmission topology and generation dispatch co-optimization problems, optimal solutions have been obtained using a linearized de-coupled power flow model. While this model is useful for many approximations, it fails to describe reactive power flows and voltage magnitudes; two critical parameters when considering the feasibility of a generation dispatch. However, topology optimization presents an intractable problem when implemented in the nonlinear and non-convex AC power flow model. The discrepancies between the AC and linearized DC power flow models have created speculation that the cost savings generated by optimizing transmission topology in the DC network may not translate into cost savings in the AC network. Using a method developed to achieve feasible OTS solutions in both the AC and linearized DC power flow models, cost savings are achieved and enhanced in the topologically reconfigured AC power flow model.

Table of Contents

Table of Figures

List of Tables

Notation

The following notation is used throughout this document. The text introduces additional notation as necessary.

$v(t)$	Time varying voltage
$i(t)$	Time varying current
V	Peak voltage magnitude
I	Peak current magnitude
θ	Voltage phase angle
φ	Current phase angle
t	Time
ω	Radial frequency
$p(t)$	Time varying power
P	Average power
Q	Reactive power
S	Complex power
P_k	Power flow along line k
P_{ij}	Power flow along line connecting bus_i and bus_j
P_g	Power output of generator g
P_d	Power demand of load d
NB	Number of busses in the power system
NL	Number of transmission lines in the power system
$\tilde{\boldsymbol{Z}}$	Complex impedance matrix (NB x NB)
$\boldsymbol{X}$	Reactance matrix (NB x NB)
$\boldsymbol{R}$	Resistance matrix (NB x NB)
$\boldsymbol{Z}$	Impedance magnitude matrix (NB x NB)

$\boldsymbol{Y}$	Admittance matrix (NB x NB)
$\boldsymbol{G}$	Conductance matrix (NB x NB)
$\boldsymbol{B}$	Susceptance matrix (NB x NB)
$\boldsymbol{\theta}$	Bus voltage phase angle matrix (NB x 1)
$\boldsymbol{A}$	Line – bus incidence matrix (NL x NB)
$\boldsymbol{E}$	Electrical distance matrix (NB x NB)
j	$(\sqrt{-1})$ imaginary number

Acknowledgements

The community that has supported, encouraged and assisted me through the completion of this research is immense. This feeble attempt to express my gratitude cannot possibly begin to repay the debts that I owe each and every member. Nevertheless, I will take this rare opportunity to acknowledge a few whose support has been particularly meaningful.

To the faculty, staff and students of the Energy and Mineral Engineering department and particularly the Energy Management and Policy option; thank you for the amazing opportunities. I am honored to represent the department as a pioneering Ph.D. student in the EMP option. Witnessing and contributing to the development of this program has been a unique and rewarding experience.

If there is one piece of advice that I have to offer people considering a graduate education, it is to find a great adviser. Seth Blumsack has been nothing short of a great adviser. We both took chances on each other in the fall of 2007 when I stumbled into his office on the verge of abandoning my graduate education. I can say without a doubt that there is no one with whom I would have rather worked throughout this journey. Seth's intelligence, ambition and mentorship have provided a benchmark that I will always strive to achieve. Thank you for creating the opportunities and showing me how to take advantage of them. If nothing else, I hope that my incessant requests have helped you learn how to say 'no'. I look forward to a lifetime of friendship with you and the rest of the Blumsack family.

Speaking of opportunities, I have been lucky enough to receive generous financial support from NSF, PJM, EPA, PSU Network Science and Earth and Environmental Systems Initiatives, and the EME department. Without these supporters, none of this would have been possible.

My internship at Los Alamos National Laboratories was one of the most rewarding experiences in my life. I would like to thank Russell Bent for providing the opportunity. It was

amazing to spend time with and learn from Russell, Carleton, Scott and the other folks at LANL and the Center for Non-Linear Studies.

Despite all of its flaws, Happy Valley is a special place. The great friends that I have found here will last a lifetime. Fortunately, there are too many of you to mention individually, but you know who you are, and thank you for the great times. Many of you belong to the cycling community, and along with the unrivaled beauty and quality of riding in Central PA, you shall take some of the blame for my procrastination.

Cycling has, until recently, dominated my thoughts and ambitions. Throughout graduate school, I have been fortunate to enjoy a life of travel and competition facilitated by bicycle racing. That lifestyle would have been impossible without the support of sponsors and teammates and the tolerance of my wife and my adviser. Again, thanks to all of you for allowing me such luxuries.

My parents and my sister deserve heartfelt thanks for the unwavering love and support throughout the last five and a half years. I love you.

Lastly and most importantly, to my wife: I started this thing because of your encouragement. The hardships that we have overcome throughout the last five and a half years are staggering. Three and half years of living half a country apart and the poverty of graduate student stipends would each be reasons enough for almost any couple to call it quits. Through all the trips on I-70, the adventures, the phone conversations, the deadlines, the late nights, the cookies and beer, and the tandem rides, we are here… together. I couldn't have done any of this without your support, encouragement and love. Here's to a lifetime of "more today than yesterday and more tomorrow than today". Shay, I love you.

Chapter 1 Introduction

The electrical transmission network is an integral part of the nearly $400 Billion electricity industry that facilitates the transport of electrical energy from supply (generation) to demand (load). Recently, the demands placed on the electrical transmission system have increased disproportionally relative to the investments made in the system [**1**]. As a result, the system has become increasingly constrained [**2**]. In constrained systems, transmission congestion occurs when the system has at least one component operating at the boundary of capability and is thus unable to transfer power to meet the desired transactions while operating within system limits. The electricity transmission system is designed in part to facilitate competition among generators. But as regional transmission markets have grown, aggregate congestion has worsened [**3**]. Transmission congestion causes barriers to competition and contributes to price fluctuations and reliability concerns. In power system planning operations congestion is typically addressed through augmentation of the transmission system. While new transmission can mitigate problems, the planning process extends over decades and incorporates large uncertainties. The non-linear nature of power flow through the transmission network creates scenarios where system extensions do not always address the goals of the planning process.

Power system operations have traditionally assumed control over generator outputs as the only means of optimization. The introduction of "Smart Grid" technologies provides additional means to control power flow through the system. Smart grid technologies include control devices, sensors, switches and communication capabilities that provide improved understanding and adaptability to power system operators [**4**]. The applications of smart grid are emerging as the potential for cost savings and reliability improvements become apparent. This research addresses a few of the emerging challenges enabled by the introduction of the smart grid. This chapter is organized as follows: Section 1.1 outlines the role of the transmission network in

restructured electricity markets and presents a conceptual example of the Optimal Transmission Switching problem. A literature review follows, describing the current state of the art of transmission switching and highlighting topics where further research is needed.

1.1 Project Motivation

Historically, the three segments of the electricity supply chain were each considered natural monopolies. Transmission and distribution were thought to be natural monopolies due to the large, lumpy investments required to build new infrastructure and low variable costs associated with operation and maintenance [**5**]. Thus, economies of scale exist in the transmission and delivery of electric power. Generation was considered a natural monopoly since economies of scale were thought to exist throughout the range of generator sizes and the efficiency of long distance transmission was relatively low [**6**]. The three natural monopolies of generation, transmission and distribution were vertically integrated and owned by singular companies or utilities that were allowed to operate in their local areas as monopolies under regulation to ensure universal access to electricity at "cost of service" prices.

By the 1960's, advances in alternating current (AC) electricity transmission technologies had improved the efficiency of long distance electricity transmission [**7**]. This increased electrical interconnection enabled the efficient transmission of electricity over long distances so that generators are no longer limited to serving local areas. The conventional wisdom of economies of scale in generation was questioned by [**6**] and [**8**], who found that economies of scale were exhausted at relatively low generator capacity levels. Additionally, improvements in generation technologies have reduced the costs of smaller generators [**9**]. Increased interconnection has made formerly "local" generation markets contestable by enabling power transfer over long distances. However, transmission and distribution are still considered to be natural monopolies

since the cost structure for these sectors has not changed even as efficiencies have improved. With open access to the transmission network, electricity generation can now be competitive.

Much of electricity restructuring was aimed at creating a competitive environment for generation. Three components have been especially important to the complex process of electricity restructuring:

1. *Vertical dis-integration of the electric utilities:*

   The unbundling of the organizations that were formerly considered natural monopolies removes the potential for collusion between different sectors within a vertically integrated utility.

2. *Regional coordination of the transmission system:*

   The formation of regional transmission organizations (RTOs) ensures independent generators access to the transmission network. RTOs are tasked with coordinating the dispatch of generators to ensure reliable system operation.

3. *Introduction of organized regional wholesale markets for electricity:*

   The formation of an electricity spot market with bid-based, security constrained, economic dispatch, enables the economically efficient trading of electricity [**10**].

Restructuring has increased competition in electricity generation by enabling the open access of generators to an electricity market and transportation network. While electricity restructuring has the long run goal of reducing electricity prices, the short term impacts are more complicated. The transmission network that was designed in a vertically integrated, regulated industry is often unable to adequately handle the electricity transmission that is desired in the competitive electricity market. The constraints associated with these inadequacies cause locational price variations and may enhance market power of some generators. There are several options to

remove these constraints and improve competition in power generation. Building new transmission infrastructure is a logical option; however the environmental, financial and political costs are high and the uncertainties created by the competitive generation market make investments risky. As an alternative to additional planning procedures, new "smart grid" technologies have enabled more flexible and smarter power systems operations procedures.

The additional control actions enabled by the smart grid can reduce the costs associated with power system operations [**11**]. Several industry and research directives seek to improve the flexibility of power system operations by utilizing the enhanced controllability of the smart grid. The Federal Energy Regulatory Commission (FERC) issued Order 890 in 2007 that calls for economic improvements in the transmission planning and operations processes that treats all resources (including non-transmission resources) comparably [**12**]. Building on Order 890, in 2011 FERC issued Order 1000 that requires the transmission planning process to consider "transmission needs driven by public policy requirements and evaluate proposed solutions to those transmission needs" [**13**]. FERC issued a statement on October 18, 2012 that it would begin enforcement of Order 1000 [**14**]. The Energy Policy Act of 2005 calls for "a comprehensive research, development, and demonstration program to ensure the reliability, efficiency, and environmental integrity of electrical transmission and distribution systems", including "advanced energy delivery technologies that enhance reliability, operational flexibility, or power-carrying capability", and "the development and use of advanced grid design, operation, and planning tools" [**15**]. These policies enforce a strong push towards incorporating flexibility into power system operations and requiring planning processes to account for such flexibility. Despite these policies and the associated cost savings and reliability improvement potentials, many flexible operations procedures remain largely avoided by the electricity industry.

One example of system flexibility that can improve power system operations is highlighted in the Energy Policy Act of 2005, where "Advanced energy delivery technologies" are defined, in part as "optimized transmission line configurations". In certain scenarios, optimizing transmission line configurations, or transmission switching, can improve system efficiency without the need to build new infrastructure. The benefits of transmission switching to deregulated systems are twofold. The improved generator competition can lower system costs and spur new generation investments. Despite the lack of a competitive generation market, deregulated systems utilize a transmission constrained economic generation dispatch. Thus the potential system cost reduction benefits of transmission switching extend to regulated systems.

In addition to highlights in recent regulatory policy, transmission switching is a recurring topic in FERC's technical conferences. Since June of 2010, the annual meetings bring together representatives from the electricity and software industries, academia and government to "promote market efficiency through enhanced software" [**16**]. The motivation of these conferences is to promote smarter software to model flexible assets and flexible operation procedures (such as reconfigurable transmission topologies) that enables electricity industry efficiency improvements.

1.1.1 Transmission switching example

The following example demonstrates the concept of transmission switching by illustrating the Braess paradox [**17**] on a Wheatstone network [**3**].

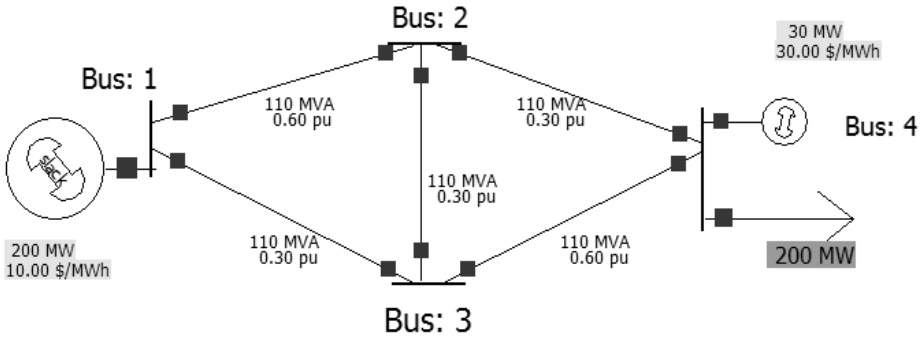

Figure 1: Symmetric Wheatstone network

Figure 1 shows the symmetric Wheatstone network where the impedance (Z) of line 1-2 is equal to the impedance of line 3-4 and the impedance of lines 1-3, 2-3, and 2-4 are equal to each other. The real components (resistance) of the line impedances are ignored, enabling the analysis of a system without resistive losses. The imaginary component of the line impedances is the "series reactance" and is displayed using the normalized per unit (pu) values for the SI units of impedance (ohms). The admittance (Y) of a line is the inverse of the impedance. The bus admittance matrix (Y_{bus}) is constructed with the diagonal elements representing self-admittances and the off diagonal elements representing the mutual admittance (Y_{ik}) of the line connecting bus *i* and bus *k*. The self-admittance values (Y_{kk}) are calculated as the negative sum of the admittances of all lines connected to bus *k*. By ignoring the real component of the admittances, we can represent the magnitudes of the imaginary components in the bus reactance matrix (B).

$$\boldsymbol{B} = \begin{bmatrix} \left(\frac{-1}{0.6}-\frac{1}{0.3}\right) & \frac{1}{0.6} & \frac{1}{0.3} & 0 \\ \frac{1}{0.6} & \left(\frac{-1}{0.6}-\frac{1}{0.3}-\frac{1}{0.3}\right) & \frac{1}{0.3} & \frac{1}{0.3} \\ \frac{1}{0.3} & \frac{1}{0.3} & \left(\frac{-1}{0.6}-\frac{1}{0.3}-\frac{1}{0.3}\right) & \frac{1}{0.6} \\ 0 & \frac{1}{0.3} & \frac{1}{0.6} & \left(\frac{-1}{0.6}-\frac{1}{0.3}\right) \end{bmatrix}$$

Each line in the network has a flow limit of 110 MW. The 200 MW load at bus 4 is to be served by dispatching the generators at busses 1 and 4. The 200 MW generator at bus 1 has a

marginal cost of generation of \$10/MWh while the smaller 30 MW generator at bus 4 has a marginal cost of \$30/MWh. The fixed costs for both generators are assumed to be zero. In this simple example, we would like to serve as much of the load as possible using the cheaper generator. To determine the amount of power flow from bus 1 to bus 4 that the network can handle, we must solve the power flow equations:

$$P_i = \sum_{k=1}^{N} |V_i|\,|V_k|(G_{ik}\cos\theta_{ik} + B_{ik}\sin\theta_{ik}) = P_{Gi} - P_{Di} \;\; \forall\, i \qquad (1)$$

$$Q_i = \sum_{k=1}^{N} |V_i|\,|V_k|(G_{ik}\sin\theta_{ik} - B_{ik}\cos\theta_{ik}) = Q_{Gi} - Q_{Di} \;\; \forall\, i \qquad (2)$$

Where V_i, P_i, and Q_i are the voltage, real power injected, and reactive power injected at bus i; G_{ik} and B_{ik} are the real and imaginary parts of the elements of Y_{bus}; and θ_{ik} is the voltage angle difference between bus i and bus k. By making the linearized decoupled optimal power flow (DCOPF) simplification, we can assume that all voltages remain at 1 pu and we can ignore reactive power injections [**18**]. Thus, the power flow equations of (1) and (2) can be reduced to:

$$P_i = \sum_{k=1}^{N} B_{ik}\sin\theta_{ik} = P_{Gi} - P_{Di} \;\; \forall\, i \qquad (3)$$

Additionally, we can make the small angle approximation of (4) which we can use to further simplify the power flow equations; the resulting linearized power flow equation is shown in **(5)**:

$$\sin(\theta_i - \theta_k) \approx \theta_i - \theta_k \qquad (4)$$

$$P_i = \sum_{k=1}^{N} B_{ik}(\theta_i - \theta_k) = P_{Gi} - P_{Di} \;\; \forall\, i \qquad \textbf{(5)}$$

The sensitivity of the power flow on each line with respect to a power injection can be calculated by solving for the voltage angles at each bus, as in (6), and dividing the difference in

voltage angles across each line by the line susceptance (B). The line flow sensitivities, given by (7), represent the change in power flow on each line due to a power injection at bus *r*.

$$\theta = B^{-1}P \qquad (6)$$

$$\frac{\partial F_{ik}}{\partial P_r} = B_{ik}(B_{ir}^{-1} - B_{kr}^{-1}) \;\; \forall\, i,k,r \qquad (7)$$

The system of 4 equations given by (6) in addition to the power balance requirement that generation must equal load gives 4 unknown bus voltage angles, and two unknown power injections corresponding to each generator. Thus, we have more equations than unknowns. By controlling a generator bus, called a slack bus, to maintain a constant voltage angle, we can remove one of the unknown voltage angles. Designating bus 1 as a slack bus we can set θ_1 equal to zero and we can solve for the remaining voltage angles using (6) and the B matrix excluding the row and column associated with the slack bus:

$$\begin{bmatrix}\theta_2\\ \theta_3\\ \theta_4\end{bmatrix} = \begin{bmatrix}-0.28 & -0.16 & -0.24\\ -0.16 & -0.22 & -0.18\\ -0.24 & -0.18 & -0.42\end{bmatrix}\begin{bmatrix}0\\ 0\\ 1\end{bmatrix} = \begin{bmatrix}-0.24\\ -0.18\\ -0.42\end{bmatrix}$$

Applying the results of equation (6) to (7) yields the line flow sensitivities to a power injection at bus 1 as:

$$\begin{bmatrix}\partial F_{12}/\partial P_1\\ \partial F_{13}/\partial P_1\\ \partial F_{23}/\partial P_1\\ \partial F_{24}/\partial P_1\\ \partial F_{34}/\partial P_1\end{bmatrix} = \begin{bmatrix}0.4\\ 0.6\\ -0.2\\ 0.6\\ 0.4\end{bmatrix}$$

Dispatching the less expensive generator at bus 1 to meet all of the 200 MW load at bus 4 introduces a 200 MW power injection at bus 1. Since we are only considering a power injection from a single bus, we can determine the line flows that result from this dispatch by multiplying the line flow sensitivities by the power injection:

$$F_{ik} = P_j \times \frac{\partial F_{ik}}{\partial P_j} \quad \forall\, i, j, k \tag{8}$$

$$F_{ik} = 200MW \cdot \begin{bmatrix} 0.4 \\ 0.6 \\ -0.2 \\ 0.6 \\ 0.4 \end{bmatrix} = \begin{bmatrix} 80 \\ 120 \\ -40 \\ 120 \\ 80 \end{bmatrix}$$

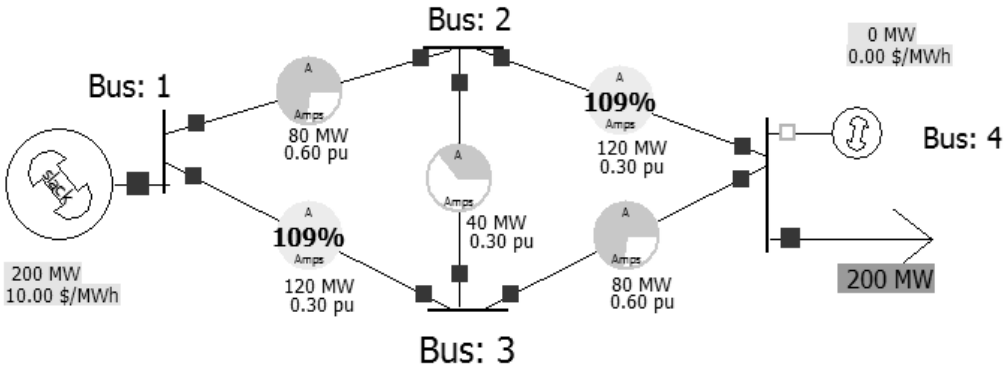

Figure 2: Wheatstone network DCPF solution without enforcing line limits

Figure 2 shows that the 120 MW flows on lines 1-3 and 2-4 are in excess of the 110 MW line limitations. By solving for the maximum flow on lines 1-3 and 2-4, we can determine the maximum power injection at bus 1:

$$\frac{F_{13max}}{\partial F_{13}/\partial P_1} = \frac{110\ MW}{0.6\ pu} = P_{1max} = 183.33\ MW$$

Therefore, the generator at bus 1 can have a maximum output of 183.33 MW and we must dispatch the generator at Bus 4 to serve the remaining 16.67 MW of load. The resulting system cost for the generation dispatch is:

$$Cost = \sum_{i=1}^{N} P_i GenCost_i = 183.33MW\frac{10\$}{MWh} + 16.67MW\frac{30\$}{MWh} = \frac{2333.33\$}{MWh}$$

Figure 3 shows the Wheatstone network with the bridge line (line 2-3) removed from service. The resulting B matrix is:

$$B = \begin{bmatrix} \left(\frac{-1}{0.6}-\frac{1}{0.3}\right) & \frac{1}{0.6} & \frac{1}{0.3} & 0 \\ \frac{1}{0.6} & \left(\frac{-1}{0.6}-\frac{1}{0.3}\right) & 0 & \frac{1}{0.3} \\ \frac{1}{0.3} & 0 & \left(\frac{-1}{0.6}-\frac{1}{0.3}\right) & \frac{1}{0.6} \\ 0 & \frac{1}{0.3} & \frac{1}{0.6} & \left(\frac{-1}{0.6}-\frac{1}{0.3}\right) \end{bmatrix}$$

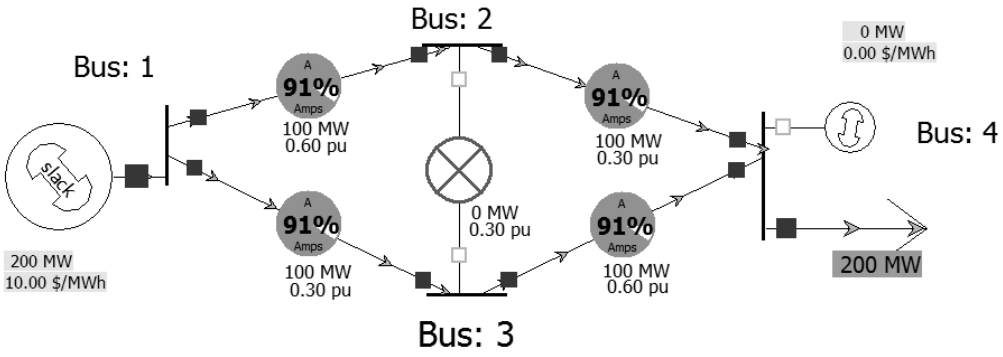

Figure 3: Switched Wheatstone network and DCOPF solution

Applying the same analysis from above, the resulting voltage angles and line flow sensitivities for the switched Wheatstone network are:

$$\begin{bmatrix}\theta_2\\ \theta_3\\ \theta_4\end{bmatrix} = \begin{bmatrix}-0.4 & -0.1 & -0.3\\ -0.1 & -0.25 & -0.15\\ -0.3 & -0.15 & -0.45\end{bmatrix}\begin{bmatrix}0\\ 0\\ 1\end{bmatrix} = \begin{bmatrix}-0.3\\ -0.15\\ -0.45\end{bmatrix}$$

$$\begin{bmatrix}\partial F_{12}/\partial P_1\\ \partial F_{13}/\partial P_1\\ \partial F_{23}/\partial P_1\\ \partial F_{24}/\partial P_1\\ \partial F_{34}/\partial P_1\end{bmatrix} = \begin{bmatrix}0.5\\ 0.5\\ 0.5\\ 0.5\end{bmatrix}$$

With this network topology, the power injected at bus 1 divides equally to flow along path 1-2-4, and path 1-3-4. When 200 MW is injected at bus 1, the flow along each of these paths is 100 MW < $F_{max\text{-}ik}$ and there is no need to dispatch the generator at bus 4 since all of the load can be met by the cheaper bus 1 generator. The system cost for the switched Wheatstone network in Figure 3 is thus \$2000.00/MWh, which is a 15% cost savings over the un-switched Wheatstone network in Figure 2.

This example demonstrates a circumstance where the system operator would not dispatch line 2-3 to reduce the cost of operating the system. However, it is easy to imagine a scenario where the system cost is reduced by the in-service status of line 2-3. Shifting the 200 MW load from bus 4 to bus 3; the optimal dispatch with all lines in service has a system cost of \$3222. Removing line 2-3 from service; the optimal system cost increases to \$4266. Thus, in a system with continuously changing loads, allowing system operators to control the network topology along with the generator dispatch can reduce the costs associated with power system operations.

1.2 Optimal Transmission Switching Problem Definition

Previous work has shown that the removal of specific transmission lines from operation can reduce the costs associated with power system operation [**19**]. This phenomenon, known as

Braess' Paradox, could be avoided in electric transmission networks through the use of emerging "smart-grid" technologies that enable a flexible network topology. Transmission switching enables system cost reductions by relieving transmission constraints and enabling the re-dispatch of low cost generators. The transmission switching problem extends the traditional power system optimization by controlling the network topology in addition to the generator dispatch.

The optimal power flow (OPF) problem determines the cost minimizing generator dispatch to satisfy system load subject to system constraints and Kirchhoff's laws.

$$min \sum_{g} c_g P_g \tag{9}$$

s.t.

$$\theta_n^{min} \leq \theta_n \leq \theta_n^{max}, \qquad \forall\, n \text{ busses} \tag{10}$$

$$P_g^{min} \leq P_g \leq P_g^{max}, \qquad \forall\, g \text{ generators} \tag{11}$$

$$P_k^{min} \leq P_k \leq P_k^{max}, \qquad \forall\, k \text{ lines} \tag{12}$$

$$\sum_{i=n} P_{k_{ij}} - \sum_{j=n} P_{k_{ij}} - \sum_{g} P_{ng} - \sum_{d} P_{nd} = 0, \forall\, n \tag{13}$$

$$B_k(\theta_n - \theta_m) - P_k = 0, \qquad \forall\, k \text{ lines} \tag{14}$$

For the linearized model above, known as a DCOPF, c_g and P_g represent the generator cost and power output and the system constraints include: bus voltage angles (10), generator outputs (11), and power flow along each transmission line (12). The power balance is represented in Equation (13) and Kirchhoff's laws are represented in (14) where B_k represents the susceptance of $line_k$.

OTS extends the DCOPF problem by multiplying an integer variable, $z_k \in \{0,1\}$, to the P_k^{min} and P_k^{max} limits of the branch power flow constraint (12), representing the out-of-service/in-service state of each transmission line. The OTS problem formulation replaces constraints (12)

and (14) of the DCOPF by Equations (15) and (16), where M_k*'s* are user-specified values that are large enough to relax the constraints associated with Kirchhoff's laws when a line is removed from service.

$$P_k^{min} z_k \leq P_k \leq P_k^{max} z_k, \qquad \forall\, k \tag{15}$$

$$\begin{aligned} B_k(\theta_n - \theta_m) - P_k + (1 - z_k)M_k \geq 0, \qquad \forall\, k \\ B_k(\theta_n - \theta_m) - P_k - (1 - z_k)M_k \leq 0, \qquad \forall\, k \\ z_k \in \{0,1\}, \qquad \forall\, k \end{aligned} \tag{16}$$

1.3 Optimal Transmission Switching Review

Transmission systems are built through a power system planning process that seeks to optimally design the system for use under an extremely large variety of conditions over long time horizons. A significant body of literature considers the optimal transmission expansion planning problem **[20-24]**. However, the transmission planning process fails to take into account flexible network topology operations into optimal network design.

Traditional transmission planning processes result in systems that are operated with static topologies that are sufficient, but are nevertheless sub-optimal in nearly all conditions. Section 1.1.1 outlines how, in certain situations, the presence of transmission lines can cause economic inefficiencies. The grid's transmission elements are equipped with relays, or switches, that facilitate the removal of transmission lines from service during power system operations. This design, originally intended for fault protection and maintenance procedures, enables the control over the topology of the transmission network. These control actions, known as "transmission switching", can be used to alleviate a variety of problems.

Transmission switching was originally proposed as a corrective action to reduce transmission line overloads [**25**]. Previous literature surveys by Glavitsch [**26**] and Rolim [**27**] document the

use of corrective switching transmission lines for solving line overload problems **[28-45]**, solving voltage problems [**35**,**28**,**42**,**43**], reducing costs and/or losses [**29**,**39**,**41**], and for security enhancement [**46**,**39**]. Regardless of the objective, the computational burden presented by corrective switching problems is a common theme in the literature. Thus, most illustrative examples have been applied to relatively small systems (<100 busses). Additionally, several strategies have been proposed to reduce the search space of switching problems. The most common search space reduction technique for switching actions has been to limit the number of lines considered switchable. Several studies simply set an upper bound on the number of switched lines while considering any line for inclusion in the set of switched lines **[11, 47-49]**. This technique provides some tractability improvements but appears to significantly degrade the quality (optimality) of results. Bakiritzis presents a method to limit switchable lines through a ranking system based on each lines effect on system security [**35**]. The method is applied to alleviate under/over voltages resulting from line outages in a 981 bus, 1175 line system of the Georgia Power Company and produces favorable, nevertheless sub-optimal results. Evolutionary algorithms are employed by Doll for the purpose of congestion management on small test systems [**50**]. Mazi, followed similarly by Wrubel, consider corrective switching on a set of lines limited by a screen and ranking system based on the sensitivities of network flows to the removal of individual lines [**34**,**44**]. Each of these corrective switching studies highlights the use of flexible network topologies as a means of alleviating post-dispatch contingencies. More recently, transmission switching has been proposed as a method to introduce a dispatchable transmission network into the optimal power flow (OPF) problem [**51**].

Optimal transmission switching was first discussed in [**51**]. Up to 25% reductions in system cost were obtained when transmission switching was applied to the IEEE 118-bus network [**11**].

In order to reduce the solution time, the authors limit the number of switchable lines to range between 1 and 7. Savings ranged from 6.3% for j=1 switchable lines to 22.3% for j=7 switchable lines. With the switchable line quantity restriction removed, 24.9% cost savings were produced by switching 38 lines.

Transmission switching on the RTS-96 system was first presented with an N-1 generation and transmission contingency analysis [**49**]. Hedman et al. present an extension that considers the commitment optimization of both transmission and generation assets [**52**]. The transmission switching problem is decomposed into two sub problems. First, a 24 hour unit commitment problem without transmission switching is solved. Since generator ramp rates are not binding in this model, 24 N-1 DCOPF optimal transmission-switching problems can then be solved simultaneously with fixed generator commitments. Finally the effect of transmission switching can be determined by solving the generation commitment problem with a fixed transmission topology. This process is repeated until solutions yield no change in unit commitment. Transmission switching generated 3.7% savings over the static un-switched DCOPF solution over the course of a single 24-hour period on the RTS-96 system.

An economic analysis of the 24-hour OTS results on the RTS-96 network is presented by O'Neil et al. [**53**]. In electricity markets, energy is considered a private good and thus the definition of which market participants benefit from energy consumption is straightforward. Transmission switching actions are considered "club goods" where every market participant benefits from the consumption of the good. The OTS problem objective by definition maximizes social welfare. While individual consumers may see deviations in electricity prices from transmission switching, in the aggregate, social welfare is improved by transmission switching. Generator benefits are more complex. Topology reconfigurations cause production increases for

some generators and decreases for others. These shifts in generation dispatch also affect the clearing prices for energy. Existing markets typically assign the benefits of transmission use through financial transmission rights [**54**]. Such frameworks can experience revenue adequacy problems when applied to topologically flexible transmission topologies [**51**]. A more complete real time electricity market design could alleviate the revenue adequacy problems and enable the pricing of topology reconfigurations [**55**].

Despite the potential for savings demonstrated in the literature, OTS has not been adopted by power system operators. Several technical challenges remain to demonstrate the feasibility of implementing OTS into the operation of existing power systems. Thus, the following overarching research question remains open: "How can we co-optimize generation dispatch and network topology to achieve reliable, cost-reducing dispatches within operational timeframes?" The effects on relays and other equipment, financial transmission rights markets and revenue adequacy and many other issues must be addressed before OTS implementation [**56**]. However, two areas are of critical interest:

1. The OTS problem is too computationally complex to solve to optimality on large systems within operational time horizons *(< 1 hour).*
2. Since the problem is formulated using the linearized-DC load flow model, the effects of voltage magnitude and reactive power flow are not captured. Thus, the ability of the system to operate reliably under optimal topology reconfigurations is not well understood.

The first problem is addressed in Chapters 2, 3, and 4 through the identification and development of a two part solution heuristic (described in Figure 4) aimed reducing the feasible solution space of the OTS problem. Network partitioning and a candidate switchable line screen together reduce the feasible space by reducing the number of transmission lines considered in

each optimization problem. The developed heuristic solution methods improve the adoptability of transmission switching operations by enabling solutions of the OTS problems on shorter timelines.

The second problem is addressed in Chapter 5, where for the first time, OTS solutions are modeled with a complete AC power flow model. By modeling reactive power flows and voltage magnitudes in addition to the real power flows and voltage phase angles, we gain an understanding of the corrective actions required to ensure feasibility of topology reconfigurations. Additionally, topology reconfigurations are shown to produce cost savings in both the AC and DC power flow models.

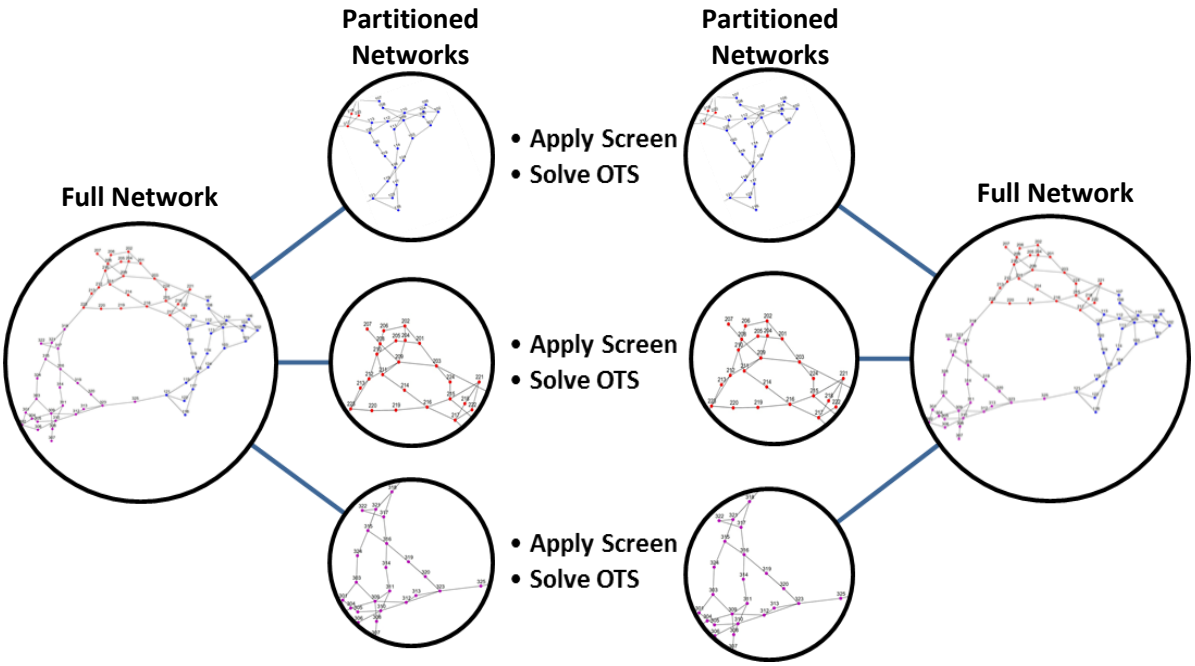

Figure 4: Schematic of the OTS solution evolution using the 2-part heuristic implemented in Chapter 4

The remainder of the document is organized as follows: Chapter 2 presents a marginal analysis of OTS results that identifies two strategies for improving the problem tractability. The results of Chapter 2 inform the transmission line screening and network partitioning approaches

presented in Chapters 3 and 4. Chapter 5 presents an analysis of topology reconfigurations in the more realistic AC system model. Finally Chapter 6 concludes highlighting the contribution of this dissertation. Appendix A at the end of the document provides the reader with an introduction to some of the engineering notation and computations surrounding electrical power flow analysis that is used throughout the document.

Chapter 2 Marginal Analysis of Optimal Transmission Switching[1]

The concept of transmission switching and OTS cost savings produced on test systems is outlined in Chapter 1. However, the nature of electricity flow through a network makes it difficult to ascribe savings to specific elements. This Chapter reports on an analysis that decomposes the solutions of OTS to investigate whether common electrical network metrics are useful predictors of the frequency with which a line will be switched and to understand the contributions of each switched line on aggregate savings.

Through the cost reduction objective of OTS, the optimal solutions determine the in/out of service state of each transmission line and the generator dispatch for the entire system. Hedman, [**52**], solves the OTS problem on the IEEE Reliability Test System – 1996. The 73 bus IEEE Reliability Test System - 1996 (RTS-96) was developed as a standardized database for testing reliability evaluation methodologies [**57**]. RTS-79, derived in 1979 provided the template for two updated systems created in 1986 (RTS-86) and 1996 (RTS-96). The system was developed to include a variety of technologies and configurations found in typical power systems. However since the RTS-96 includes many of these characteristics within one system, it is not intended to represent any particular system. One particularly useful aspect of the RTS-96 is the inclusion of 24 load cases corresponding to the hours of a single day. RTS-96 consists of three virtually identical 24-bus power systems that are loosely connected. Hence, RTS-96 is often referred to as the three area reliability test system. The RTS-96 network, shown in Figure 5, is a commonly used benchmark for power system analysis and in its published form consists of 73 buses, 120 transmission lines and 99 generators and has no binding transmission constraints. The following modifications are made to each area of the network to facilitate a constrained optimal dispatch

[1] The research presented in this chapter has been published in *IEEE Transactions on Power Systems* [**125**].

[**52**]: Line 11-13 was removed, 480MW of load was shifted from buses 14,15,19 and 20 to bus 13, and the capacity of line 14-16 was decreased to 350MW. It is important to note that generator ramp rate constraints are not considered in the RTS-96 model. Generator fuel costs are reported in Table 1. The complete system data is reported in the Matpower data format in Appendix C.1.

Table 1: RTS-96 Generator Fuel Costs

Gen	Fuel	Fuel Cost/Mbtu	Out_{Min}%	Out_{Max}%	Marginal Cost $/MWh
U12	#6 oil	$8.40	20	100	$85.50
U20	#2 oil	$15.17	79	100	$149.56
U50	Hydro	$0.00	100	100	$0.10
U76	Coal	$1.78	20	100	$17.00
U100	#6 oil	$8.40	25	100	$67.95
U155	Coal	$1.78	35	100	$14.71
U197	#6 oil	$8.40	35	100	$70.12
U350	Coal	$1.78	40	100	$14.96
U400	LWR	$0.60	25	100	$22.00

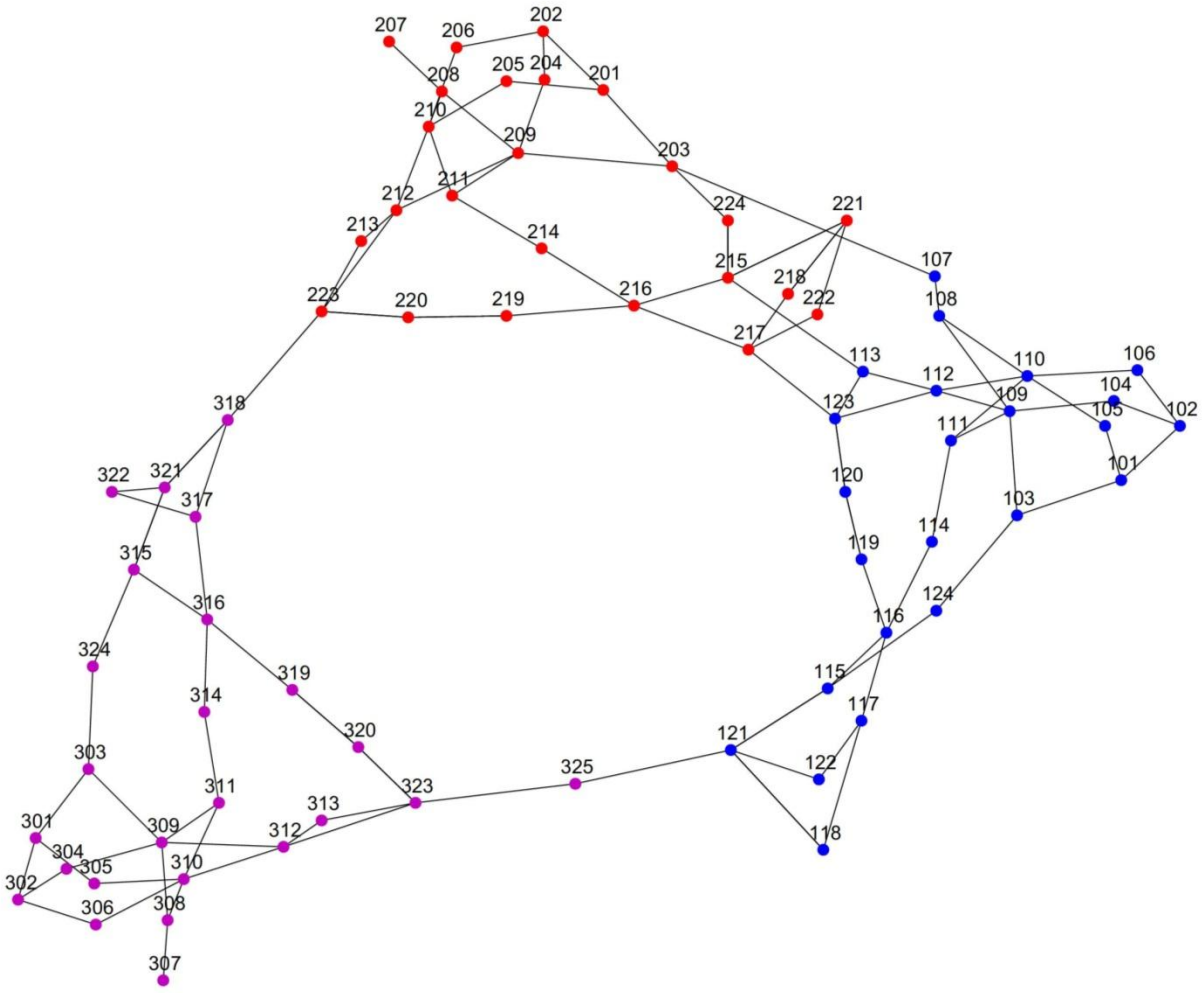

Figure 5: Topological representation of the RTS-96

The results of [**52**] provide 24 optimally switched solutions for the RTS-96 test network. The authors of [**52**] were kind enough to provide the dataset of OTS results on the RTS-96 network. Specifically, the dataset contains the in-service/out-of-service state of each transmission line in the network as 120 binary variables for each of the 24 load periods. This dataset provides the foundation for a meta-analysis of OTS results. The meta-analysis objectives are twofold. First, the simulated infrastructure of electrical transmission networks provides several constants that could identify "switchable" lines. An analysis of various network constants investigates this

theory. Second, analysis of the changes induced by switching lines indicates areas of interest for heuristic development.

2.1 Correlation of Various Network Parameters to Switched Line Probability

The significance of various network properties on the likelihood of a particular line removal through OTS is investigated using the set of optimally switched lines for each load case of the RTS-96. For each hour, the dataset identifies which lines are removed from service. The number of lines that are removed from service ranges from one (*hour 22*) to 7 (*hours 7, 12, and 13*). The sum of the switched elements is recorded in Table 2.

Table 2: # of Switched Lines in Each Period

HR1	HR2	HR3	HR4	HR5	HR6	HR7	HR8
6	3	3	2	2	2	7	3
HR9	**HR10**	**HR11**	**HR12**	**HR13**	**HR14**	**HR15**	**HR16**
6	3	5	7	7	6	7	7
HR17	**HR18**	**HR19**	**HR20**	**HR21**	**HR22**	**HR23**	**HR24**
4	3	5	6	3	1	2	5

Table 3 shows various electrical and network parameters of the transmission lines that were switched anytime during the 24 hours of OTS on the RTS-96 network. The last column of Table 3 reports the number of times that each line was switched. This value is used as a proxy for switching probability for the analysis of each of the network parameters (described below). The correlation of each network parameter to the number of times each line is switched is shown in Figure 6.

2.1.1 Branch Resistance, Reactance and Susceptance

The resistance of a transmission line is the real component of the branch impedance which describes the difficulty of electrical current flow along a conductor. However, since this analysis uses the linearized, lossless DC power flow model, where losses are neglected, the resistance of

the transmission lines is ignored. Therefore, resistance has no effect on the probability that a transmission line is removed from service.

The reactance of a transmission line is a measure of the resistance to a change in power flow. Susceptance is simply the inverse of reactance, describing the ease of changing current flow. Figure 6 plots the reactance of every line in the system against the number of times each line is switched. The highest reactance branches are never switched, however Table 4 shows that no significant correlation was observed between reactance or susceptance and the number of times that lines were switched.

2.1.2 Branch Capacity

The branch capacity represents the maximum power flow path rating. Ratings are calculated depending on a variety of factors including: transmission line material, tower spacing, tower height, surrounding geography (trees, water, etc.) and expected weather. Branch capacities are set to avoid operating instabilities and over-heating which typically leads to the stretching and breaking or short-circuiting of transmission lines. Although the highest-capacity transmission line is never switched, Figure 6 shows that branch capacity is not a significant identifier of the number of times that a line is switched.

2.1.3 Degree of Branch Endpoints

The number of transmission lines connected to a bus is represented as the bus degree. The degrees of the busses connected by a switched transmission line likely have little to do with the potential cost savings gained by switching that transmission line. Except in the case where both the origin and destination busses have degree ≤ 2. In this case transmission switching would cut a loop in the system, or remove a bus from the network altogether. For this reason, the *From-Bus Degree* parameter, which represents many of the low-degree connections in the system, has a significant positive correlation.

2.1.4 Branch Centrality

The branch centrality describes the number of shortest topological (number of hops) paths between any two nodes that utilize each branch. Again, Figure 6 shows that the branch centrality parameter provides little indication of the switching potential of specific transmission lines.

Table 3: Switched Transmission Line Data

Fr Bus-To Bus	Resist-ance (p.u.)	React-ance (p.u.)	Suscept-ance (p.u.)	Line Rating (MW)	From Degree	To Degree	Centrality	# Periods Switched
109-111	0.002	0.08	0	400	5	3	71.55	15
112-113	0.006	0.05	0.1	500	4	3	92.743	1
113-215	0.01	0.08	0.158	500	3	5	144.94	10
201-202	0.003	0.01	0.461	175	3	3	58.8	4
209-211	0.002	0.08	0	400	5	3	74.291	3
215-216	0.002	0.02	0.036	500	5	4	124.1	4
215-221	0.006	0.05	0.103	500	5	5	79.167	2
217-218	0.002	0.01	0.03	500	4	3	65.917	14
218-221	0.003	0.03	0.055	500	3	5	14.75	1
218-221	0.003	0.03	0.055	500	3	5	14.75	4
219-220	0.005	0.04	0.083	500	3	4	252.87	1
219-220	0.005	0.04	0.083	500	3	4	252.87	1
220-223	0.003	0.02	0.046	500	4	5	263.21	6
220-223	0.003	0.02	0.046	500	4	5	263.21	1
309-311	0.002	0.08	0	400	5	3	89.213	18
310-311	0.002	0.08	0	400	5	3	130.88	1
318-321	0.003	0.03	0.055	500	4	5	273.45	7
318-321	0.003	0.03	0.055	500	4	5	273.45	8
320-323	0.003	0.02	0.046	500	4	5	206.6	2
320-323	0.003	0.02	0.046	500	4	5	206.6	2

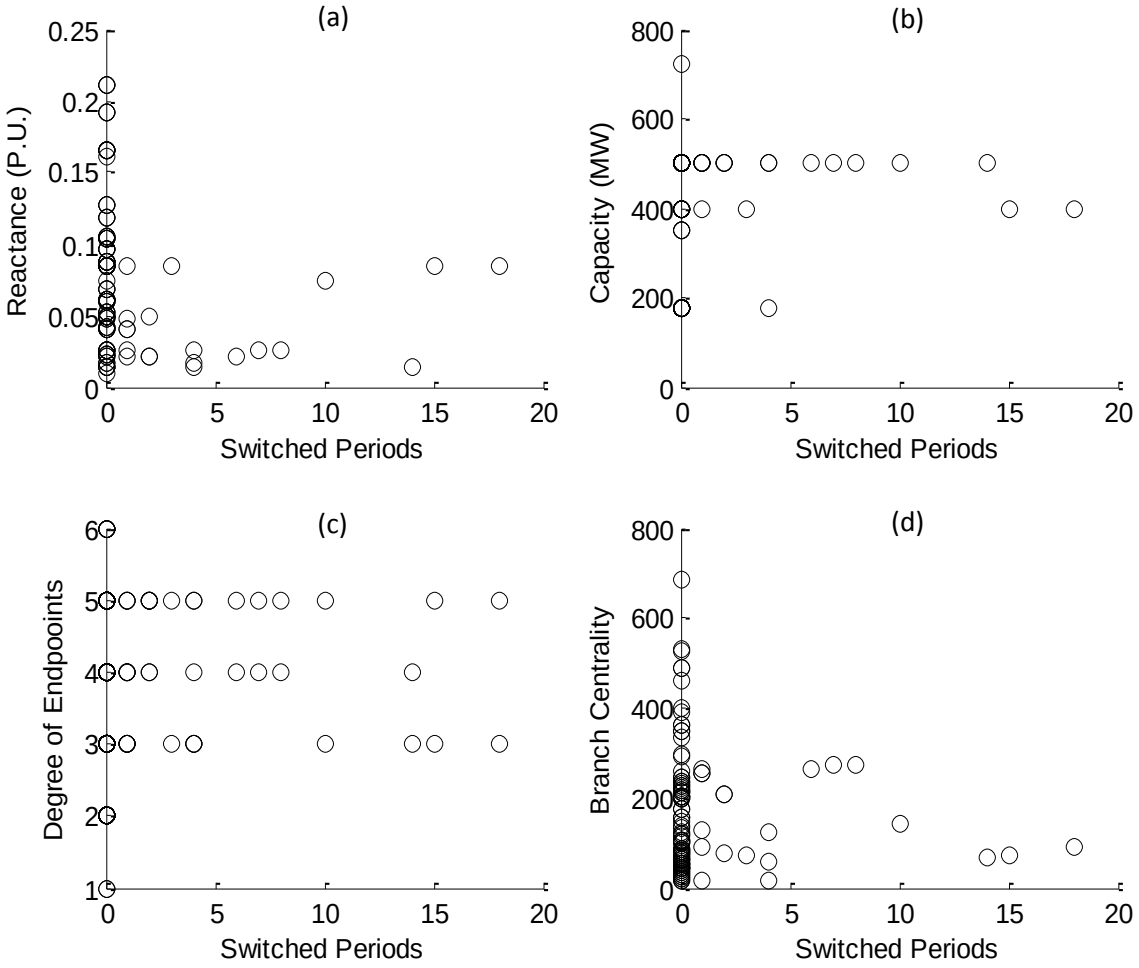

Figure 6: Various transmission line parameters are plotted as functions of the number of periods each transmission line is removed from service.

Table 4: Correlations Between Various Network Parameters and # Times a Line is Switched

Parameter	Correlation Coefficient
Branch Reactance (a)	-0.1593
Branch Susceptance	-0.0652
Branch Capacity (b)	0.1470
From-Bus Degree (c)	0.2259
To-Bus Degree (c)	0.0244
Branch Centrality (d)	-0.0647

Table 5: Marginal Savings as a % x 10^{-1} of Un-Switched System Cost

	Periods (Hours)																							
Lines	**1**	**2**	**3**	**4**	**5**	**6**	**7**	**8**	**9**	**10**	**11**	**12**	**13**	**14**	**15**	**16**	**17**	**18**	**19**	**20**	**21**	**22**	**23**	**24**
109-111	-.001	---	---	---	---	---	-.001	---	.193	.420	.463	.470	.463	.470	.470	.445	.436	.436	.387	.372	.372	---	---	---
112-113	---	---	---	---	---	---	---	---	---	---	---	---	---	---	---	---	---	---	---	---	---	---	---	.011
113-215	-.027	.000	.000	.000	.000	.000	-.027	---	---	---	-.251	---	---	---	-.252	---	---	---	---	---	---	---	-.335	---
201-202	.000	---	---	---	---	---	.000	---	---	---	---	---	---	---	-.002	---	---	---	---	---	---	---	---	-.006
209-211	---	---	---	---	---	---	.035	---	---	---	.374	---	---	---	---	---	---	---	---	---	---	---	.199	---
215-216	---	---	---	---	---	---	---	---	---	---	---	.015	.010	---	.015	-.002	---	---	---	---	---	---	---	---
215-221	---	---	---	---	---	---	---	---	---	---	---	-.024	-.024	---	---	---	---	---	---	---	---	---	---	---
217-218	---	.000	.000	.000	.000	.000	---	.017	.024	.033	.032	---	---	.032	---	---	---	---	---	.035	.035	.034	---	.016
218-221	---	---	---	---	---	---	---	---	---	---	---	---	---	---	---	.003	---	---	---	---	---	---	---	---
218-221	---	---	---	---	---	---	.000	---	---	---	---	---	---	---	.003	---	.003	---	.003	---	---	---	---	---
219-220	---	---	---	---	---	---	---	---	.025	---	---	---	---	---	---	---	---	---	---	---	---	---	---	---
219-220	---	---	---	---	---	---	---	---	---	---	---	---	---	---	---	---	---	---	---	.050	---	---	---	---
220-223	---	---	---	---	---	---	---	---	.018	---	---	.027	.028	.027	---	.029	.030	---	---	---	---	---	---	---
220-223	---	---	---	---	---	---	---	---	---	---	---	---	---	---	---	---	---	---	---	.034	---	---	---	---
309-311	.020	---	.000	---	---	---	.020	.175	.342	.429	.450	.444	.450	.444	.444	.447	.439	.439	.412	.402	.402	---	---	.106
310-311	---	.000	---	---	---	---	---	---	---	---	---	---	---	---	---	---	---	---	---	---	---	---	---	---
318-321	.000	---	---	---	---	---	---	---	-.001	---	---	-.003	-.003	-.003	-.003	-.003	---	---	---	---	---	---	---	---
318-321	---	---	---	---	---	---	.000	-.001	---	---	---	-.003	-.003	-.003	---	-.003	---	---	-.003	-.003	---	---	---	---
320-323	-.001	---	---	---	---	---	---	---	---	---	---	---	---	---	---	---	---	---	---	---	---	---	---	.002
320-323	---	---	---	---	---	---	---	---	---	---	---	---	---	---	---	---	---	.017	.018	---	---	---	---	---
# Sw'd[1]	6	3	3	2	2	2	7	3	6	3	5	7	7	6	7	7	4	3	5	6	3	1	2	5
Cost $k[2]	7.27	7.26	7.25	7.25	7.25	7.25	7.27	7.34	7.44	7.54	7.59	7.60	7.59	7.60	7.60	7.56	7.55	7.55	7.51	7.50	7.50	7.51	7.44	7.31
$[S_1]$[3]	-0.01	0.00	0.00	0.00	0.00	0.00	0.03	0.19	0.60	0.88	1.07	0.93	0.92	0.97	0.68	0.92	0.91	0.89	0.82	0.89	0.81	0.03	-0.14	0.13
$[S_2]$[4]	0.00	0.00	0.00	0.00	0.00	0.00	0.05	0.19	0.55	0.82	1.03	0.76	0.76	0.93	0.72	0.86	0.89	0.84	0.74	0.83	0.72	0.03	0.00	0.10

[1]#switched lines produced by Optimal Transmission Switching. [2] Total system cost of the un-switched system in thousands of dollars.
[3] S_1 represents the hourly sum of the marginal % savings of all of the switched lines. [4] S_2 is the Optimal Transmission Switching % savings.

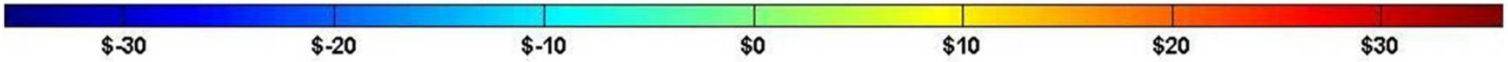

2.2 Marginal Transmission Switching

To investigate the relative value of switching individual lines, the results of a baseline DC OPF run over 24 hours (with no transmission switching) were compared to a series of DC OPF simulations with individual lines switched out. Marginal system cost reductions produced by individually switching transmission lines are determined as the system cost reduction from the nominal (no switching) case. N-1 transmission security is considered by individually removing transmission elements and verifying that the dispatch remains unaffected. Additionally, N-1 generation security is considered by verifying a feasible dispatch under the removal of any one generator. The calculations follow the broad steps below for each of the 24 load periods:

1. Run the un-switched DC OPF to obtain a baseline total system cost for hour *h.*
2. Using the set *S* of optimally switched lines for hour *h*, remove from service line *i=1* of set *S* to obtain the marginally-switched system.
3. Run the DC OPF on the marginally-switched system to obtain the total system cost for hour *h* with line *i* removed from service.
4. Subtract the un-switched system cost from the marginally-switched system cost to obtain the marginal contribution of switching line *i* during hour *h*.
5. Replace line *i* so that it is no longer out of service.
6. Increment *i* and repeat Steps 2-6 until each line in the optimally switched set *S* for hour *h* has been considered.
7. Sum the marginal savings produced by individually switching each line in the set *S* to obtain the aggregate marginal savings.
8. Simultaneously remove all of the lines in set *S* from service to obtain the optimally-switched system.

9. Run the DCOPF on the optimally-switched system to obtain the total optimal system cost for hour *h.*
10. Subtract the un-switched system cost from the optimal system cost to obtain the OTS savings during hour *h.*
11. Increment *h* and repeat Steps 1-10 until each period has been considered.

These calculations were performed running Matlab on a PC in roughly 5 minutes. The results are shown in Table 5 where the colored cells correspond to the magnitude of the cost (negative) or savings (positive) produced by individually switching transmission lines. The values within the colored cells of Table 5 are the tenths of a percentage of savings over the un-switched system cost generate by individually switching lines.

The number of switched lines in each of the 24 periods is displayed at the bottom of Table 5 in the row denoted by "*# Sw'd*". The optimal savings produced by OTS (simultaneous switching) is reported in the "*Savings*" row, while the total system cost in thousands of dollars is reported in the "*Cost $k*" row. The bottom section of Table 5 warrants three observations:

1. System cost reductions are not an increasing function of the number of switched transmission lines.
2. Peak hours (9-21) experience the greatest cost reductions from transmission switching.
3. The highest cost hours (10-18) have a consistently high system cost, however the percentage Savings varies significantly.

Table 5 reports the sum of marginal savings (from switching individual lines) in the row denoted by "S_1". As shown in Figure 7, the sum of marginal savings does not completely reflect the cost savings produced by the results of [**52**], although the two are close. The average difference between the sum of marginal savings (S_1) and the savings produced by OTS (S_2) is

0.05%. During periods 9-21, these calculations suggest that the majority of cost savings are produced by switching line 109-111 and line 309-311.

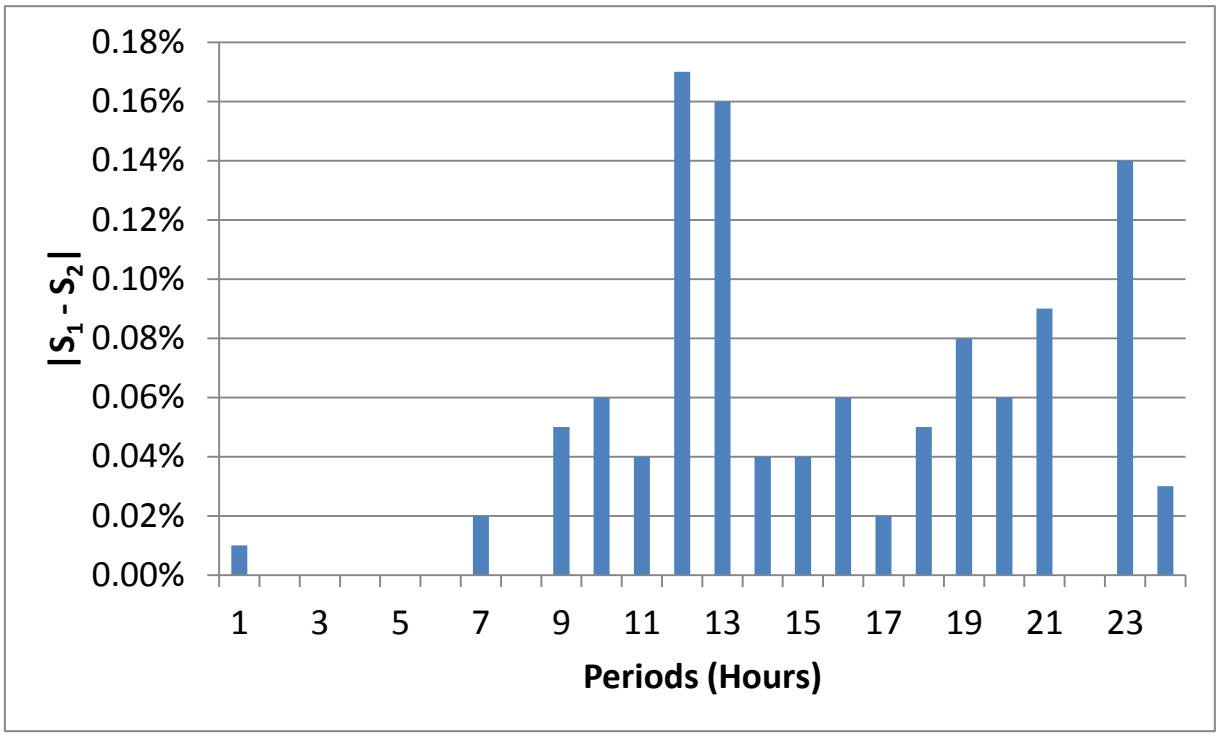

Figure 7: The difference between the sum of marginal savings from switching lines individually (S_1) and the OTS savings (S_2)

The RTS-96 system consists of 3 loosely interconnected sub-networks or areas. The first digit of each bus number indicates the area in which the bus is located. Table 5 indicates that switched lines with significant marginal savings (>0.5%) are lines 109-111 and 309-311 during hours 8-21, line 309-311 in hour 24 and line 209-211 in hours 11 and 23. Never over the course of the 24 hours do two lines with significant marginal contributions to savings reside within the same area.

2.3 Marginal Switching Conclusions

Analysis of the metadata gathered here, leads to two primary conclusions. First, these results suggest that the savings produced by OTS are primarily due to the switching actions of a small number of transmission lines. While lines 109-111 and 309-311 appear to contribute most

significantly to savings in total system cost, we found no network properties that distinguish these lines. No evidence was found to suggest that these lines could be identifiable through a simple examination of line characteristics or network topology metrics.

The second conclusion is slightly less obvious. The difference between the sum of marginal savings and OTS savings is small. This suggests that the effects of transmission switching are relatively localized. While the effects of transmission switching on power flows are, by definition, system wide; the magnitudes of the changes in flow across lines diminish as the electrical distance from the switched line increases. Additionally, the unit commitment changes that produce the cost savings are nonlinear. Thus, the results presented here show that transmission switching effects are relatively localized since it is not necessary to switch all lines (in the OTS solution) simultaneously to achieve similar benefits. In particular, since the lines that contribute most to the observed savings reside in different areas, it is likely that transmission switching effects are localized to within areas.

Chapter 3 Screened Optimal Transmission Switching

Previous research has demonstrated the significant savings potential of implementing OTS into power system operations [**11**,**19**]. Operators could adopt OTS as a part of the day-ahead market, or real-time markets. While day-ahead implementation would allow for longer solution times than real-time implementation, the current problem complexity of OTS on real systems remains much too large to obtain feasible solutions on operational time horizons through traditional optimization solution techniques. This chapter develops a new approach for improving the computational tractability of the OTS problem. The approach presented here aims to reduce the problem complexity so that traditional optimization techniques can be applied to a slightly modified OTS problem to produce improving results on much shorter time horizons.

The conclusions presented in Chapter 2 suggest that two approaches may be useful to reduce the problem complexity of OTS. The observation that the majority of savings is produced through switching a small subset of lines suggests that the majority of lines need not be considered in the OTS problem. The following Chapter develops and implements a pre-screening method for limiting the lines considered switchable in the topological optimization problem.

3.1 Switchable line limiting heuristic development

Transmission switching actions produce system cost savings by relieving transmission congestion and enabling generation re-dispatch. Through the use of the linearized DC power flow model, we can use sensitivity factors to identify lines that, when switched, relieve congestion on other lines, possibly enabling a cost saving generation re-dispatch.

The Line Outage Distribution Factors (LODF) are derived from the Power Transfer Distribution Factors (PTDF) using the linearized de-coupled system model [**58**] and describe the change in real power flow on every line in the system due to the removal of a single line. In (17

), $PTDF_{ij,k}$ describes the change in power flow across the line connecting bus_i and bus_j (P_{ij}) due to a power injection at each bus_k (P_k) and a corresponding power removal at the slack bus. B_{ij} is the i^{th} entry of the j^{th} column that represents the network susceptance between bus_i and bus_j

$$PTDF_{ij,k} = \frac{\partial P_{ij}}{\partial P_k} = B_{ij}\left(B_{ik}^{-1} - B_{jk}^{-1}\right) \quad (17)$$

$$LODF_{ij,mn} = \frac{PTDF_{ij,m} - PTDF_{ij,n}}{1 - PTDF_{mn,m} + PTDF_{mn,n}} \quad (18)$$

$$\Delta P_{ij} = LODF_{ij,mn} \times P_{mn}^{*} \quad (19)$$

$LODF_{ij,mn}$ describes the change in power flow across the line connecting bus_i and bus_j due to the removal of the line connecting bus_m and bus_n. $LODF_{ij,mn}$ is derived by calculating the *PTDF* for line *ij* corresponding to a power removal at bus_m and a power injection at bus_n. By designating bus_n as the slack bus and setting the power injection/removal equal to the pre-switching flow along line *mn* we simulate the removal of line *mn*. $LODF_{ij,mn}$ represents the pre-switched $line_{mn}$ flow distributed to $line_{ij}$. The change is power flow along $line_{ij}$ is achieved using Equation (20), where P^{*}_{mn} represents the pre-switched power flow along $line_{mn}$.

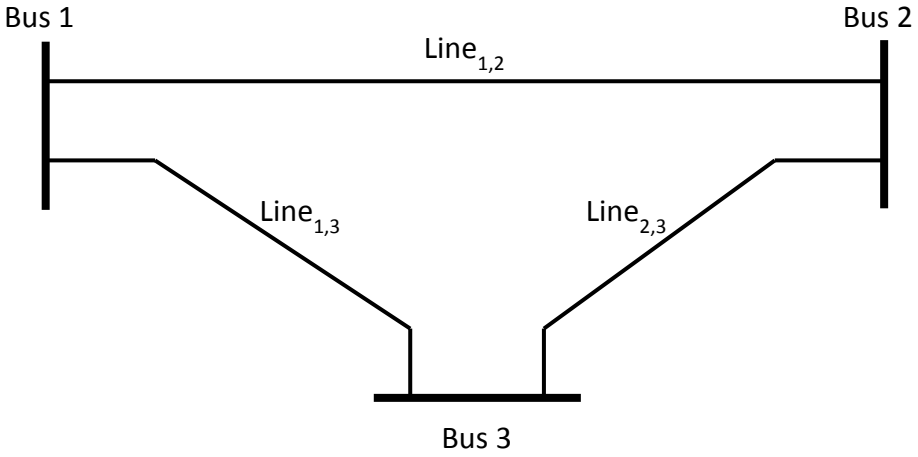

Figure 8: Simple 3 bus, 3 line network

Figure 8 shows a simple network with 3 buses and 3 lines with equal impedances. We can describe the flow along $line_{12}$ and $line_{23}$ due to the removal of $line_{13}$ with $LODF_{12,13}$ and $LODF_{23,13}$. We can see that the removal of $line_{13}$ would result in a transfer of all of the power that was flowing from bus_1 to bus_3 along $line_{13}$ to the path created by $line_{13}$ and $line_{23}$. Thus $LODF_{12,13}$ and $LODF_{23,13}$ are both equal to the fraction of the original, pre-switched $line_{13}$ flow that is now carried by the respective $line_{12}$ and $line_{23}$ ($LODF_{12,13} = LODF_{23,13} = 1$).

We further define Available Branch Capacity (*ABC*) as a simple measure of spare capacity on a transmission line. In equation (20), *ABC* describes the additional power flow each line can handle without reaching its thermal limit. Equation (21) scales ΔP_{ij}, by the Lagrange multipliers on the thermal flow limits of $line_{ij}$ (μ_{ij}). Since the μ_{ij} are only non-zero for $line_{ij}$ with a binding thermal flow limit constraint, ΔABC_{mn} represents metric of the congestion relieved by removing $line_{mn}$. The upside down triangle symbols in Figure 9 shows that three branches experience binding maximum flow constraints over the course of 24 periods.

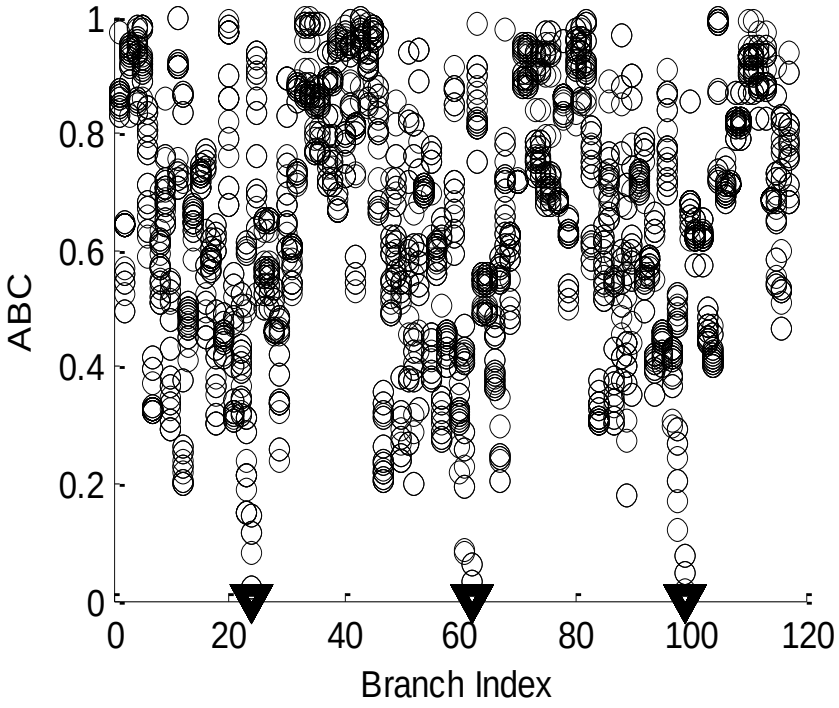

Figure 9: RTS-96 branch index vs. Available Branch Capacity for 24 periods (hours)

$$ABC_{ij} = 1 - \frac{P_{ij}}{P_{ij}^{max}} \quad (20)$$

$$\Delta ABC_{mn} = \sum_{ij} LODF_{ij,mn} \times \left(P_{mn}^{*}\mu_{ji} - P_{nm}^{*}\mu_{ji}\right) \quad (21)$$

Equation (21) serves as a ranking metric for considering switchable transmission lines. By limiting the switchable lines to those that, when switched, cause increases in ΔABC, and thus reductions in flow on congested lines, we can eliminate many of the switching variables from the topological optimization problem. For instance, Figure 10 shows that in hour 14, lines with indices 24, 62 and 99 connecting busses 114-116, 214-216 and 314-316 are congested.

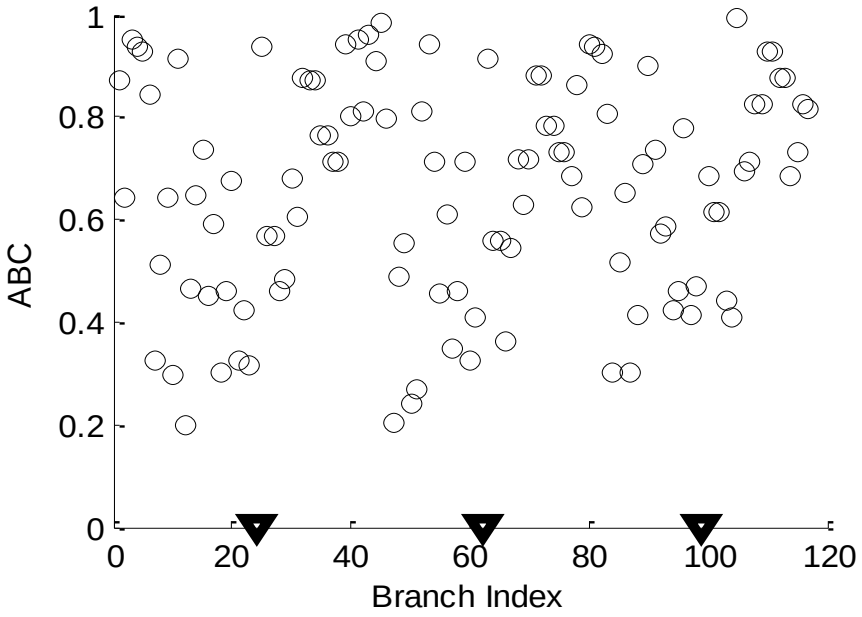

Figure 10: RTS-96 branch index vs. Available Branch Capacity for period (hour) 14

Figure 11 identifies the effect of switching each line in the system on the three congested lines. Note that if line *ij* is congested in the pre-switched case, then ΔABC is equal to one when that line is switched. Figure 11 shows that there exist relatively few lines where removal increases ΔABC for each congested line. This subset outlines the reduced set of decision variables for the OTS problem for hour 14 on the RTS-96 network. When compared with hour 14 in Table 5, removal of the two lines that exhibit significant marginal switching benefits generates increases in ΔABC on congested lines. In particular, switching line 109-111 increases the *ABC* of congested line 114-116 by 14% and switching line 309-311 increases the *ABC* of congested 314-316 by 13.9%

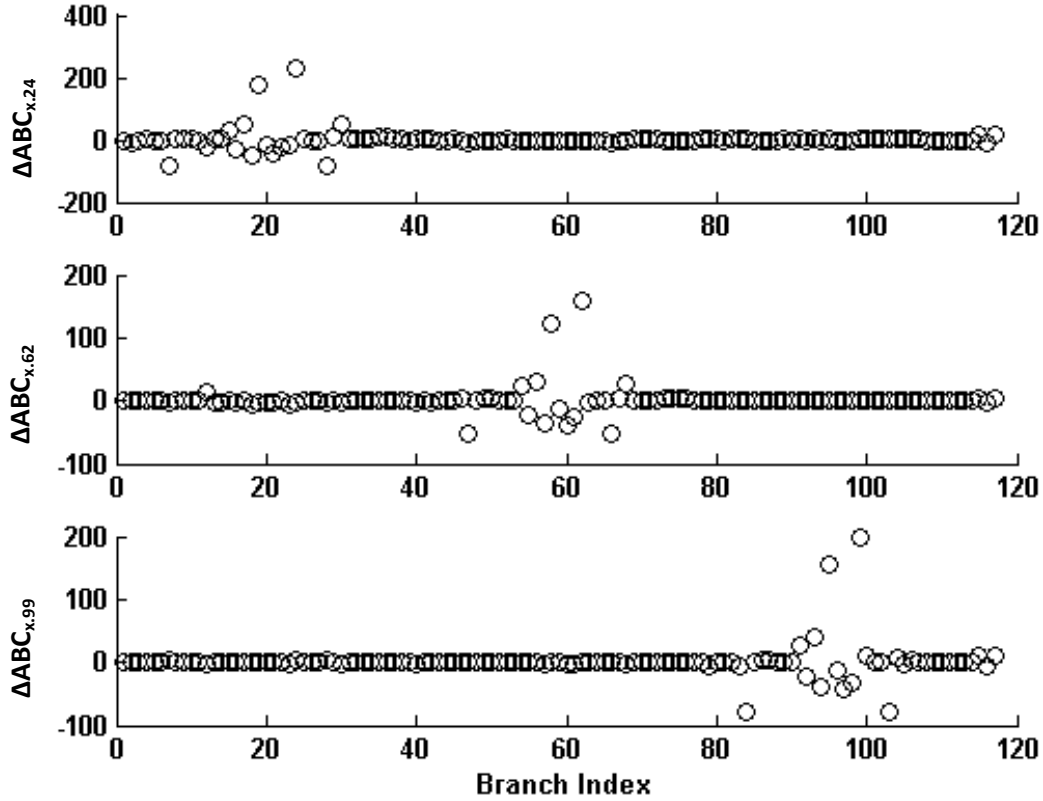

Figure 11: ΔABC on lines 24, 62 and 99 corresponding to a removal of line x for RTS-96 period (hour) 14

.

Table 6: Imputation/Refutation Map

Optimally Switched / Identified by Screen	Y	N
Y	True Imputation	False Imputation
N	False Refutation	True Refutation

Table 7: Probabilities of pre-screening success (lines with >0.5% marginal savings)

Optimally Switched / Identified by Screen	Y	N	Total
Y	37.8% (100%)	36.8% (0%)	1036
N	62.1%	63.2%	1772
Total	105	2703	2808

I define an "Imputation" as the event where the Δ*ABC* screen suggests that a line be eligible for switching. Likewise, I define a "Refutation" as the event where the Δ*ABC* screen suggests that a line not be eligible for switching. A True Imputation thus describes the event where the Δ*ABC* screen suggests that a line be eligible for switching, and the OTS algorithm also identifies that line to be switched. A True Refutation describes a similar event where both the Δ*ABC* screen and the OTS algorithm suggest that a line not be switched or eligible for switching. Similarly, I define False Imputation as the event where the Δ*ABC* screen identifies a line to be eligible for switching but is not switched in the OTS algorithm. Finally, a False Refutation describes the event where the Δ*ABC* screen suggests that a line not be eligible for switching but the OTS algorithm identifies that line to be switched. These events are summarized in Table 6, which shows the conditions that determine the imputation/refutation state based upon whether or not a line is actually switched by OTS and/or identified by the Δ*ABC* screen. Table 7 reports the occurrences of these events based on analysis of the RTS-96 network. This analysis of the RTS-96 test system has found that pre-screening based on *ΔABC* accurately identifies all lines whose

marginal contribution to system cost savings when switched is greater than 0.5% of pre-switched system cost (these lines are identified in Table 5). The "True Refutation" and "False Imputation" values for the lines with large savings contributions are not calculated, since we do not know if any lines with a large savings benefit were not identified by the OTS algorithm. Since [**52**] reports that the OTS problem has been solved to optimality on the RTS-96, the likelihood of the OTS algorithm failing to identify beneficial line switching is very low. Pre-screening based on ΔABC less accurately identifies lines with very small contributions to system cost savings (i.e., less than 0.5% of total system cost) from switching. When considering all optimally switched lines the pre-screen accurately identifies 37.8% and accurately rejects 63.2%. Table 7 shows that pre-screening based on ΔABC is a useful solution heuristic that will identify the lines that contribute most to cost savings as switchable. The solutions generated through implementation of this heuristic may not be optimal; however the results of Chapter 2 suggest that the majority of savings may be achieved through switching the lines identified here.

3.2 Transmission Switching Model

In order to test the ability of heuristic solution techniques to reduce solution times, an optimal transmission switching solver was created. By modeling the optimal transmission switching problem in a programming language interpretable by a commercially available optimization package, we can apply standardized optimization techniques to unique problem formulations. While there exist several commercially available optimization software options, each with their own set of advantages/disadvantages, the Comet Optimization Studio was chosen primarily for is clear modeling language and free distribution [**59**]. The economic generation dispatch – topological optimization problem presents a Mixed Integer Linear Programming problem when

modeled using the linearized DC power flow assumptions. The SCIP MIP solver contained in the Comet distribution is utilized to solve the MIP and LP problems.

The developed model has the capability to solve the economic generator dispatch problem under a variety of user specified parameters. The dispatch model can be selected from one of the following 3 options:

1. Optimal Power Flow

$$min \sum_{g} c_g P_g \tag{22}$$

s.t.

$$\theta_n^{min} \leq \theta_n \leq \theta_n^{max}, \qquad \forall\, n \text{ busses} \tag{23}$$

$$P_g^{min} \leq P_g \leq P_g^{max}, \qquad \forall\, g \text{ generators} \tag{24}$$

$$P_k^{min} \leq P_k \leq P_k^{max}, \qquad \forall\, k \text{ lines} \tag{25}$$

$$\sum_{i=n} P_{k_{ij}} - \sum_{j=n} P_{k_{ij}} - \sum_{g} P_{ng} - \sum_{d} P_{nd} = 0, \forall\, n \tag{26}$$

$$B_k(\theta_n - \theta_m) - P_k = 0, \qquad \forall\, k \text{ lines} \tag{27}$$

2. Unit Commitment

$$min \sum_{t} \sum_{g} c_g P_{g,t} + c_g^{up} g c_{g,t}^{up} + c_g^{dn} g c_{g,t}^{dn} \tag{28}$$

s.t.

$$\theta_n^{min} \leq \theta_{n,t} \leq \theta_n^{max}, \qquad \forall\, n \text{ busses}, t \text{ periods} \tag{29}$$

$$P_g^{min} u_{g,t} \leq P_{g,t} \leq P_g^{max} u_{g,t}, \qquad \forall\, g \text{ generators}, t \text{ periods} \tag{30}$$

$$P_k^{min} \leq P_{k,t} \leq P_k^{max}, \qquad \forall\, k \text{ lines}, t \text{ periods} \tag{31}$$

$$\sum_{i=n} P_{k_{ij},t} - \sum_{j=n} P_{k_{ij},t} - \sum_{g} P_{ng,t} - \sum_{d} P_{nd,t} = 0, \forall\, n, t \tag{32}$$

$$B_k\left(\theta_{n,t} - \theta_{m,t}\right) - P_{k,t} = 0, \qquad \forall\, k \text{ lines}, t \text{ periods} \tag{33}$$

$$u_{g,t} - u_{g,t-1} = gc_{g,t}^{up} - gc_{g,t}^{dn}, \qquad \forall\, g \text{ generators}, t \text{ periods} > 1 \tag{34}$$

$$gc_{g,t}^{up} \leq u_{g,t}, \qquad \forall\, g \text{ generators}, t \text{ periods} \tag{35}$$

$$gc_{g,t}^{dn} \leq 1 - u_{g,t}, \qquad \forall\, g \text{ generators}, t \text{ periods} \tag{36}$$

$$u_{g,t} \in \{0,1\}, \qquad \forall\, g \text{ generators}, t \text{ periods} \tag{37}$$

3. Optimal Transmission Switching

$$min \sum_{g} c_g P_g \tag{38}$$

s.t.

$$\theta_n^{min} \leq \theta_n \leq \theta_n^{max}, \qquad \forall\, n \text{ busses} \tag{39}$$

$$P_g^{min} \leq P_g \leq P_g^{max}, \qquad \forall\, g \text{ generators} \tag{40}$$

$$P_k^{min} \leq P_k \leq P_k^{max}, \qquad \forall\, k \text{ lines} \tag{41}$$

$$\sum_{i=n} P_{k_{ij}} - \sum_{j=n} P_{k_{ij}} - \sum_{g} P_{ng} - \sum_{d} P_{nd} = 0, \forall\, n \tag{42}$$

$$P_k^{min} z_k \leq P_k \leq P_k^{max} z_k, \qquad \forall\, k \tag{43}$$

$$B_k(\theta_n - \theta_m) - P_k + (1 - z_k)M_k \geq 0, \qquad \forall\, k \tag{44}$$

$$B_k(\theta_n - \theta_m) - P_k - (1 - z_k)M_k \leq 0, \qquad \forall\, k \tag{45}$$

$$z_k \in \{0,1\}, \qquad \forall\, k \tag{46}$$

The Unit Commitment model is a multi-period dynamic programming model that has the ability to consider integer generation unit commitment variables and corresponding generator startup and shutdown costs. The OTS model is a single period model that considers integer branch switching and linear generator dispatch variables. The OTS model utilizes the Big M method to enhance the optimization routines ability to find an initial feasible solution [**60**]. The

user specified value of the M_k*'s* in Equations (44) and (45) must be sufficiently large so that when $line_k$ is removed from service (z_k=0) the power flow between bus_n and bus_m is no longer constrained to the power flow rating of $line_k$. Since B_k and P_k are constants in Equations (44) and (45), the value for M_k must be at least as large as $B_k(\theta_{max}-\theta_{min})$. Although bus voltage angle limits (θ_{max}, θ_{min}) are not explicitly necessary for power flow optimization problems, they provide useful constraints for selecting M_k*'s*. Additionally, tightening bus voltage angle constraints limits the feasible search space for the optimization problem and enhances tractability. Thus, the user must carefully select θ_{max} and θ_{min} values large enough to allow transmission line power flows to vary within path ratings but small enough to provide tractability improvements. For simulations on the RTS-96 network, the bus voltage angles are constrained to: -0.9 rad $\leq \theta \leq$ 0.9 rad.

Each model has the option to include security constraints. A user specified contingency vector indicates each of the transmission and generation elements considered in the security constraints. For each transmission or generation element included in the contingency vector, the model posts a copy of the system constraints with that element removed. Thus, for a complete N-1 secure dispatch, the model posts N^2 constraints for the optimization. The additional constraints typically increase the problem complexity. A primal feasible solution to the complete N-1 secure model is a solution where the system will remain within operating constraints with any single in-service branch or any committed generator removed from service. In the case where a committed generator is removed from service, the system requires a generation re-dispatch. The N-1 security ensures that the generation re-dispatch is handled only from committed generators and the resulting power flow satisfies all other system constraints.

3.3 Switchable Line Screening Heuristic Application

The offline screening method developed in Section 3.1 is applied before the system is submitted to the Optimal Transmission Switching routine. However, nominal un-switched or pre-OTS system state is a necessary input to the screening method. Therefore, a power flow solution for the operating state of interest must be obtained prior to screening for switchable lines. The process diagram in Figure 12 shows the steps and corresponding data required to obtain an optimally switched power system. The application environment in which each process was implemented is highlighted (Blue for Comet and Red for MATLAB).

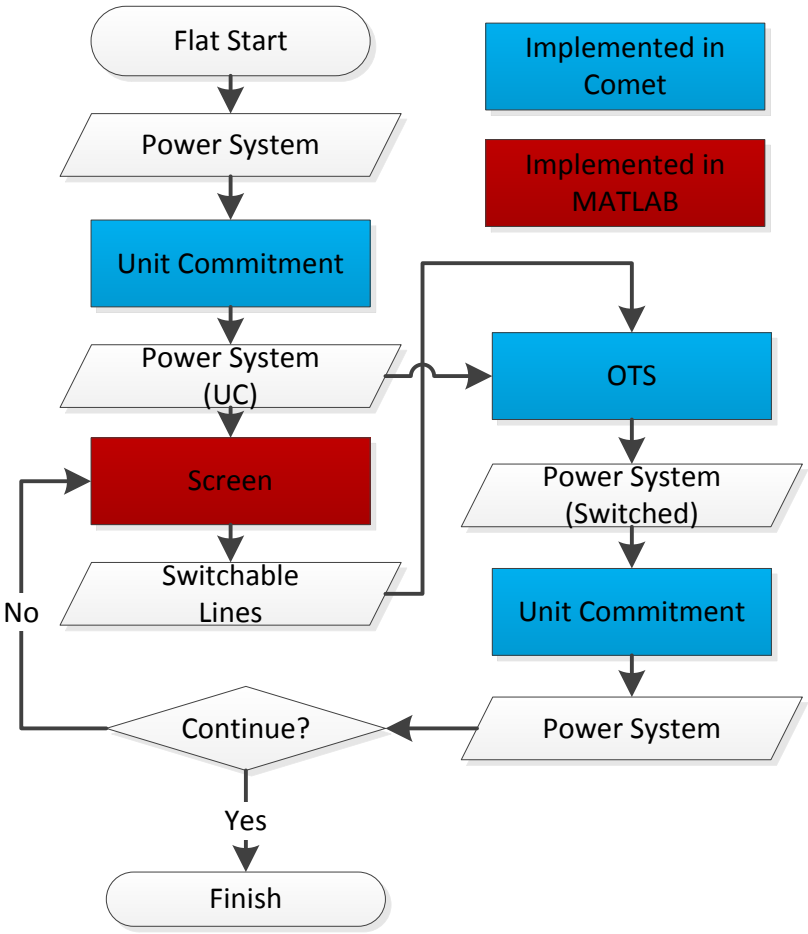

Figure 12: Process diagram for obtaining screened Optimal Transmission Switching solutions

Application of the ΔABC screen generates a set $S_{ABC,t}$ of switchable lines for each period, t. The number of switchable lines identified by the ΔABC screen is denoted by η_t. The screening

technique where $S_{ABC,t}$ includes all switchable lines that reduce flow on congested lines is denoted "Inclusive Screening". To form a basis of comparison, we form same-sized switchable line sets by:

- Randomly selecting η_t lines by averaging 100 uniformly random permutations to form the set $S_{RAND,t}$;
- Ranking the line capacity to form the set, $S_{CAP,t}$ consisting of the η_t lines with the highest rated thermal flow capacity (RTS-96 only);
- Ranking the line reactance to form the set, $S_{REAC,t}$ containing the η_t lowest reactance lines;
- Ranking the branch betweenness centrality to form the set, $S_{CENT,t}$ containing the η_t highest centrality lines. Branch (line) centrality is defined as the sum of the fraction of shortest paths between any two nodes that pass through the branch:

$$c_B(b) = \sum_{i,j \in N} \frac{\sigma(i,j|b)}{\sigma(i,j)} \qquad (47)$$

  Where N is the set of nodes (buses), $\sigma(i,j)$ is the number of shortest paths between $node_i$ and $node_j$, and $\sigma(i,j|b)$ is the number of shortest paths between $node_i$ and $node_j$ passing through $branch_b$.

To further examine the effects of applying a switchable line limiting heuristic to the OTS problem we rank lines according to each metric described above. The line rankings enable a "Progressive Screening" analysis where the transmission switching problem is solved with a progressively larger switchable set. The switchable set of transmission lines starts with the highest ranked line (according to the above ranking metrics). After solving the OTS problem with a single switchable line, the switchable set is increased to include the two highest ranked lines. The switchable set is iteratively appended to include lower ranked lines and screened OTS is solved at each iteration.

3.3.1 RTS-96 Inclusive Screening Results

The methods of [**52**] are used to solve the 24-hour unit commitment problem for the summer weekday RTS-96 load cases without transmission switching. The same system modifications described in Chapter 2 and reported in Appendix C.1 are utilized to introduce congestion to the 24 summer weekday load periods of the RTS-96. The OTS MIP is then applied to the 24 fixed unit commitment solutions. We enforce the same limits on the bus voltage angle ($\theta_{min/max}$= $\pm 0.6 rad$) and choose the same big M value ($M_k = 1.2|B_k|$) as [**52**]. Generator costs are modeled as linear functions between the minimum and maximum outputs reported in [**57**] and the assumed fuel costs shown in Table 1.

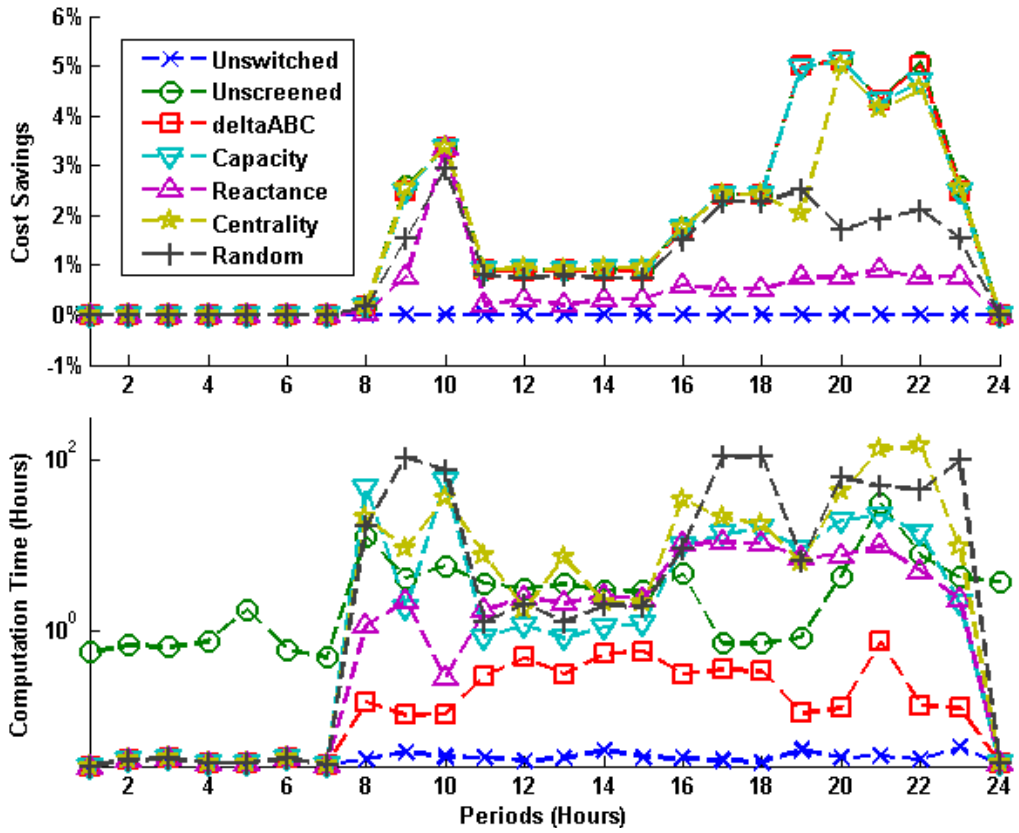

Figure 13: Inclusive screen switching results for each of the 24 load periods in the RTS-96 network. The system cost savings over the DCOPF solution (top) and computation time (bottom) is displayed for the following solution techniques: un-switched DCOPF, unscreened OTS, and ΔABC, line capacity, line reactance, line centrality, and random line screened switching

The savings generated by the six transmission switching screening methods are shown in the top panel of Figure 13. Cost savings are calculated as the system cost reduction over the un-switched DCOPF for load period *t.*

$$Savings_t\% = \left(C_{DCOPF,t} - C^*_{switched,t}\right)/C_{DCOPF,t} * 100 \qquad (48)$$

The bottom panel of Figure 13 shows the solution time in hours. For periods {1-7, 24}, $\eta_t=0$, that is, the *ΔABC* screen identified no lines to be added to the switchable set. Thus, the screened switching problems are equivalent to the DCOPF (without transmission switching) for the periods where $\eta_t=0$. The total 24-hour solution time for the un-screened OTS problem was 103.91 hours. Table 8 reports the system cost savings and computation time for each of the solution methods; Unit Commitment (UC, no-switching), Optimal Transmission Switching (OTS, no-screening), and screened OTS where lines are screened based on *ΔABC*, capacity, reactance, branch centrality and random inclusion. These results provide evidence that *ΔABC* screen can achieve high quality results quickly. The capacity screen is also able to achieve very good results, but requires substantially more computation time.

Table 8: 24 Hour RTS-96 Screening Method Performance

	UC	**OTS**	**Δ*ABC***	**Capacity**	**Reactance**	**Centrality**	**Random**
Savings (%)	0	0.36	0.35	0.34	0.1	0.32	0.22
Comp Time (hours)	3.7	104	4.97	220	81	495	695

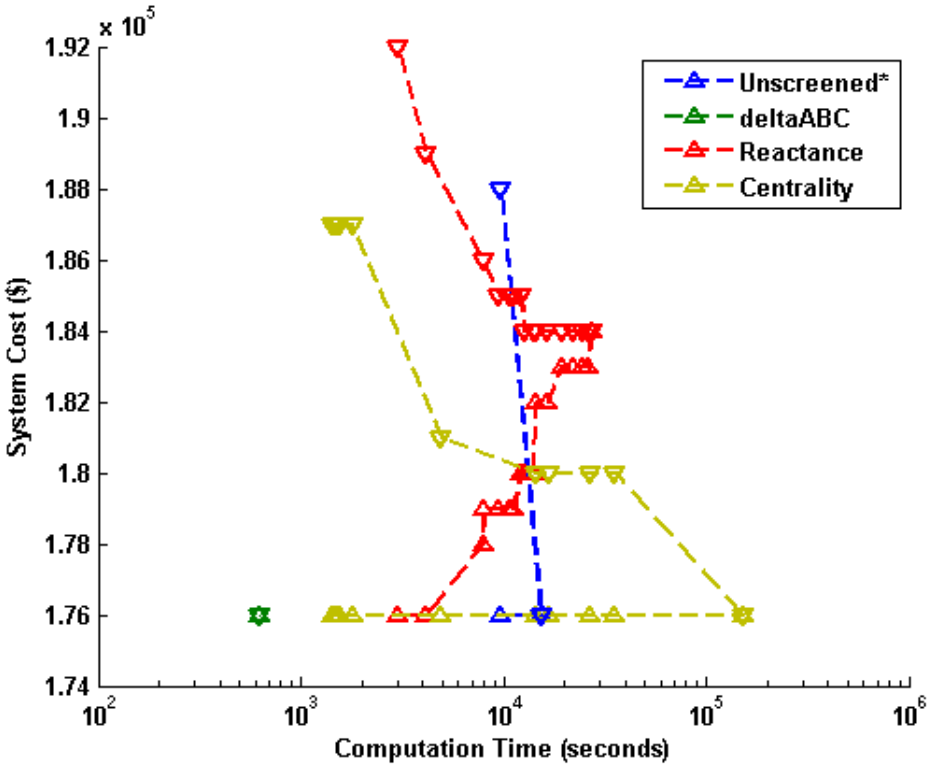

Figure 14: Fig. 5. Primal (▼) and Dual (▲) OTS objective function values for the ΔABC, reactance and centrality screens in the RTS-96 hour 20 network.

3.3.2 Progressive Screening Results on the RTS-96 Network

The marginal switching analysis in [8] found that most of the cost-reduction benefits could be achieved by switching a relatively small number of lines. To further examine this finding with our proposed screening tool, we progressively increased η_{14} and η_{20} to consider up to 50 switchable lines and solved the screened OTS problems on hours 14 and 20 in the RTS-96 test system. The hour 14 results are shown in Figure 15 and Figure 16 shows the hour 20 results

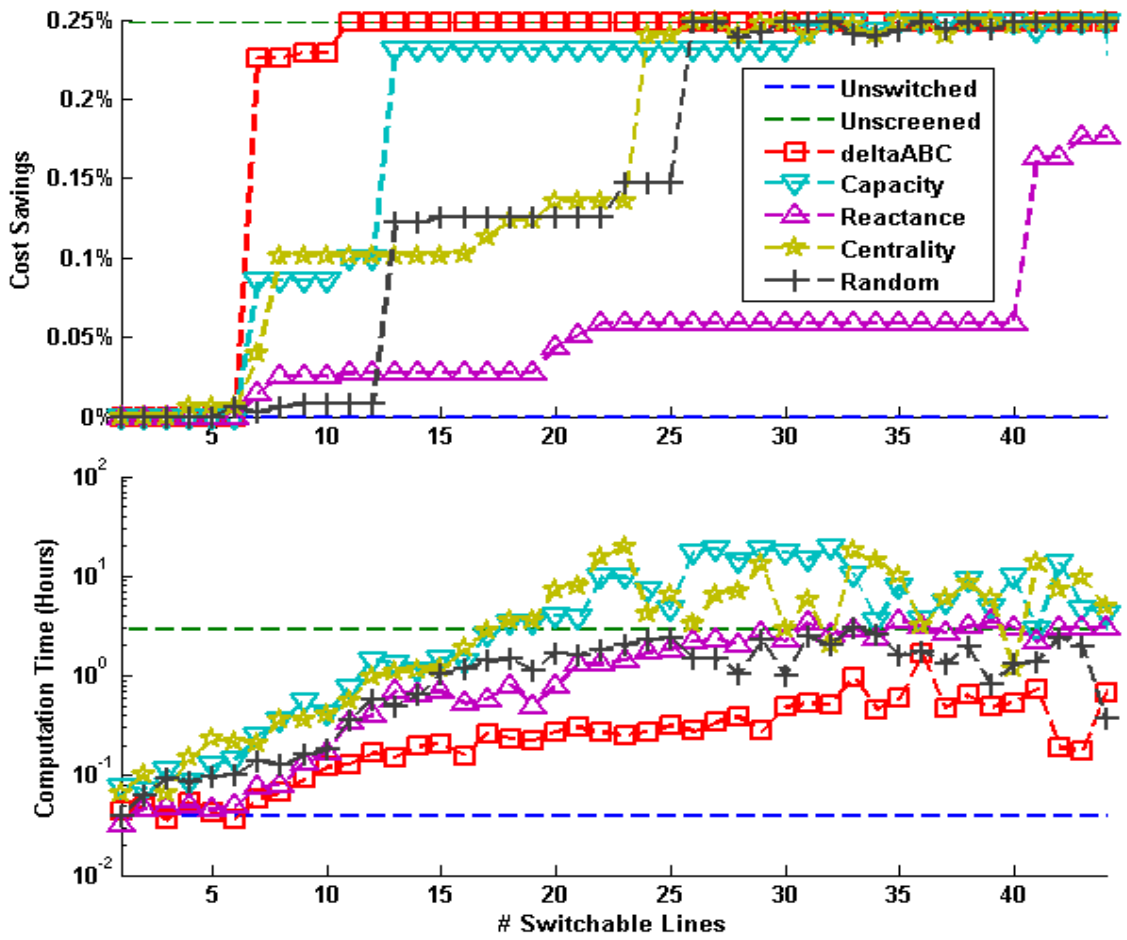

Figure 15: System cost savings (top) and computation time(bottom) considering 1-50 switchable lines for each of the *ΔABC*, capacity, reactance, centrality and random screens in the RTS-96 hour 14. The lower and upper cost savings bounds are shownl with lines representing the no-switching (0% savings) and OTS (Unscreened) solutions.

Figure 15 shows that with only 7 candidate switchable lines considered in hour 14, the ΔABC screened problem takes only 3.46 minutes to generate a solution with 0.226% cost reduction over the un-switched case (90% of optimal savings). In comparison, the optimal solution generated by OTS takes 2.9 hours and yields a 0.248% cost reduction.

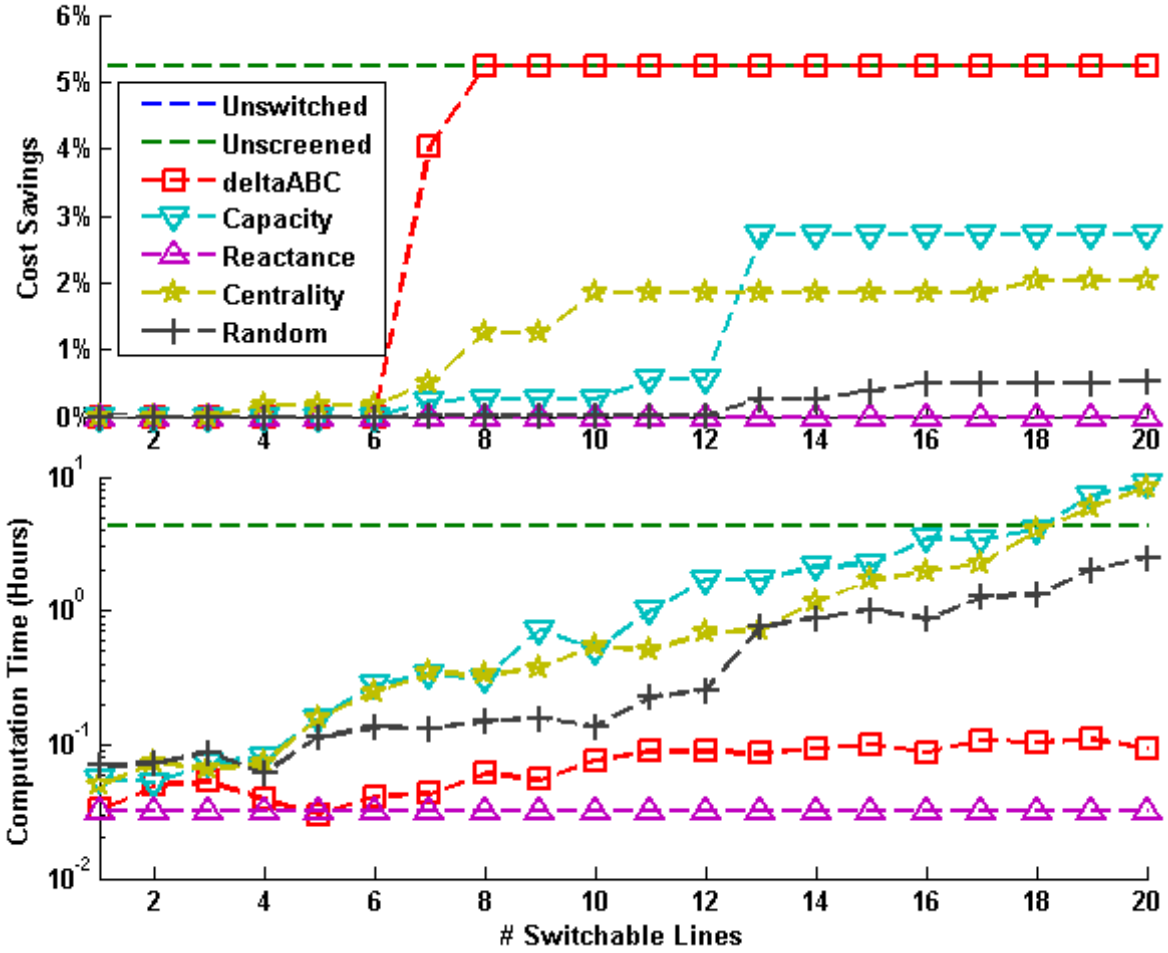

Figure 16: System cost savings (top) and computation time (bottom) considering 1-20 switchable lines for each of the *ΔABC*, capacity, reactance, centrality and random screening techniques in the RTS-96 hour 20. The lower and upper cost savings bounds are shown in the top panel with lines representing the no-switching (0% savings) and OTS (Unscreened) solutions. The computation time for OTS in hour 20 is 4.3hours

Figure 16 shows that with 7 and 8 candidate switchable lines, the Δ*ABC* screened switching problem yields 4% and 5.2% savings, respectively. The un-screened OTS problem also yields an optimal savings of 5.2%. However, the un-screened OTS problem takes 4.3 hours to converge, while the Δ*ABC* with 8 switchable lines generates the optimal savings in 3.6 minutes.

3.3.3 Progressive Switching on the IEEE 118-Bus Test Network

OTS and the screened OTS techniques described earlier are applied to a constrained version of the IEEE 118-Bus test network. The IEEE 118-Bus test network in its published form has no

transmission line flow ratings and therefore is un-congested in the DC model [**61**]. To create some congestion in the network, transmission line flow limits were added according to Appendix A in reference [**3**]. The complete system data as used in the analysis in this document is available in Appendix C. The un-switched DCOPF results have binding thermal power flow constraints on two transmission lines. Since the IEEE 118-Bus network is not N-1 secure, we consider a complete N-1 transmission and generation contingency model with the exception of 11 transmission lines and 4 generators which are critical to the reliable operation of the network. The 11 critical transmission lines removed from the N-1 contingency analysis are those that connect buses: 77-82, 82-83, 83-85, 85-86, 85-88, 85-89, 88-89, 89-90, 89-92, 90-91, and 91-92. The four critical generators are those connected at buses: 69, 80, 87, and 100.

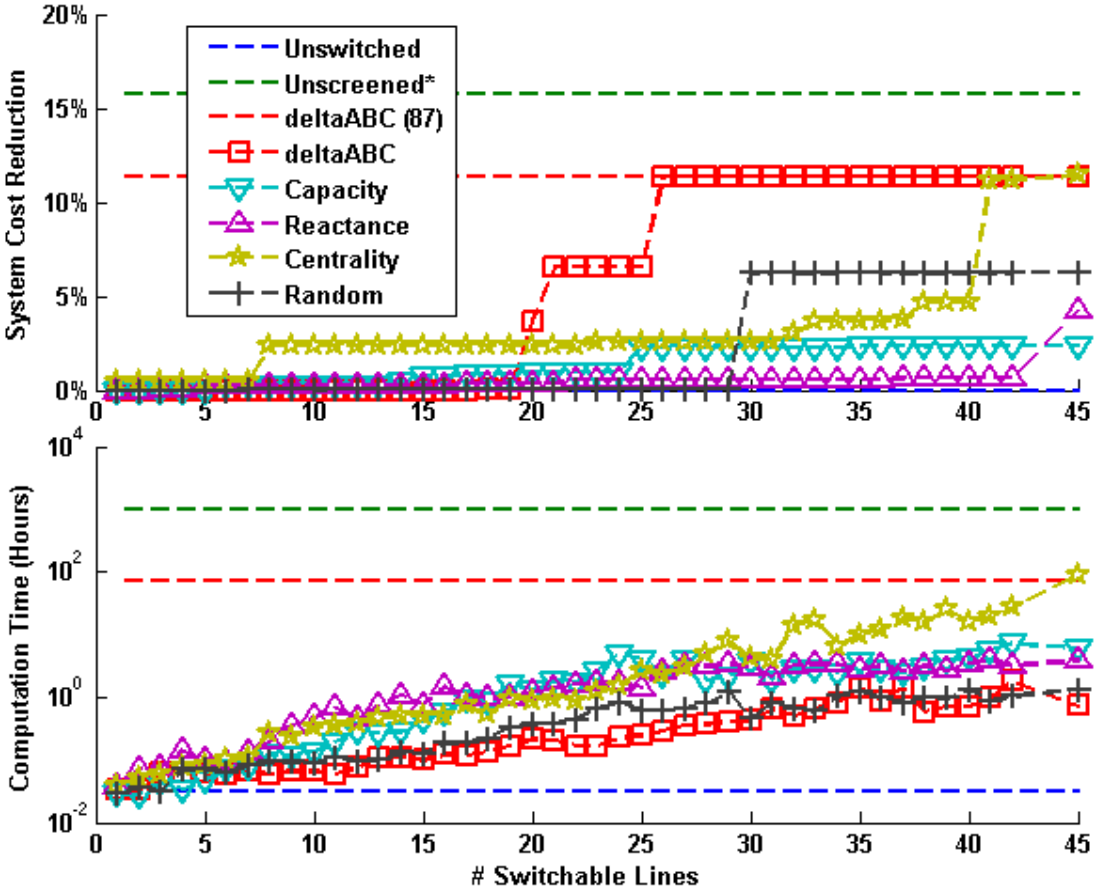

Figure 17: System cost savings (top) and computation time (bottom) considering 1-45 switchable lines for each of the *ΔABC*, capacity, reactance, centrality and random screening techniques in the IEEE 118-bus network. The dashed red lines for "*ΔABC* (87)" represent the cost and time for the case that considers the maximal switching set identified by the *ΔABC* screen. The dashed green lines identify the unscreened OTS problem status after 1000 computation hours.

Figure 17 shows the screened OTS results on the IEEE 118-Bus network. Again, the Δ*ABC* screen outperforms all other screening techniques. After 1000 hours of computation, the un-screened OTS did not converge to optimality. After 115 hours the un-screened OTS problem had generated 15.8% savings with an optimality gap of 20%. For comparison, Figure 17 shows the results of including 87 switchable transmission lines (chosen by Δ*ABC* screening) in the OTS problem. The 87 line Δ*ABC* produced 11.3% savings in 70.4 hours. Figure 18 shows that by identifying 27 switchable lines using the Δ*ABC* screening technique, the solver finds a feasible

solution and converges to optimality in roughly 20 minutes, much quicker than when other screening techniques are employed.

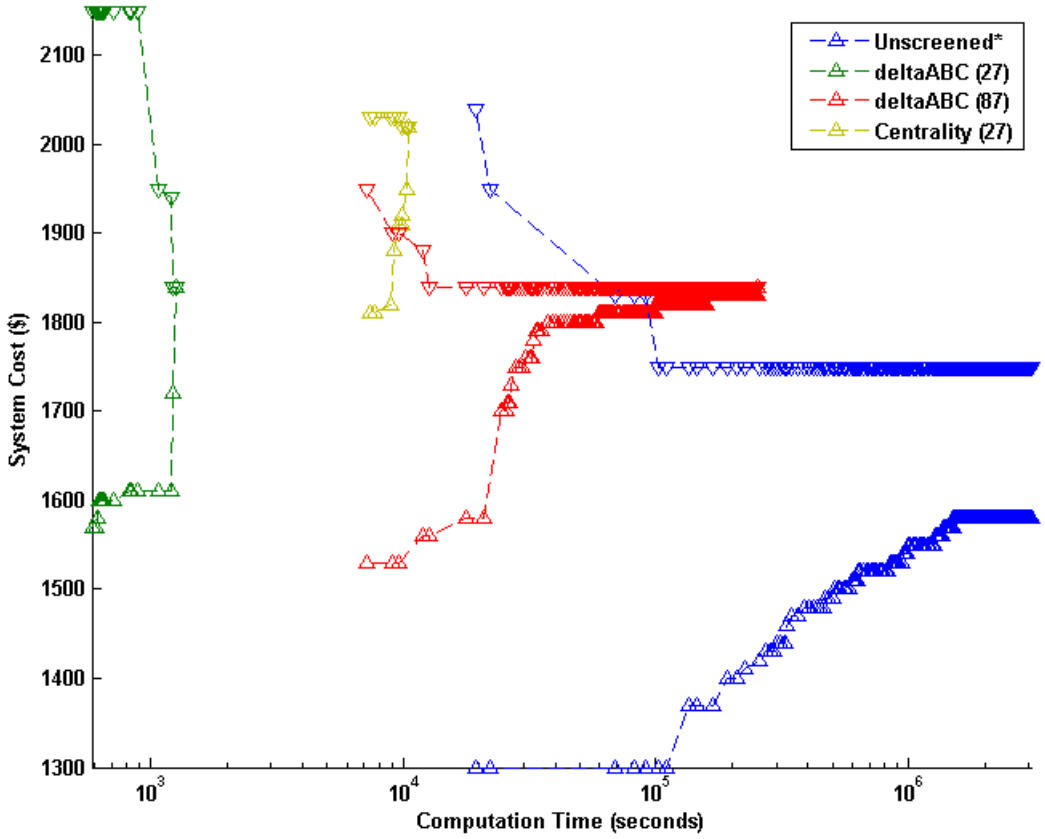

Figure 18: Primal (▼) and Dual (▲) OTS objective function values for the *ΔABC* screen including 27 and 87 switchable lines, and the 27 line centrality screen in the IEEE 118-bus network.

3.4 Screened Switching Conclusions

The results of previous research in Optimal Transmission Switching [**52**] have been analyzed to support the development of heuristics (search space reduction techniques) to facilitate faster solutions to the OTS problem [**62**]. Faster solution techniques will enable electrical networks to become more adaptive as smart-grid communication and control systems are rolled out. In particular, the marginal analysis of Chapter 2 suggested a search space reduction method for faster solving of the transmission switching problem. The observation that switching relatively

few lines has a significant contribution to the savings generated by OTS suggests that a screening rule to limit the number of lines considered for transmission switching may be applied.

A screen is developed for candidate switchable lines based on a network's sensitivity, the Line Outage Distribution Factor (LODF). The LODF is employed to identify lines that, when switched, increase the available branch capacity of constrained transmission lines. This screen (ΔABC screen) successfully identifies 100% of the lines that reduce system costs by at least 0.05% in RTS-96 OTS simulations (relative to pre-switched costs). Application of the ΔABC screen to the transmission switching problem yields near optimal results in significantly less computational time. Analysis of the RTS-96 hour 14 and hour 20 results in suggest that further solution time reductions may be achieved without significantly sacrificing cost reductions by reducing the number of lines selected by the ΔABC screen.

As presented here, the ΔABC screening rule requires that congestion relief depend primarily on the switching actions of only one line. That is, switching only one line is required to increase *ABC* on a constrained line. The ΔABC screen does not identify the cases where switching two or more lines is required to relieve congestion. The results presented here suggest, however, that the majority of OTS savings can be produced by switching single lines to relieve a particular transmission congestion. The significant reduction in solution times associated with switching only lines highlighted in the ΔABC screen vs. considering all lines for switching, suggests that ΔABC screening represents a promising approach to improving the tractability of the OTS problem. It is noted that an extension to the presented ΔABC screening rule is required to consider the effects of removing multiple lines simultaneously. A sensitivity analysis of the increased computational burden versus the improved optimality of results is required to

determine the value of screening for simultaneously switched lines that relieve transmission constraints.

The analysis and results of this research have, thus far, been limited to applications on the RTS-96 and IEEE 118-Bus networks using DC approximations. Thus, empirical conclusions presented here are limited to these benchmark networks under the assumptions relevant for the DC approximation. Research presented in Chapter 4 and Chapter 5 applies the developed heuristics to transmission switching on larger test systems as well as real system models. This approach will be critical for scaling OTS algorithms to larger problems that are currently computationally intractable. The analysis presented here focuses on an economic transmission topology optimization considering a full set of N-1 transmission and generation constraints. Other AC reliability constraints, such as voltage stability and reactive power are problems that are addressed in Chapter 5 to validate the potential of transmission switching to improve utilization of transmission assets and increase system performance.

Chapter 4 Partitioned Transmission Switching

The results of the marginal switching analysis in Chapter 2 suggest that the effects of transmission switching are separately additive and can be relatively localized within properly defined area boundaries. This observation suggests that network decomposition may enable parallelization of the OTS problem to obtain solutions on distinct sub-networks without degrading cost savings performance. The stochastic nature of power system operations and planning procedures often require multiple simulations for each decision period. Since, in their worst case, optimal power flow (OPF) problem complexities scale exponentially with system size, simulations can be extremely computationally expensive on large power systems [**63**]. Therefore, it is common to partition power networks so that simulations can be run in parallel on the subsystems of interest while the remainder of the network is represented by a reduced equivalent. Partitioning (or clustering) of data has a variety of applications in statistics and artificial neural networks (ANN's) [**64**,**65**]. Network partitions, often referred to as zones or areas, have traditionally been made along arbitrary geographic or asset ownership boundaries. The optimality of zonal power system calculations can depend on zonal definitions. This Chapter presents a network partitioning method that produces electrically cohesive power system zones and thus improves the performance of network reductions for many zonal power system calculations. The presented method is used to decompose the OTS problem into sub-problems that can be solved and then aggregated to form near optimal total-system solutions.

Optimal vehicle routing problems have been solved on partitioned transportation networks to reduce the computational burden [**66**]. The division of electrical networks into zones or clusters has a long history; Kron [**67**] and Happ [**68**,**69**] pioneered the study of diakoptics, or "tearing" to reduce the computational requirements for analyzing large-scale systems. Network clustering has been proposed to assess voltage security and define control areas for reactive power markets

[**70**,**71**]. The adaptation of existing clustering methods to power systems analysis problems is described in [**72**,**73**]. Kamwa et al. [**74**,**75**] have utilized clustering methods to evaluate the dynamic vulnerability of real-sized systems (Hydro-Québec). Many of the studies regarding power system partitioning are based either on the slow coherency approach [**76**] or disturbance simulation approaches [**77**,**74**]. The goal of this section is thus to develop methods for identifying zones that cluster together electrically similar busses. That is, electrical changes originating from within a zone should primarily affect busses inside the zone relative to those busses outside the zone. A secondary requirement of the partitioning method is to generate zones using only the electrical properties of the network, rather than the operating state, to avoid the need to simulate a priori different contingency scenarios. This Chapter develops a partitioning method based on a measure of electrical distance and applies the transmission switching problem to the partitioned networks[2].

4.1 Electrical Distance and Electrically Cohesive Clusters

In order to partition the network so that the inter-partition effects are minimized, we need to understand the structure of the electrical network. Representation of the structure of a power grid as a graph requires both its topological structure (node-edge connectivity) and its electrical structure (which represents the influence of Kirchhoff's Laws). To understand the electrical structure of a power grid we need a measure of electrical connectedness (or conversely distance). While electrical distance has been used in a number of power systems problems [**70**,**71**,**78**,**79**], the concept has not been used extensively in the context of structural network analysis.

[2] The partitioning methods developed in 4.1 and 4.2 have been submitted for publication in IEEE Transactions on Power Systems [**126**]

Reference [**78**] showed that the logarithmic voltage magnitude sensitivity in a power grid can qualify as a distance metric, under some conditions. In Appendix B, a distance metric based on the relationship between electric power transactions that occur in a power grid is developed.

$$e(a,b) = B_{a,a}^{-1} + B_{b,b}^{-1} - B_{b,a}^{-1} - B_{a,b}^{-1} \quad (49)$$

Where B^{-1} is the inverse of the node to node susceptance matrix, the electrical distance metric is defined for a linearized system by Equation (49). $e(a,b)$ represents the electrical distance between $node_a$ and $node_b$ and is dependent upon the elements corresponding to the a^{th} and b^{th} rows and columns of B^{-1}. Electrical distance is closely related to the voltage phase-angle differences between nodes in the grid, which is a common measure of stress in power systems [**80**]. While other measures of electrical distance exist (see, for example [**79**,**78**,**70**,**71**,**81**,**82**], some of which are also based on equivalent impedance), this measure of distance is useful because it approximates the extent to which changes in real power injections will result in voltage phase angle changes, which are of particular interest for applications requiring the calculation of real power flows. By assuming that voltages are 1.0 p.u. and that voltage phase angle differences θ_{ab} are small, the distance measure is independent of operating state. Operating state independence is an important feature for an electrical distance measure that will be utilized for calculations in future, unknown operating states.

From electrical distance (where E is the matrix of all distances and e_{ij} is the distance between buses i and j) it is possible to measure the total electrical distance within a cluster, and the strength of the connections between clusters. Equation (50) measures the total electrical distance within clusters for a clustering solution C, that divides the network into p clusters:

$$\hat{e}(C) = \sum_{i=1}^{n} \sum_{j \in M_i} e_{ij} \qquad (50)$$

where M_i is the set of nodes that are in the same cluster as node i, and n is the number of buses in the system. The clustering distance measure ranges between zero, when all nodes are in separate clusters (a completely atomistic clustering), and the sum $\sum_i \sum_j e_{ij}$ when all nodes are in a single, fully connected, cluster. High-quality clusters will have lower electrical distances between nodes in each cluster (and thus high intra-cluster cohesiveness).

Equation (50) incorporates the within-cluster distances for a clustering solution, but does not consider the connections across zonal boundaries. If a cluster boundary cuts through a low-impedance connection, such as a very short transmission line or a transformer, the effect on E would be insignificant. Equation (51) provides a measure of the connection strengths across cluster boundaries.

$$h(C) = \sum_{i=1}^{n} \sum_{j \notin M_i} \frac{1}{e_{ij}} \qquad (51)$$

The use of the inverse distance ($1/e_{ij}$) increases the contribution of low-impedance connections to h. Note that this measure is similar to the graph "efficiency" measures proposed in [**83**] and adapted for power grids in [**82**].

4.2 Clustering Results

This section presents the results of electrical distance clustering on two test power systems. Spectral, K-Means and Genetic Algorithm (GA) clustering methods (presented in Appendix B) are employed to partition power systems. The results show that clustering on electrical distance can generate partitions that are electrically cohesive and thus suitable for topological optimization calculations.

4.2.1 Electrical distance clustering results in reduced loop flows

A common use for zonal analysis in power system planning and operations is for monitoring transactions between locations. In transmission planning applications, for example, it is desirable that intra-zonal transactions do not significantly affect currents, voltages or power flows outside of the zone. Similarly, for applications of reducing the complexity of transmission switching problems, it is desired to limit the effects (changes in currents, voltages and power flows) of transmission switching outside of the zone. In this section the measures of clustering quality that are presented in Appendix B.2 are used to test the hypothesis that when zones are designed to have higher connectedness and cohesiveness while controlling for the number and size of clusters, the intra-zonal real power injections result in less power flow changes on branches outside of the zone. That is, clustering to achieve higher Between Cluster Connectedness Index (BCCI) and Electrical Cohesiveness Index (ECI) scores, while controlling for the Cluster Count Index (CCI) and the Cluster Size Index (CSI), limits the occurrence of loop flows. To measure this, (52) provides a measure of "transaction leakage" for zone z, which includes buses in the set M_z:

$$T_z = \sum_{\forall i,j \in M} \sum_{a,b \notin M_z} |I_{ab}(0) - I_{ab}(i \to j)| \qquad (52)$$

where $I_{ab}(0)$ is the current magnitude on the branch between Nodes a and b, and I_{ab} $(i \to j)$ is the current on the same branch after adding an additional 1 MW of demand at Bus j and allowing a "slack bus" at Bus i to meet this additional demand. The calculated current magnitudes result from a standard Newton-Raphson AC power flow calculation. T_z is divided by the change in branch currents on all branches (not just those outside of M_z) to obtain a normalized measure of transaction leakage $\overline{T_z}$ which has the range [0,1]. The transaction leakage measures the amount

that currents, and thus real power flows, change outside of a zone, given transactions within the zone. Transaction leakage is generally referred to as "loop flow".

The concept of transaction leakage is well suited to measure the extent to which the effects of transmission switching actions are localized. The removal of transmission elements from service is akin to the power injection/removal described in the transaction leakage calculation above where the magnitude of the power injection/removal is equal to the negative of the pre-switching real power flow along $line_{ij}$. With this slight modification, the result of the transaction leakage calculations would measure the change in current magnitude along $line_{mn}$ due to the removal of $line_{ij}$. By partitioning the network such that inter-zonal transaction leakages are minimized, we can minimize the inter-zonal effects of transmission switching and examine the zonal transmission switching problems independently.

4.2.1.A IEEE-RTS-96 Test Network

To illustrate how the use of the electrical distance clustering method could reduce the complexity of the transmission switching problem, the IEEE-RTS-96 bus test case is partitioned into three zones. Each set of partitions is used to compare the quantity of transaction leakage to the product of ECI and BCCI (the portion of Eq. (123) that is explicitly based on electrical distance). This comparison is made for 100 randomly generated divisions of the IEEE-RTS-96 case into three zones (using the random centroid method) and solutions that resulted from the evolutionary algorithm. To avoid distortions that might result from unbalanced cluster sizes, only random solutions with a CSI score of 0.9 or higher are considered.

The results shown in Figure 19 indicate a strong ($\rho = -0.9418$) and statistically significant ($P < 10^{-5}$) negative correlation between $\mathrm{BCCI}\cdot\mathrm{ECI}$ and transaction leakage. Relative to the correlation between transaction leakage and the independent values of ECI and BCCI

($\rho(\overline{T}_z, ECI) = -0.8729, \rho(\overline{T}_z, BCCI) = -0.8886$), this is interpreted as strong evidence in support of the hypothesis that defining network partitions with high electrical cohesiveness limits the inter-zonal effects of transmission switching and enables the analysis of transmission switching on isolated sub-networks. Additionally, the solution achieved by spectral clustering and the GA clustering routine (Δ in Figure 19) yields identical clusters to those found by disturbance-based coherency [**74**] yet don't require state dependent simulations.

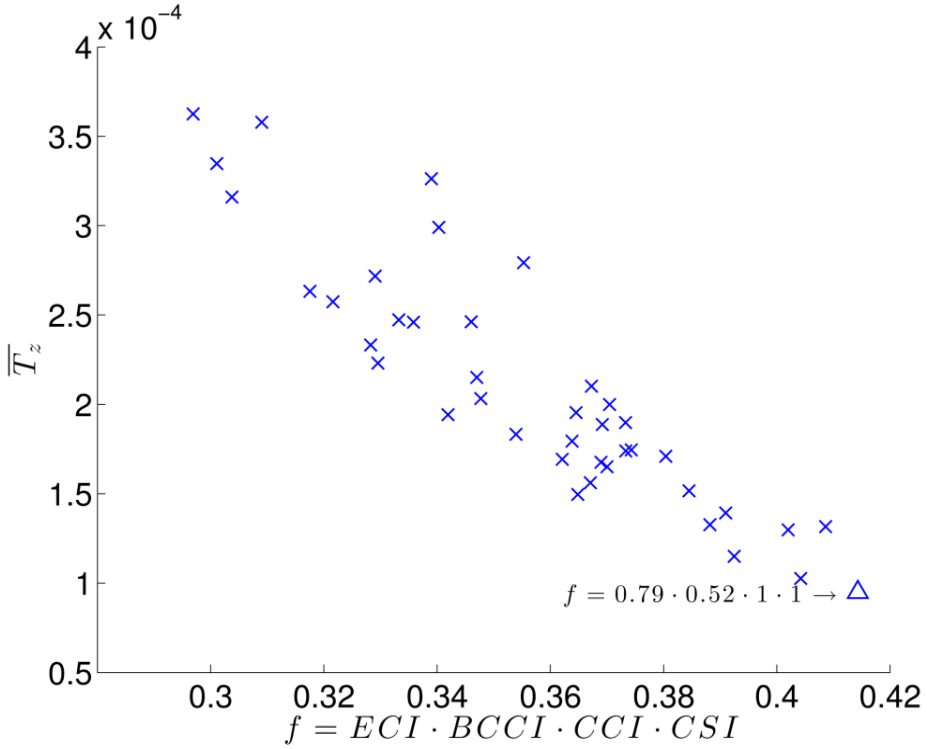

Figure 19: Scatter plot showing clustering quality and the amount of loop flow for random clustering solutions (X) and solutions generated by spectral clustering (Δ) for the IEEE RTS-96 network with 3 clusters.

4.2.1.B 2383-Bus Winter Peak Polish Network

The electric power infrastructure from Poland corresponding to the winter peak load profile is used as an example of an real power system [**84**]. The Polish power network is composed of 2383 buses, 2896 transmission lines and 327 generators. Figure 20 shows the transaction

leakage resulting from random, k-means and GA clustering solutions. The correlations between the transaction leakage and the BCCI, ECI and the product of ECI and BCCI are: $\rho(\overline{T_z}, BCCI) = -0.6295$, $\rho(\overline{T_z}, ECI) = -0.2383$, $\rho(\overline{T_z}, ECI \cdot BCCI) = -0.5543$. In this case, the correlations between transaction leakage and BCCI and BCCI*ECI were statistically significant with $P<10^{-5}$, and the correlation between transaction leakage and ECI was statistically significant with $P=0.036$.

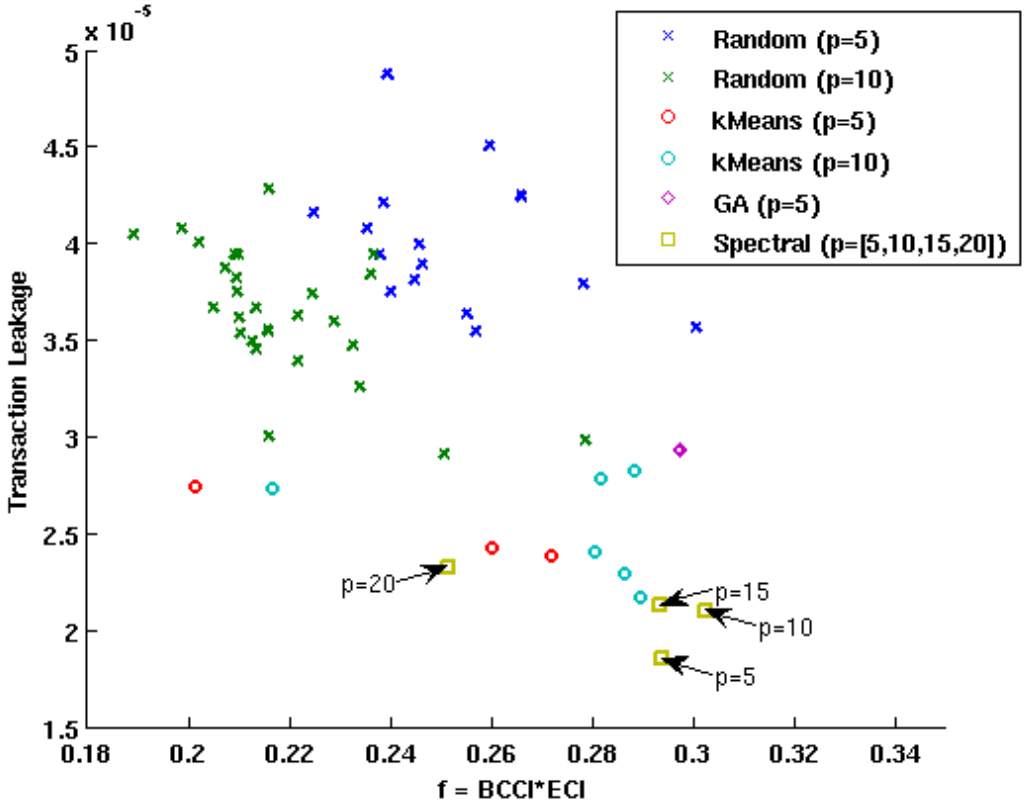

Figure 20: Where p represents the goal number of clusters, the scatter plot shows clustering quality (f) and the amount of loop flow (transaction leakage) for 42 random clustering solutions (X), 13 k-means solutions (○), a GA solution (◊) and 4 spectral clustering solutions (□) for the Polish power grid.

4.3 Partitioning for Transmission Switching

Electrical power systems can consist of tens of thousands of nodes and even more transmission lines. The physical properties of electrical networks and Kirchhoff's laws dictate that, by definition, changes in power injections/withdrawals at one node will affect the power

flows on every line in the network. However in practical terms, with a network that spans thousands of miles, the distant effects of power injections/withdrawals are often immeasurably small. Likewise, the results of Chapter 2 demonstrate that the effects of transmission switching are relatively localized. That is, congestion relief is primarily limited to lines that are relatively close to the switched line. This observation suggests that, for the purpose of transmission switching, the network may be decomposed so that the OTS problem may be solved on distinct sub networks. The benefits of this decomposition stem from the scaling of the feasible space to the number of switchable lines. If *n-lines* are considered switchable, the number of feasible network topologies is $2^{n\text{-}lines}$. Therefore, partitioning a network with n = 1000 lines into a 10 networks with 100 lines would decrease the number of feasible network topologies from about 10^{301} to about 10^{31}. The results of Chapter 2 suggest that this significant reduction in complexity would result in only minor reductions in the optimality of results. However, the quality of the results likely depends upon the ability to partition the network such that the inter-partition effects of transmission switching are minimized.

In [**75**], an electrical distance metric is defined to partition a large-scale network into zones, such that electrical changes within a zone (such as current injections) affect other nodes within the same zone, while the remainder of the network (outside the zone) is largely unaffected. This partitioning method identifies zones within electrical networks where power transfer between zones is minimized. When the partitioning method in [**85**] is applied to the RTS-96 network, the method exactly reproduces the 3 pre-defined areas in the RTS-96 test system. This result verifies the method performance and reinforces the earlier conclusion that the effects of transmission switching are largely localized – i.e., switching a line in area *k* produces system-wide cost savings because it enables low-cost generation resources within area *k* to be dispatched at greater

levels. Additionally, we can observe from Figure 11 that the switched line that create the greatest increases in *ABC* for the congested lines reside in the same area/zone as the congested line. Consequently, these zonal boundaries largely limit the impacts of transmission switching to intra-zonal effects and the transmission switching problem can be formulated on smaller sub-systems rather than the global network. Figure 21 shows a process diagram for solving the partitioned – screened Optimal Transmission Switching problem.

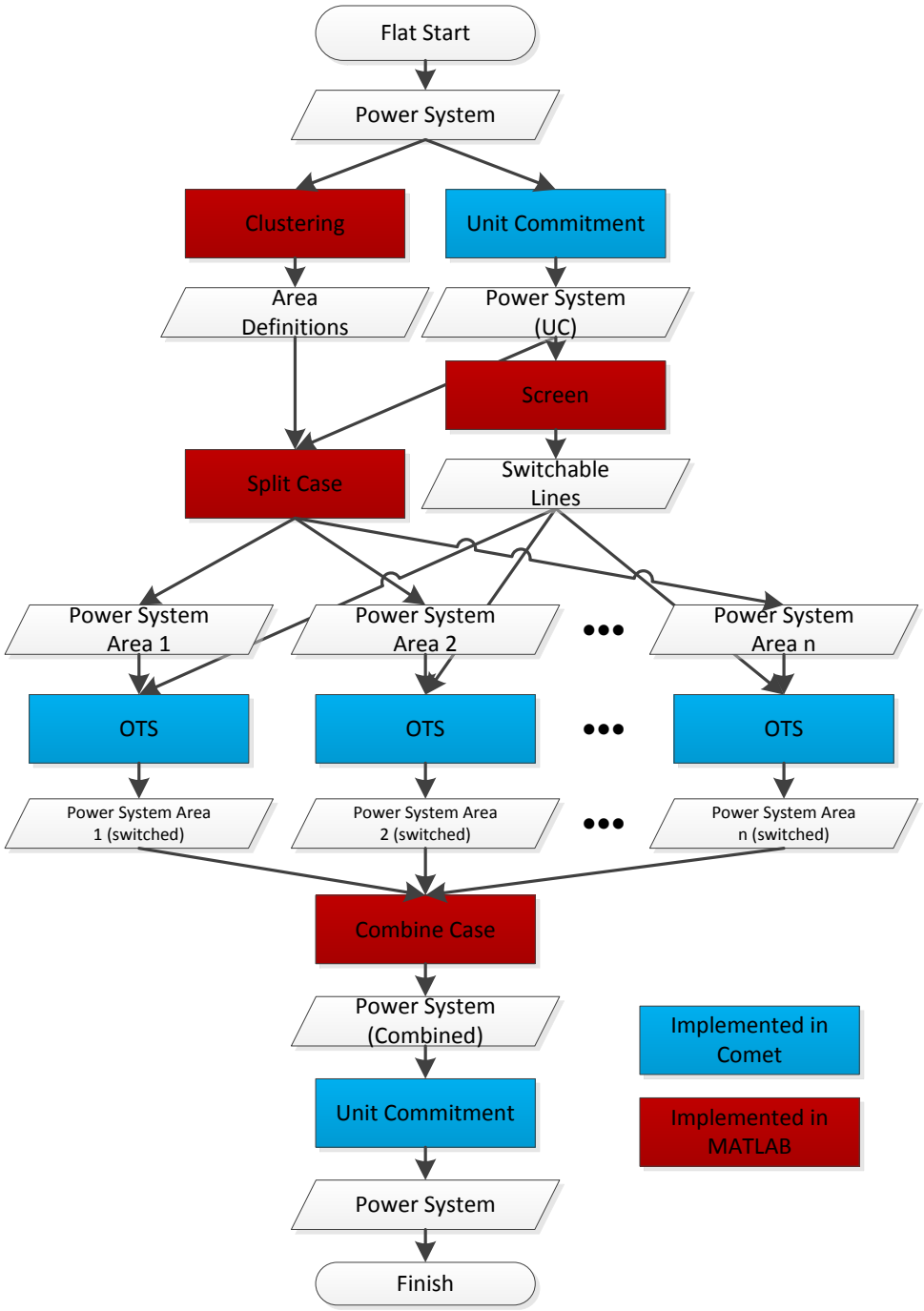

Figure 21: Process diagram for obtaining partitioned and screened Optimal Transmission Switching solutions

In order to apply the OTS solution algorithm to distinct partitions within the power network, we must first decompose the network according to the defined zones. The inability for electrical transmission systems to store significant quantities of energy requires that equivalent power

supply (generation) and power demand (load) within a power system. While this balance is certainly achieved for the aggregated system, individual zones do not necessarily achieve generation/load balance and inter-zonal power transfers are required. Thus, when decomposing the system, we must preserve the inter-zonal power transfers so that each zone may have an excess generation or load but the aggregate system is balanced.. Additionally, from the calculation of the *B-matrix* in Appendix A, the electrical impedance along a path between any two nodes in the system depends on the properties of every transmission element in the system. In order to properly define the impedance between two nodes within a zone, we must account for the properties of the network outside in addition to the network within the zone of interest. While it is necessary to preserve these properties for intra-zonal power flow calculations, it is reasonable to abstract the external network to achieve the preservation through network equivalence methods [**86**].

The most common equivalence method for DC power flow calculations is known as the Ward reduction method [**87**]. The Ward method represents the network influence between each pair of border nodes through a single impedance value. The method is very useful in modeling power flows on large networks where the external network is not of interest. However, the Ward reduction does not preserve transmission constraint or generation characteristics for system elements at the borders or external to the zone of interest. When many border nodes exist in a zone, the number of equivalent impedances representing the outside system can become enormous, and in some cases can exceed the size of the original system. For example, a zone with n nodes connected to external zones has $(n^2-n)/2$ Ward reduced impedance values for the external network. The electrical distance partitioning methods developed in Appendix B do not explicitly minimize inter-zonal connections. Thus, in this case the Ward reduction method is not

very successful in reducing power system complexity. Instead, the external network remains completely represented and the OTS problem is solved on the zone of interest while decision variables (P_g, u_g, *and* z_k) outside the zone of interest are fixed to their un-switched or previous switching iteration state. This simplification significantly improves the problem tractability and enables parallel solution of OTS problems on distinct zones while maintaining a level of network detail necessary to improve the feasibility of switching results.

4.4 Partitioned Switching Results

To illustrate the effectiveness of network partitioning for optimal topology reconfigurations, the OTS problem is applied to zones of the RTS-96 test network and the 2,383 bus Polish power network. The un-screened and ΔABC-screened partitioned switching results in this section are produced using a single iteration of the process diagram shown in Figure 21. Additional cost reductions may be achievable by performing additional iterations of the partitioned switching optimization process, however the analysis presented here is intended to explore the computational time reductions associated with generating cost reducing solutions through partitioned OTS and thus the process is limited to a single iteration. The processes implemented in the Comet optimization studio (UC and OTS in Figure 21) use the same solvers developed in Section 3.2.

4.4.1 Partitioned Switching on the IEEE RTS-96 Network

The IEEE Reliability Test System – 1996 consists of three essentially identical 24-bus networks loosely interconnected together. The structure of the network makes partitioning on the RTS-96 relatively straightforward. The GA and spectral electrical distance clustering methods presented in Appendix B.3 both reproduce the RTS-96 pre-defined zones perfectly. Thus, the RTS-96 is partitioned into the three pre-defined zones for partitioned OTS. Similar to the screened OTS presented in Section 3.3, the partitioned OTS presented here includes a

complete set of N-1 security constraints. That is, a successful solution results in a transmission topology and generation dispatch that allows the system to operate with any single transmission or generation element removed from service. Again, the same system modifications described in Chapter 2 are utilized to introduce congestion into the RTS-96. The complete system data as used is reported in Appendix C.1.

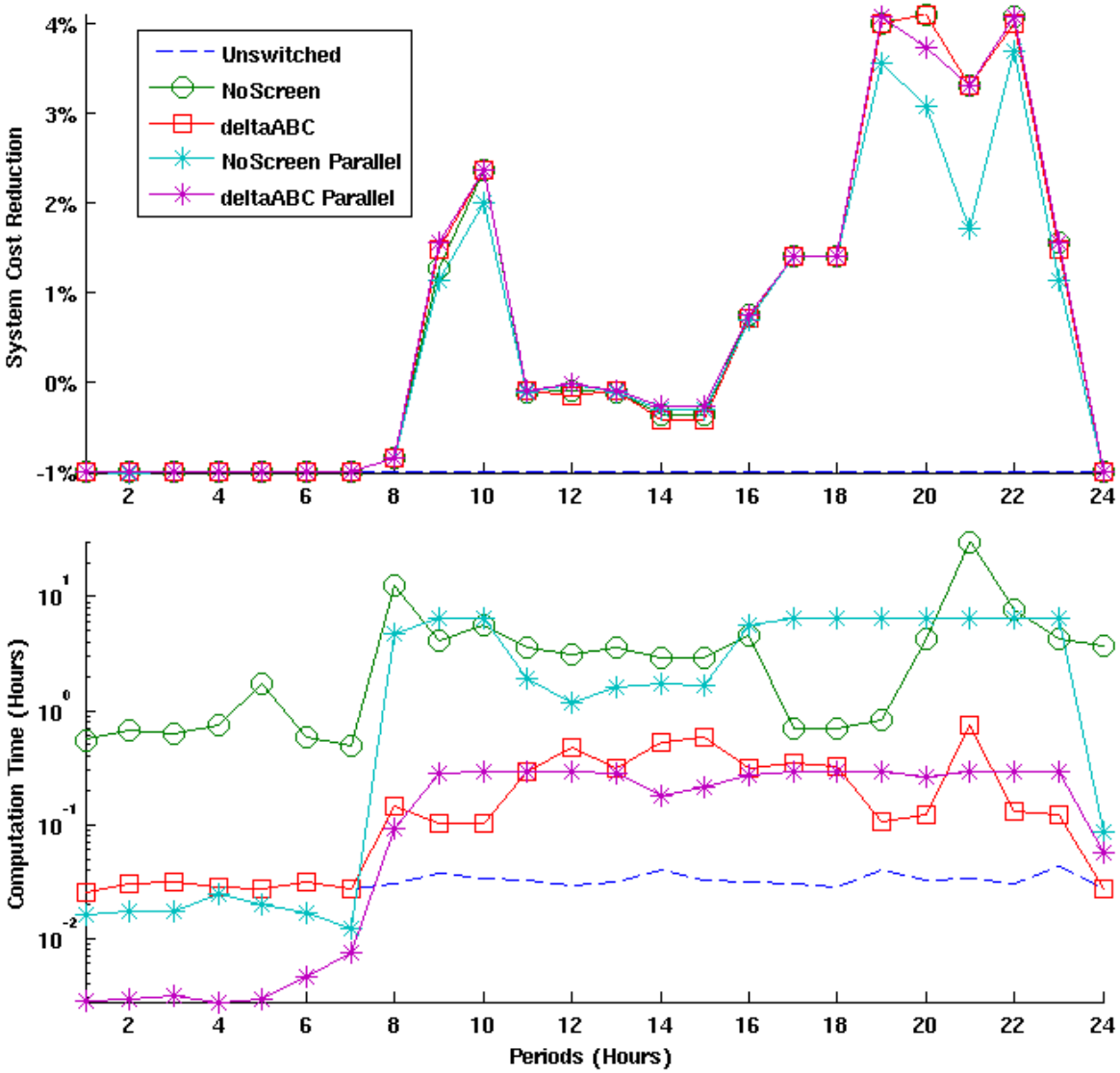

Figure 22: Partitioned and screened switching solutions on 24 periods of the RTS-96 network.

Figure 22 shows the results of partitioned switching on the RTS-96 network. The objective of partitioned switching is to create a method to parallelize the OTS problem. Thus, the solution time for each period depends upon the solution times for each partition. Since, we are interested in the computation time required to obtain a solution for a given load period, the solution time is reported in the bottom panel of Figure 22 as the maximum partition solution time. As in Chapter 3, only the OTS process in the diagram of Figure 21 is considered in the solution time. The other process solution times are both trivial and relatively constant with respect to screening and partitioning methods.

Table 9 shows that unscreened partitioned switching achieves near optimal cost reductions. The computation times are reported as follows: The "sum hourly" column describes the sum of the computation times of all 24 periods where partitioned computation times are the maximum time of all partitioned solutions for each hour (53).

$$T_{sum\ hourly} = \sum_{h=1}^{24} max\left(t_h^i\right) \forall\ i \qquad (53)$$

The "sum part" column describes the sum of all partitioned solution times for all partitions and all periods (54).

$$T_{sum\ part} = \sum_{h=1}^{24} \sum_{i=1}^{N} t_h^i \qquad (54)$$

Finally, the "total" solution time represents the actual solution time, where the hourly problems and the partitioned problems can all be solved simultaneously. Thus, the "total" solution time is the maximum solution time for any single period, or any single partition (55).

$$T_{total} = max\left(max\left(t_h^i\right)\right) \forall\ h, i \qquad (55)$$

The results show that significant computation time reductions are generated by partitioned switching. The partitioned problems converge to within 0.07% of the optimal savings for both the un-screened and screened OTS. When compared to the un-partitioned counterparts, the partitioned solution methods achieve the optimal, or near optimal solution in less than half the computation time. Similarly to the results of Chapter 3, the ΔABC-screened OTS problems solve in significantly less time than the un-screened OTS problems. However, the screened partitioned solution method achieves a better objective function value than the un-screened partitioned switching method. This somewhat counter-intuitive result likely arises in the case that un-screened partitioned switching solutions remove a transmission line in one area that causes transmission congestion in another area. By limiting the switchable lines through the ΔABC-screening method, switching events that cause inter-area congestion are minimized.

Table 9: Solution details for RTS-96 partitioned switching

Solution Method	Cost		Savings		Time		
	24 Hour	Avg Hourly	24 Hour	Avg Hourly	Sum Hourly	Sum Part	Total
OPF	$3,814,765	$158,948	--	--	0.76h	--	0.04h
OTS (un-screened & un-partitioned)	$3,740,344	$155,872	1.950%	1.615%	100.93h	--	30.48h
OTS (screened & un-partitioned)	$3,741,219	$155,847	1.928%	1.599%	4.97h	--	0.74h
OTS (un-screened & partitioned)	$3,748,638	$155,954	1.733%	1.426%	76.98h	148.3h	6.48h
OTS (screened & partitioned)	$3,740,344	$155,847	1.950%	1.615%	4.27h	8.27h	0.29h

For example, in period 21 of Figure 22 we can see that the partitioned un-screened OTS (denoted by the blue "*") generates significantly less savings than the partitioned screened OTS solution (denoted by the purple "*"). The partitioned un-screened solution removes 20 lines from service (7 in zone 1, 7 in zone 2 and 6 in zone 3), while the partitioned screened solution

only removes 12 lines (3 in zone 1, 5 in zone 2 and 4 in zone 3). The power flow obtained from the two solution methods yields two congested lines in the un-screened case (line 113-215 and line 213-223) and no congested lines in the screened case. If we eliminate the switching actions of zone 1 of the un-screened solution method (keep all transmission lines that originate and end in zone 1 in service) and keep the branch status resulting from the zone 2 and zone 3 calculations, all congestion is relieved and the optimal savings is achieved. This suggests that the un-screened partitioned switching solution of zone 1 is causing the congestion on lines 113-215 and 213-223. ΔABC-screening the partitioned network seems to eliminate the occurrence of this phenomenon and facilitate obtaining optimal solutions in significantly less time than traditional OTS methods. Additionally, the reduction in switching events is likely better in terms of circuit breaker wear.

4.4.2 Partitioned Switching on the 2383-bus Winter Peak Polish Network

Section 4.2.1.B illustrates the results of electrical distance clustering on the 2383 bus Polish power network when partitioned into 5 zones. The winter peak load case included in the Matpower distribution (case2383wp) is used to illustrate the effects of partitioning on OTS results [**84**]. Case2383wp contains quadratic generator production cost functions. To simplify the cost minimization of OTS, the generator production cost functions are linearized between the minimum and maximum generator MW outputs.

Unlike the RTS-96, the five pre-defined zones included in the case2383wp do not correlate well to the five zones generated by electrical distance clustering. The top panel of Figure 23 shows the cost savings generated through unscreened and ΔABC-screened OTS when the case2383wp network is partitioned into 5, 10, 15 and 20 zones. The figure shows that cost reductions are highly sensitive to the chosen number of partitions. In theory, we would expect to see a negative correlation between the number of partitions in the network and the savings

generated by partitioned switching. This theoretical correlation would exist due to the inability for each partitioned switching solution to relieve congestion across zonal boundaries. In practice, the top panel of Figure 23 shows that the results are more complicated.

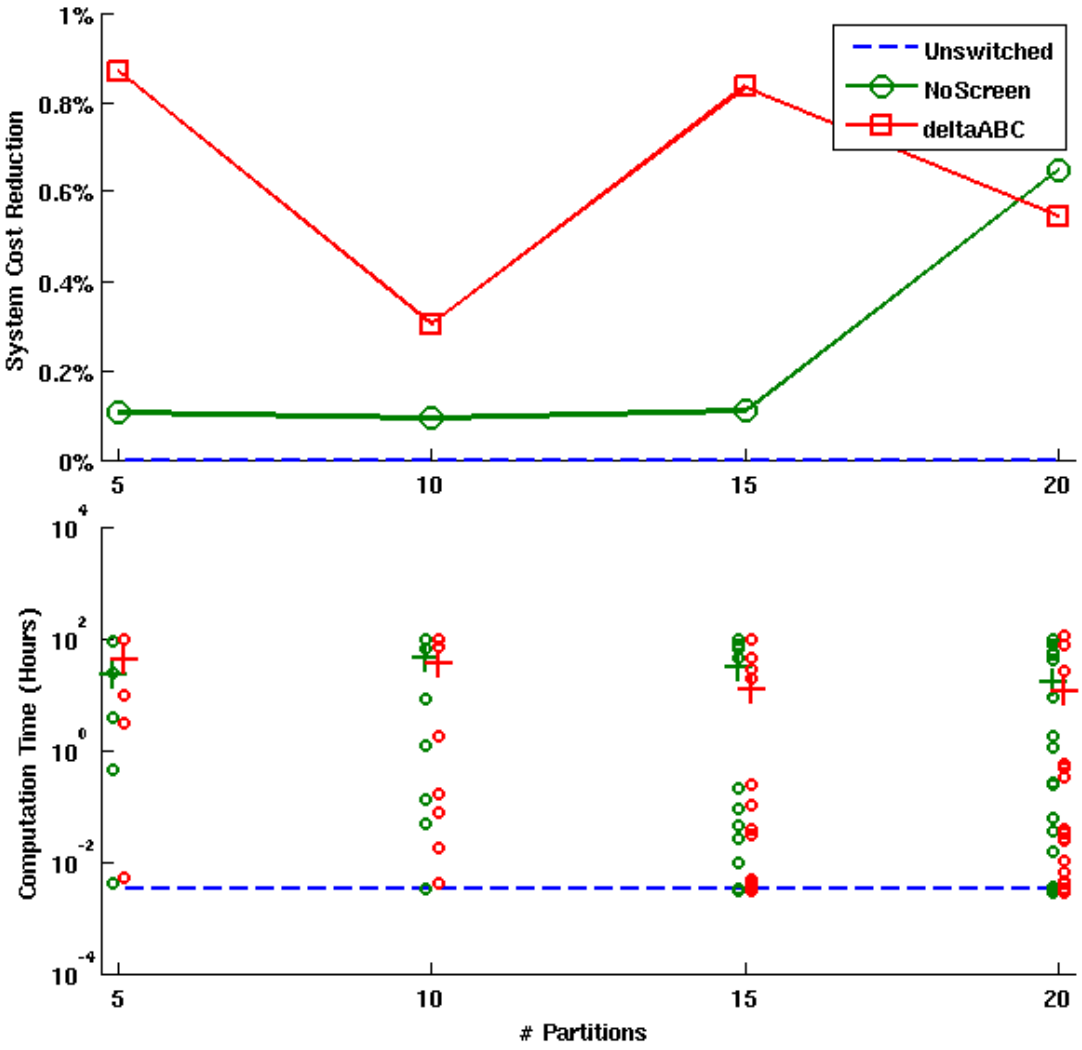

Figure 23: Spectral partitioned and screened switching savings (top panel) and computation time (bottom panel) on Polish Winter Peak network. The computation times are reported in the bottom panel for each partition ('o') and the mean of all partitions computation times ('+') for each partitioning solution.

The scatter plot in the bottom panel of Figure 23 shows the OTS solution times for each partition ('◯') and the average of the partition solution times ('+'). Due to computational resource constraints, the optimization routines were terminated after 100 hours. However, the

average solution times show that by increasing the number of partitions, the computation time for partitioned OTS generally decreases. The results also show that the ΔABC-screened OTS again solves faster and generates greater savings than the unscreened OTS problems. In Chapter 3 we saw that ΔABC screened OTS generated near optimal solutions, but the un-screened OTS solution method was the benchmark for generating optimal savings. Here, the partitioning assumes that switching actions within an area relieve congestion within the same area. By treating every transmission line within an area as switchable, the un-screened solutions have greater chances of switching a line that causes inter-area congestion. The ΔABC screen reduces the chance of causing inter-area congestion by considering the global effects on congestion, rather than just the local (intra-area) effects. In other words, the ΔABC screen will not select a line in $zone_k$ that could increase congestion within $zone_j$ for topology modifications. Table 10 shows that the screened solutions generally have fewer switched lines than the unscreened solutions.

Table 10: Partitioned Switching Results for the 2383-bus Polish Winter Peak Power Network

Problem	Partitioning	Screen	System Cost	Savings %	Avg Sol'n Time (hours)	# Switched lines
OPF	None	None	$ 1,789,640.00	--	0.0034	--
OTS	Spectral w/ 5 zones	None	$ 1,785,591.73	0.106%	23.16	43
		ΔABC	$ 1,771,952.89	0.869%	40.13	125
	Spectral w/ 10 zones	None	$ 1,785,826.08	0.090%	45.8	73
		ΔABC	$ 1,782,093.45	0.302%	35.69	58
	Spectral w/ 15 zones	None	$ 1,785,543.58	0.109%	30.44	70
		ΔABC	$ 1,772,565.47	0.835%	12.56	59
	Spectral w/ 20 zones	None	$ 1,775,905.16	0.648%	16.42	142
		ΔABC	$ 1,777,757.58	0.544%	10.92	98
	Random w/ 5 zones	None	$ 1,792,262.52*	-0.147%*	48.6*	33.8*
		ΔABC	$ 1,788,864.18*	0.043%*	43.8*	84*
	Random w/ 10 zones	None	$ 1,787,194.39*	0.137%*	22.7*	99.4*
		ΔABC	$ 1,789,640.00*	0.000%*	25.3*	137.4*

In order to understand the effectiveness of spectral clustering for partitioned OTS, the partitioned OTS technique is applied to randomly generated clusters. Random clusters are

formed using a random centroid method, where centroid nodes are chosen at random and clusters are formed by iteratively adding nodes to the cluster associated with their nearest (topologically) centroid. This method ensures that zones are topologically connected. ΔABC-screened and unscreened OTS was performed on 10 samples of random clustering with 5 partitions and 10 samples of random clustering with 10 partitions. The results are shown in Figure 24 and Table 10. The top panel of Figure 24 shows that the savings is highly dependent upon zonal definition. We can see that the 5-partition random sample #4 generates negative savings for both screened (deltaABC 5) and unscreened (NoScreen 5) switching. Other solutions approach the savings generated by the spectral partitioning method (Figure 23), but in general the random clustering solutions yield significantly less cost savings. The lower panel of Figure 24 again shows that the ΔABC-screened solutions typically solve in less time than the unscreened solutions. Again, solutions were terminated after 100 computation hours. We can see that the solution times are highly variable. The average solution times and savings (*) generated by the 10 samples of random partitioned OTS (for both 5 and 10 partitions) are shown in Table 10. When compared with the results of the spectral partitioned OTS, the random partitioned OTS method underperforms in both cost savings and solution time.

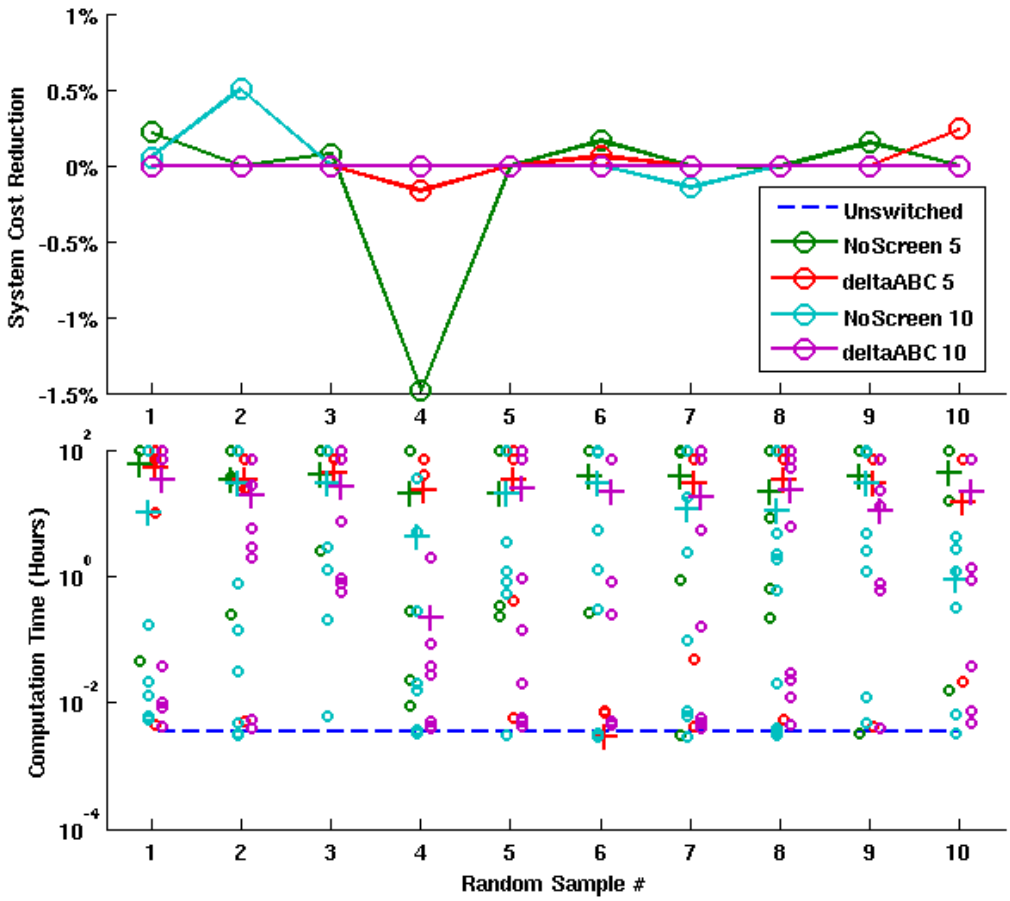

Figure 24: Random partitioned switching savings (top panel) and computation time (bottom panel) on Polish Winter Peak network. The computation times are reported in the bottom panel for each partition ('o') and the mean of all partitions computation times ('+') for each randomly partitioned sample.

4.5 Partitioned Switching Conclusions

The results of partitioned transmission switching on the RTS-96 network and the 2383-bus Polish Power network show that network partitioning can improve OTS problem tractability without significantly compromising solution quality. The analysis presented here on the Polish power network model represents a pioneering application of OTS on large power systems. Additionally, the RTS-96 partitioned switching results achieve near optimal solutions; an indication that properly defined partition boundaries enables the recombination parallel OTS solutions to achieve a cost saving dispatch.

The non-polynomial scaling of the OTS problem complexity dictates that by partitioning a system and solving OTS problems on distinct sub-networks, the problem complexity is reduced. The partitioned networks preserve the interaction between sub-networks while assuming minimal inter-area perturbations from transmission switching actions. This enables further reductions in computation time by solving all sub-network OTS problems simultaneously on parallel processors. The results on the RTS-96 show a significant (typically an order of magnitude or more) reduction in computation time when comparing partitioned and un-partitioned OTS. These tractability improvements have enabled, for the first time, OTS solutions on the 2383-bus Polish power network. Without partitioning, OTS is simply infeasible on a system as large as the Polish network.

While the partitioning (or clustering) problem on the RTS-96 network is trivial, partitioning the Polish power network presents an interesting challenge. The results presented here show that the optimality of partitioned OTS solutions is dependent upon the quantity and quality of network partitions. By comparing the results of OTS on random partitions and partitions that minimize the inter-zonal effects of transmission switching (spectral partitions), we can see that properly defined partitions are crucial to generating globally optimal solutions. As expected, the

results show a tradeoff between the number of partitions and the quality of solutions as measured by computation times and generated cost savings. As we increase the number of partitions in a network, the problem complexity is reduced and solutions are obtained in reduced computation times. The effect of the number of partitions on solution quality is more complex. Generally we would expect that as the number of partitions increases, the ability to neglect inter-zonal transmission switching effects would diminish. However, nature of the OTS problem and the Polish power network make it difficult to demonstrate such properties empirically. The relatively small number of congested lines (only 3 congested transmission lines) and the nonlinear nature of the OTS problem produces a highly variable relationship between the number of clusters and the savings generated by OTS (see the top panel of Figure 23).

The combination of the ΔABC-screening method developed in Chapter 3 generates the greatest savings in the least computation time. Simply invoking either solution heuristic can itself improve the tractability of OTS problems. However, the results shown here demonstrate the additive nature of the improved problem tractability. Figure 22 shows how ΔABC-screened switching and partitioned ΔABC-screened switching incrementally reduce the solution times while achieving near optimal solutions. Spectral clustering on electrical distances to partition the network in combination with the switchable line screen improves the OTS problem tractability so that transmission switching may be applied to large power systems.

Chapter 5 Correcting OTS for AC Power Flows

Thus far in the evolution of OTS literature and research, the transmission switching problem has been formulated and solved on a simplified and linearized model of a power grid, which neglects important variables such as variations in voltage magnitudes and reactive power (see Appendix A). The approximate effects of transmission switching on economic dispatch have been documented in previous literature using the linearized DC OPF model [**11**,**48**,**49**,**52**,**53**]. The voltage magnitude and reactive power flows, which are neglected in the linearized DC OPF, are crucial parameters when considering system reliability. Ignoring these parameters, the reliability of OTS results is uncertain on real systems. By analyzing the voltage magnitude response and reactive power flows resulting from topology reconfigurations under OTS, we can characterize the effects of OTS operations on AC power flows. This chapter develops a method to achieve OTS solutions that are demonstrably feasible in both the AC and linearized DC power flow models.

5.1 The Accuracy of DC Power Flow Approximations When Considering AC Power Flow Constraints

The vast majority of electrical power systems components operate under an alternating current (AC) framework. AC systems have time-dependent voltage and current wave-forms that oscillate in the pattern of a sine wave. The average real (P) and reactive (Q) power at each point in a power system is governed by the set of non-linear equations:

$$P_i = \sum_{k=1}^{N} |V_i||V_k|\,|Y_{ik}|\cos(\theta_i - \theta_k - \varphi_{ik}) \qquad (56)$$

$$Q_i = \sum_{k=1}^{N} |V_i||V_k|\,|Y_{ik}|\sin(\theta_i - \theta_k - \varphi_{ik}) \qquad (57)$$

Where $|V_i|$ is the root-mean-squared voltage magnitude at bus_i, Y_{ik} is the entry corresponding to the i^{th} row of the k^{th} column of the bus admittance matrix (Y_{bus}), θ_i is the bus voltage angle, and φ_{ik} represents the difference in current phase angles between bus_i and bus_k. By substituting the conductance (G) and susceptance (B) components of the complex admittance (Y) we can rewrite the equations for real and reactive power as follows.

$$P_i = \sum_{k=1}^{N} |V_i||V_k| \left(G_{ik} \cos(\theta_i - \theta_k) + B_{ik} \sin(\theta_i - \theta_k)\right) \quad (58)$$

$$Q_i = \sum_{k=1}^{N} |V_i||V_k| \left(G_{ik} \sin(\theta_i - \theta_k) + B_{ik} \cos(\theta_i - \theta_k)\right) \quad (59)$$

Due to the nonlinearity of the real and reactive power equations and the difficulty associated with obtaining a solution, many power flow analyses are formulated using the linearized de-coupled (DC) system model (see Appendix A).

The commodity traded in most electricity markets is electrical energy which is delivered by real power. Since reactive power has a net-zero transfer of energy, we are often not explicitly concerned with the generation, transmission, or consumption of reactive power when making calculations relevant to electricity markets. The economic dispatch and calculation of market prices often ignores the bus voltage magnitude variations that largely govern reactive power flows. However, power system components are sensitive to both real and reactive power flow and reliable system operations must consider bus voltage magnitudes and voltage angles. The validity of the linearized DC power flow approximations is highly dependent on the system and load profile to which it is applied. For instance, imagine two simple systems: A single lossless line system connecting two generator busses each controlled to a voltage magnitude of 1p.u. would yield feasible operating points in both the AC and the linearized DC model. On the other hand, consider a system with a single generator at one bus and constant load at the other. If the

load demands reactive power in addition to a real power quantity equal to the transmission line transfer capability, the linearized DC power flow would obtain a solution while an AC power flow would be infeasible [**88**]. Similarly, large perturbations in operating state may affect the validity of the DC power flow approximation. Joint dispatch of generation and transmission topology based on DC OTS may result in infeasible operating points in the more realistic AC model. These discrepancies in AC versus linearized DC power model results are the source of many arguments against the adoption of OTS [**19**].

In the linearized DC power flow model, transmission congestion is caused by binding transmission line flow constraints (12). However, in AC power flow models, there are some losses associated with electricity transmission and transmission line flow limits are defined with respect to the apparent power ($S = P+jQ$) flowing along a transmission line. Additionally, AC power flow congestion can arise from binding bus voltage magnitude constraints. The linearized DC power flow model typically underestimates transmission line loadings while overestimating bus voltage angle differences [**89**]. Since optimal transmission switching problems have, thus far, been implemented using a linearized DC power flow model, it is useful to examine the results of OTS solutions in an AC power flow framework.

5.2 Optimal Transmission Switching for Feasible AC Power Flows

It is well known among power system engineers that it can often be "maddeningly difficult" to obtain solutions to the AC power flow problem [**88**]. Since AC solution algorithms attempt to iteratively converge on a solution from a known operating point, solutions are particularly difficult to obtain when the operating point is dramatically altered. Conventional practice typically avoids large deviations in operating point from contingencies and control actions such as transmission switching. While many of the systems presented in this document have

demonstrably feasible AC power flow solutions prior to any transmission switching, OTS solutions in the linearized DC power flow model may present a situation where the AC power flow is infeasible. The analysis presented here is designed to gain an understanding of the conditions where OTS solutions cause AC infeasibilities and the actions required to obtain AC feasible OTS solutions. The process diagram in Figure 26 shows the methods used to ensure AC feasible OTS solutions.

The ΔABC-screening method developed in Chapter 3 is used to generate a switchable line set and improve the computation time. The OTS problems are solved using the OTS MIP solver developed in Chapter 3. The AC optimal power flow problem (ACOPF) is formulated in Equations (60)-(70). Notice that the transmission line flow constraints in Equations (65) and (66) consider only real power flows. This formulation is chosen for consistency to enable comparisons between the congestion in the linearized DC model and the AC model. Losses are accounted for in the power injection balance equations of (67) and (68). ACOPF problems are solved using the Matpower version 4.1 toolbox in MATLAB [**84**]. The optimization engine employed by the ACOPF algorithm in Matpower is the constrained nonlinear multivariate minimization tool in the MATLAB Optimization Toolbox. This research is focused on generating AC feasible OTS solutions. Here, AC feasibility is defined as an ACOPF solution that satisfies the constraints posed by (61)-(70). AC infeasible solutions can arise by violating any of the constraints.

$$min \sum_{g} c_g P_g \qquad (60)$$

s.t.

$$\theta_n^{min} \leq \theta_n \leq \theta_n^{max}, \qquad \forall\, n \text{ busses} \qquad (61)$$

$$v_n^{min} \le v_n \le v_n^{max}, \qquad \forall\, n \text{ busses} \tag{62}$$

$$P_g^{min} \le P_g \le P_g^{max}, \qquad \forall\, g \text{ generators} \tag{63}$$

$$Q_g^{min} \le Q_g \le Q_g^{max}, \qquad \forall\, g \text{ generators} \tag{64}$$

$$P_k^{min} \le \Re\left\{S_{k_{ij}}\right\} \le P_k^{max}, \qquad \forall\, k \text{ lines} \tag{65}$$

$$P_k^{min} \le \Re\left\{S_{k_{ji}}\right\} \le P_k^{max}, \qquad \forall\, k \text{ lines} \tag{66}$$

$$\sum_{i=n} P_{k_{ij}} - \sum_{j=n} P_{k_{ij}} - \sum_{g} P_{ng} - \sum_{d} P_{nd} = 0, \forall\, n \tag{67}$$

$$\sum_{i=n} Q_{k_{ij}} - \sum_{j=n} Q_{k_{ij}} - \sum_{g} Q_{ng} - \sum_{d} Q_{nd} = 0, \forall\, n \tag{68}$$

$$[V_i] Y_{ij}^* V^* - S_{k_{ij}} = 0, \qquad \forall\, k \text{ lines} \tag{69}$$

$$\left[V_j\right] Y_{ji}^* V^* - S_{k_{ji}} = 0, \qquad \forall\, k \text{ lines} \tag{70}$$

As discussed in Appendix A, network power flows are governed by Kirchhoff's laws. In the linearized DC power flow model, transmission line reactances govern real power flows and bus voltage phase angles. A feasible DC power flow solution respects transmission line flow rating constraints and generator output constraints but assumes that all bus voltage magnitudes are normalized to 1p.u. In the AC power flow model, bus voltage magnitudes result from the solution of the AC power flow equations (69) and (70). Maintaining an AC feasible power flow solution requires that system generators be able to supply real and reactive power in such a way that none of the system constraints are violated. Removing transmission lines from service changes the impedance parameters of the network (represented by the Y_{bus} matrix) and, through the complex interdependence of AC power flow, will change the bus voltage magnitude, phase angles, and transmission line power flows. OTS can present scenarios where system generators cannot always adjust to deliver load in the topologically reconfigured transmission network.

Assuming transmission switching actions do not isolate network components (create islands), switching operations will only cause flow rating (65)-(66) or voltage magnitude (61)-(62) constraint violations. As noted in Appendix A, real power flows are driven primarily by differences in bus voltage phase angles. To understand the effect of transmission line impedance parameters on voltage phase angles (and thus real power flows) and voltage magnitudes, it is useful to construct an example.

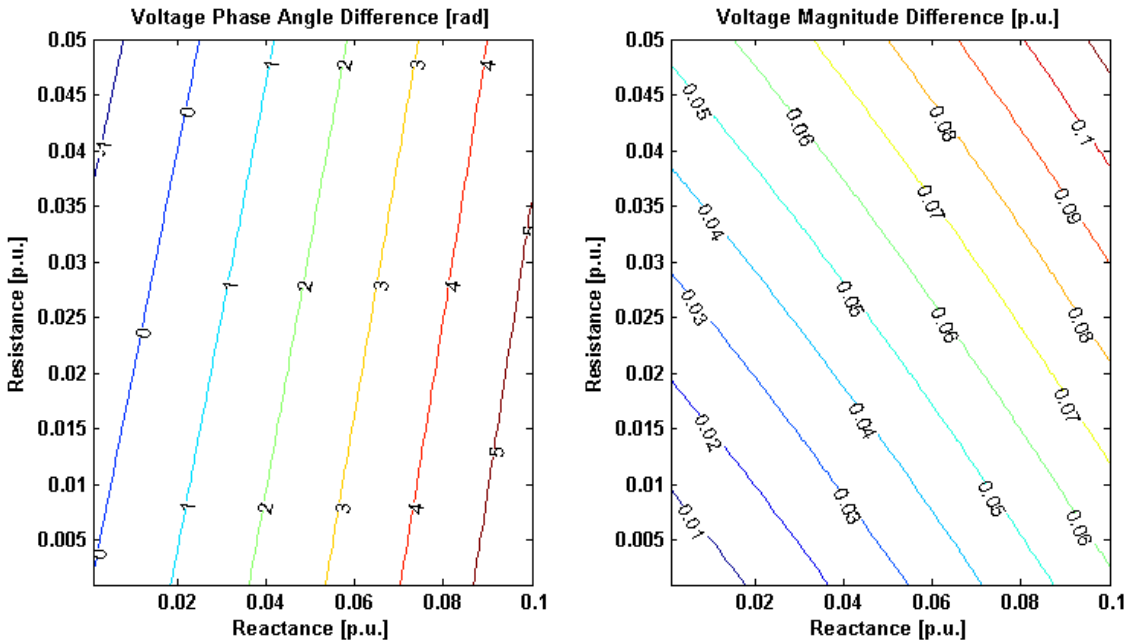

Figure 25: The resistance and reactance parameters of a single transmission line system are varied to generate Voltage phase angle (left) and magnitude (right) differences between bus_1 and bus_2 where 100MW and 50MVAr are generated at bus_1 and consumed at bus_2.

Imagine a single transmission line system where a generator located at bus_1 serves a 100MW real power and 50MVAr reactive power load at bus_2. To illustrate the effect of transmission line impedance parameters on the voltage at bus_2, the voltage at bus_1 is controlled to 1p.u. and 0° and the resistance and reactance parameters of the transmission line are varied. The contours of Figure 25 show the voltage phase angle (left pane) and magnitude differences (right pane) between bus_1 and bus_2 resulting from varying the transmission line impedance parameters. The

left pane shows that phase angle differences are highly sensitive to transmission line reactance but not very sensitive to resistance. However, the right pane shows that voltage magnitude differences are sensitive to both resistance and reactance parameters. This analysis suggests that real power flow between two busses is primarily affected by the equivalent reactance while the bus voltage magnitudes are affected by the equivalent reactances and resistances. These results can be demonstrated analytically by examining Equations (58) and (59) for the two node example:

$$P_2 = |V_2||1|(G_{12}\cos(\theta_2 - 0) + B_{12}\sin(\theta_2 - 0)) \quad (71)$$

$$Q_2 = |V_2||1|(G_{12}\sin(\theta_2 - 0) + B_{12}\cos(\theta_2 - 0)) \quad (72)$$

Substituting $G = 1/R$ and $B = 1/X$ and calculating the partial derivatives of $|V_2|$ in (71) with respect to R and X:

$$\frac{\partial|V_2|}{\partial R_{12}} = -\frac{P_2}{\cos(\theta_2)} \quad (73)$$

$$\frac{\partial|V_2|}{\partial X_{12}} = -\frac{P_2}{\sin(\theta_2)} \quad (74)$$

Similarly, substituting for G and B and calculating the partial derivatives in (72) yields:

$$\frac{\partial|V_2|}{\partial R_{12}} = -\frac{Q_2}{\sin(\theta_2)} \quad (75)$$

$$\frac{\partial|V_2|}{\partial X_{12}} = -\frac{Q_2}{\cos(\theta_2)} \quad (76)$$

If we make the small angle assumption (see Appendix A) to assume that the value of θ_2 is relatively similar to the value of $\theta_1=0$ we can see that the most significant partial derivatives of $|V_2|$ are with respect to R for real power (73) and X for reactive power (76).

If we again make the small angle assumption in Equations (71) and (72) we can assume that $\sin(\theta_2-\theta_1) \approx \theta_2-\theta_1$ and $\cos(\theta_2-\theta_1) \approx 1$. Thus we can solve for θ_2:

$$\theta_2 = \frac{P_2 X_{12}}{|V_2|} - \frac{X_{12}}{R_{12}} \quad (77)$$

$$\theta_2 = \frac{Q_2 R_{12}}{|V_2|} - \frac{R_{12}}{X_{12}} \quad (78)$$

Taking the partial derivatives of θ_2 with respect to the impedance parameters in Equation (77) yields:

$$\frac{\partial \theta_2}{\partial R_{12}} = X_{12} \quad (79)$$

$$\frac{\partial \theta_2}{\partial X_{12}} = \frac{P_2}{|V_2|} - \frac{1}{R_{12}} \quad (80)$$

Similarly, the partial derivatives of the reactive power equation (78) yields:

$$\frac{\partial \theta_2}{\partial R_{12}} = \frac{Q_2}{|V_2|} - \frac{1}{X_{12}} \quad (81)$$

$$\frac{\partial \theta_2}{\partial X_{12}} = R_{12} \quad (82)$$

If we make the realistic assumptions that the values of P_2 and X_{12} are significantly larger than the values of Q_2 and R_{12} respectively, the voltage magnitude at bus_2 is most sensitive to changes in line resistance..

In order to identify the switched transmission line properties that contribute to AC infeasible OTS solutions, the selection criteria for removing transmission lines that are optimally switched by OTS in the DC model from the set of switchable transmission lines is varied. Figure 25 and the subsequent analytical results demonstrate that AC power flow feasibility can be sensitive to both reactance and resistance, but the sensitivities of a particular system may depend on that system's parameters. So, It makes sense to consider corrective removal of lines from the switchable set based on both reactance and resistance criteria. Thus, the following five criteria serve to identify which optimally switched line to remove from the switchable set:

1. Maximum resistance optimally switched transmission line.
2. Minimum resistance optimally switched transmission line.
3. Maximum reactance optimally switched transmission line.
4. Minimum reactance optimally switched transmission line.
5. Random optimally switched transmission line.

For the analysis presented here, the OTS problem is solved without the *N-1* security constraints. Security constraints are ignored for two reasons: first, the un-secure OTS problem is significantly more tractable, enabling shorter computation times. Second, the lack of security constraints results in OTS solutions that present larger topology disruptions. That is, more transmission lines are switched in un-secure OTS than in *N-1* secure OTS solutions. Larger topology disruptions generally cause more constraint violations in the ACOPF and enable a more substantial analysis of the switched transmission lines that contribute to AC infeasibility. Despite the lack of security constraints in the problem formulation, the effects of OTS on AC system security can be described using an ex-post security analysis. By checking the ability of the system to withstand the loss of any single element before and after OTS operations, we can assess the effect of topology reconfigurations on system security. Here, the ex-post security analysis is limited to transmission security. That is, a generation dispatch and transmission topology is said to be transmission secure if the system can withstand the loss of any single in-service transmission element without violating transmission line flow ratings.

It should be emphasized that the results obtained by the process in Figure 26 are not intended to produce a co-optimal generation dispatch and network topology in the AC power flow model. Rather, the method is intended to determine whether OTS solutions obtained through the DC framework are likely to cause constraint violations in real systems (modeled in the AC power

flow framework) and appropriate modifications to the OTS problem that enable feasible real system solutions.

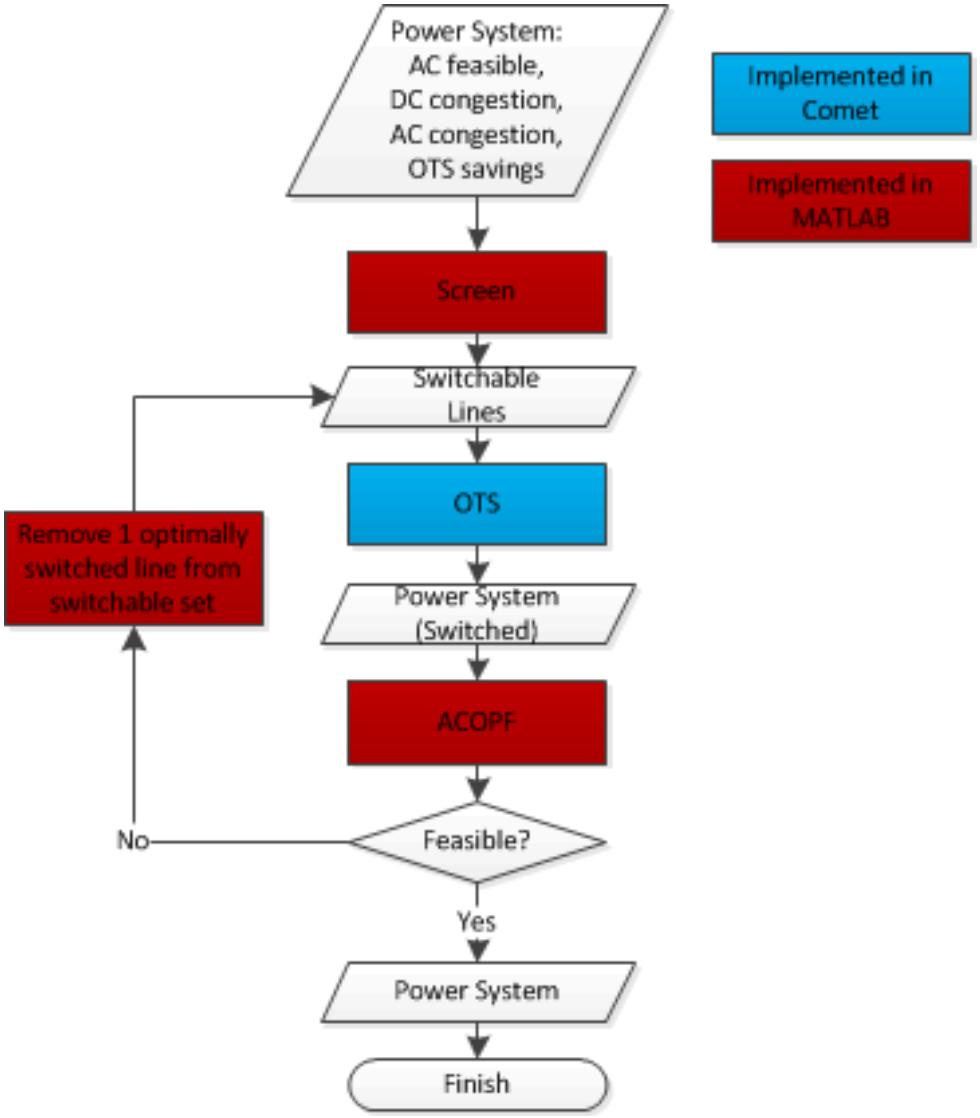

Figure 26: Process diagram for obtaining AC feasible transmission switching results.

5.3 Results

The method presented in Section 5.2 was applied to the 24 load periods of the IEEE RTS-96 network. Again, the same system modifications described in Chapter 2 are utilized to introduce congestion into the RTS-96. The complete system data as used is reported in Appendix C.1.

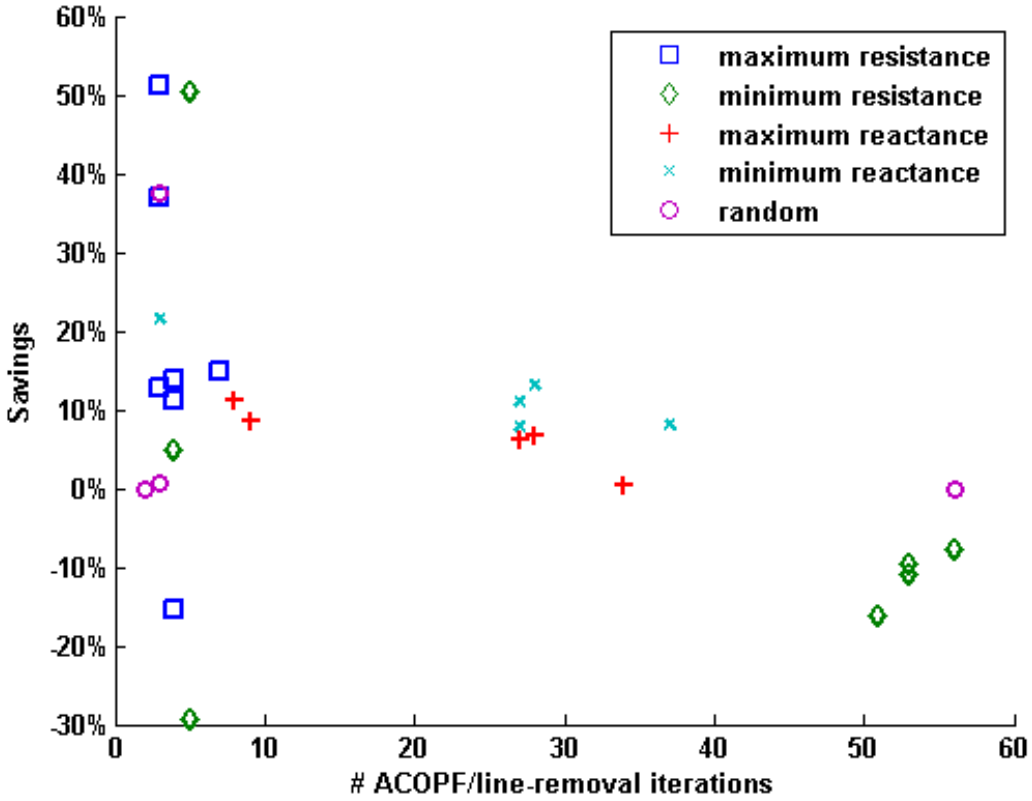

Figure 27: Optimally switched lines are removed from the switchable set until the OTS algorithm obtains a feasible ACOPF. Switched lines are selected for removal based on: maximum resistance ('□'), minimum resistance ('◊'), maximum reactance ('+'), minimum reactance ('X'), and random ('○'). The horizontal axis represents the number of lines that are removed from the switchable set (the # of iterations of the process in Figure 26), and the vertical axis shows the system cost savings obtained over the un-switched case in the AC model.

Figure 27 shows the results of the procedure presented in Figure 26 on the 24 summer peak weekday load periods of the RTS-96 network. The savings values presented on the vertical axis are the result of the following calculation:

$$Savings\ \% = \frac{\left(f(ACOPF_{un-switched}) - f(ACOPF_{switched})\right)}{f(ACOPF_{un-switched})} \times 100 \qquad (83)$$

where *f(ACOPF)* is the value of the ACOPF objective function in Equations(60). $ACOPF_{switched}$ is the result of the first feasible ACOPF solution obtained in the process in Figure 26. Each process iteration is equivalent to removing a single line from the switchable set. The number of

process iterations (switchable set reductions) required to obtain a feasible ACOPF solution is reported on the horizontal axis of Figure 27. The results show that feasible AC power flow solutions are achieved in the fewest iterations by successively removing high-resistance lines from the switchable set (see Table 11). Additionally, removing the maximum resistance line generally achieves greater system cost savings than removing lines by one of the other selection rules. This likely arises due to the effect of high resistance transmission lines on voltage magnitude differences. For a constant power flow between two busses, the bus voltage phase angle differences are driven primarily by the equivalent reactance between the two busses. Similarly bus voltage magnitude differences are driven primarily by the equivalent resistance between the two busses [**89**]. Removing a high resistance line from service can dramatically change the equivalent resistance between busses and cause significant changes bus voltage magnitudes at the line endpoints; causing voltage magnitude constraint violations if the induced changes are large enough. Thus, by removing the highest resistance optimally switched line from the switchable set of transmission lines, the next OTS solution will leave that line in service and improve the likelihood of obtaining feasible ACOPF solutions.

Table 11: Feasible ACOPF OTS Results (RTS-96)

	# Feasible ACOPF Periods	# Lines Removed from Switchable Set	24 hour OTS (DC) Savings	24 hour OTS (AC) Savings
Un-switched	13	--	--	--
Maximum Resistance	15	75	0.539%	6.019%
Minimum Resistance	18	429	0.350%	-13.300%
Maximum Reactance	15	334	0.539%	5.810%
Minimum Reactance	12	442	0.502%	10.500%
Random	10	395	0.315%	2.230%

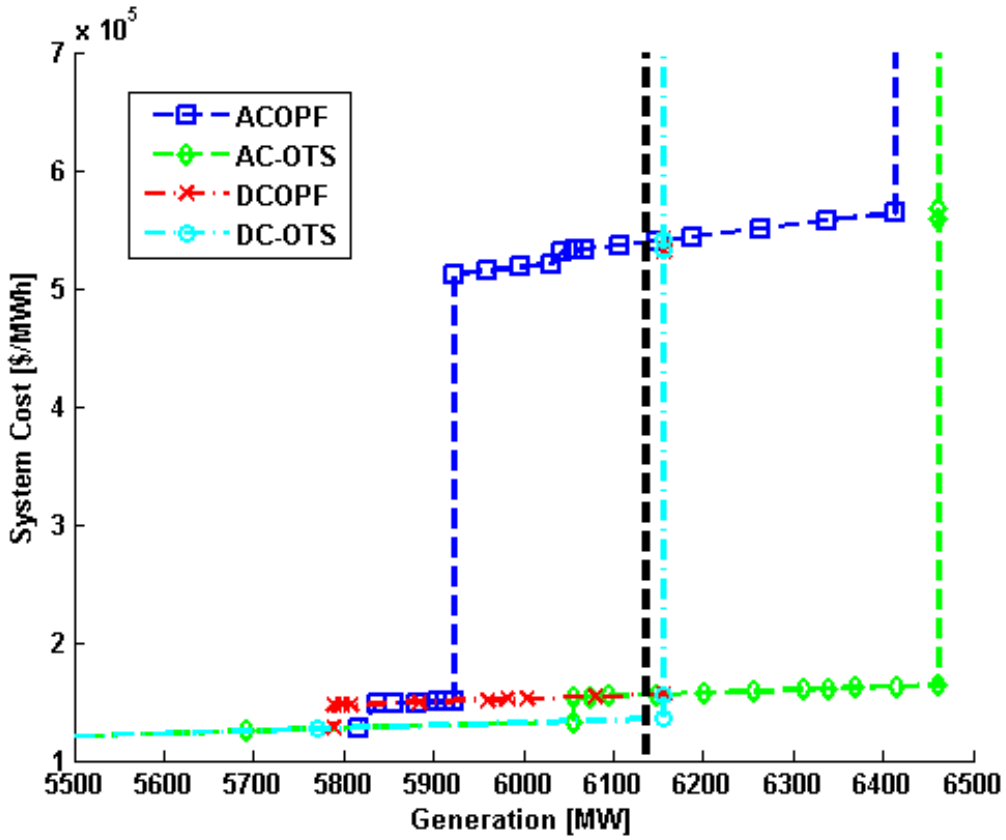

Figure 28: Total system cost (vertical axis) as a function of system load (horizontal axis) for IEEE RTS-96 hour 24 resulting from un-switched ACOPF ('□'), AC feasible OTS achieved by removing maximum resistance lines from the switchable set ('◊'), DCOPF ('X'), and DC OTS ('○'). The dotted vertical black line represents the total system load (6136 MW).

Another observation from Figure 27 is that the cost savings achieved in the ACOPF is significantly higher than the savings achieved by OTS in the DC model (see Figure 13). Further analysis suggests that this due to the definition of generator costs in the IEEE RTS-96 system (see Appendix C.1). For example, the total system cost curves are shown in Figure 28 where generators are dispatched in order of increasing marginal cost values subject to the constraints associated with relevant dispatch models. Note the large cost jump in each dispatch model's cost curve resulting from the differences in generator production costs. The cost associated with dispatching the (un-switched) system using the DCOPF model falls below the large jump in the cost curve ('x'). Due to losses and additional binding constraints, the un-switched ACOPF

system cost falls above the large jump in the corresponding cost curve ('□'). In both the AC and DC power flow models, OTS relieves some transmission congestion and enables some production shift to lower cost generators. This generation dispatch re-ordering from OTS actions effectively shifts the large cost jumps seen in the ACOPF and DCOPF curves in Figure 28 to the right. The change in generator outputs between the OPF and OTS solutions is shown in Figure 30 for both the DC and AC models. As a result, OTS moves the AC operating point to below the cost jump in the AC-OTS cost curve ('◊') and facilitates larger cost savings than would be suggested form OTS in the DC model. This result is sensitive to the system load profile and generator cost definitions as well as system constraints. Since most real electricity systems have some sort of jump in the cost curve, it is likely that this behavior could be observed in other systems under the right circumstances.

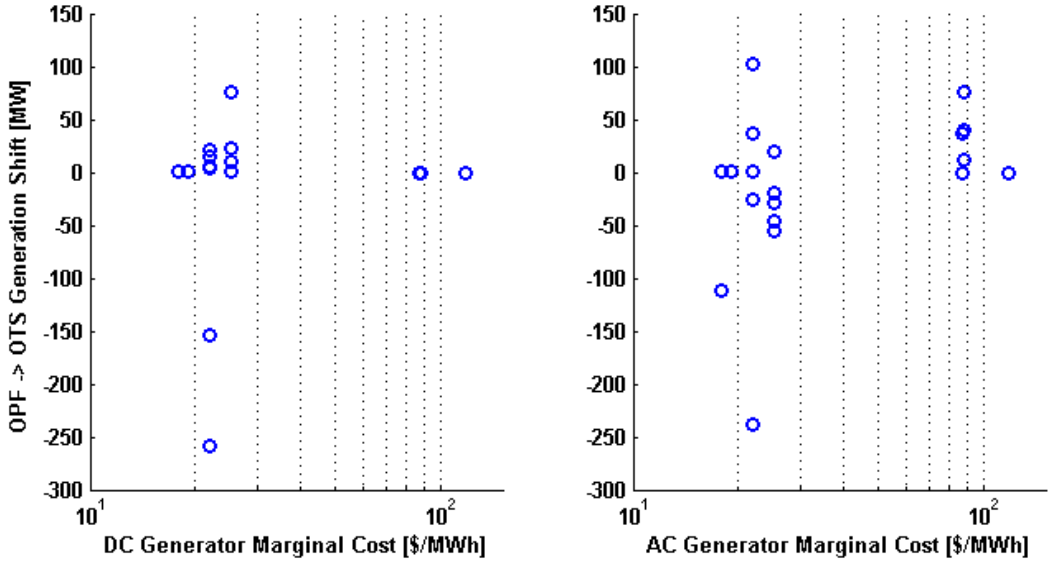

Figure 29: Marginal generator cost (horizontal axes) vs. change in generation output between OPF and OTS solutions in the DC model (left plot) and the AC model (right plot) for each generator in IEEE RTS-96 hour 24.

Table 12 shows the proportion of single transmission line outages that cause transmission line overloads in excess of 110% of the transmission line power flow ratings. In the un-switched

DCOPF and ACOPF models (calculated neglecting security constraints), 25% and 27% of transmission line outages cause transmission line power flow overloads. By comparison, the security violation rates for the AC feasible OTS results are generally lower than for the un-switched results. When security constraints are left out of the optimization model, generation is dispatched so that transmission line security violations are common. These ex-post transmission security analysis results show that OTS can reduce the occurrence of binding power flow constraints and thus reduce the proportion of line outages that cause overloads. Generalizing these results suggests that OTS (without security constraints) does not necessarily degrade transmission security.

Table 12: Ex-Post Security Violations in the RTS-96

	Un-switched	Maximum Resistance	Minimum Resistance	Maximum Reactance	Minimum Reactance	Random
DC Security Violation	25%	27%	0%	9%	0%	34%
AC Security Violation	27%	32%	11%	10%	8%	40%

5.4 Conclusions

Although OTS has shown great potential for cost savings in the linearized DC system model, concerns about system reliability of topologically reconfigured networks have remained. Due to the non-linearity and non-convexity of the ACOPF, the generation dispatch and topology optimization problem remains intractable in the AC power flow model. The uncertainty of AC system behavior under topological reconfigurations, particularly voltage magnitudes and reactive power flow behaviors, contributes to the concerns about OTS system reliability. This research presents a step toward understanding AC system reliability under optimal topology reconfigurations made in the DC model.

The analysis presented in Section 5.2 aims to generate feasible ACOPF solutions on topologically reconfigured networks by incrementally removing lines from the switchable set of transmission lines based on five selection criteria. The results show that removing the highest resistance lines from the switchable set (i.e. forcing high resistance lines to remain in service) generates feasible ACOPF solutions in fewer process iterations, relative to removing lines by other selection criteria. Additionally, when a feasible ACOPF solution is found, the cost savings over the un-switched ACOPF are significant when high resistance lines are removed from the switchable set. Removing the lowest resistance lines from the switchable set requires many more process iterations and tends to generate cost increases over the un-switched ACOPF. When compared to the maximum resistance, removing lines from the switchable set randomly or according to the minimum or maximum reactance values generates similarly positive cost savings but requires significantly more process iterations to achieve feasible ACOPF solutions. These results highlight the dependency of AC feasibility on certain lines; particularly high resistance lines. Additionally, the results here show that by screening for switchable lines, OTS

solutions obtained in the linearized DC model can translate to system cost savings in the AC model.

The ex-post transmission security analysis shows that in both the AC and DC power flow models, transmission line overloads can be less common in switched systems than in un-switched systems. Even with this relatively loose definition of transmission security, the results suggest that transmission topology reconfigurations do not necessarily degrade the security of the system.

This research presents the first known method to extend OTS results obtained in the DC power flow model to the more realistic AC power flow model. The method focuses on ensuring AC feasible power flow solutions. Specifically, the method is designed to correct steady-state voltage magnitude constraint violations caused by topology reconfigurations. The results show that the method also generates favorable cost savings in the AC network. Ultimately, this research demonstrates a voltage-corrected transmission switching method that is both feasible and still leads to system cost savings.

Chapter 6 The Smart Use of Infrastructure Resources

Total annual U.S. electricity revenues are approaching $400 Billion. In such an enormous industry, the savings potential for even miniscule efficiency improvements is vast. This research addresses just a few subjects in the quest to improve the effectiveness of reliably generating, transporting and distributing electrical energy. The "Grid of the Future" will incorporate emerging "Smart Grid" technologies to enhance the reliability, security, adaptability and efficiency of the electricity industry infrastructure [**90**]. By improving asset flexibility, sensing and communications, the smart grid provides degrees of control previously unavailable. The promise of an improved electrical system attracted $3.1 billion as part of the American Recovery and Reinvestment Act of 2009 [**91**]. As large investments increase the penetration of smart infrastructure, unlocking potential system performance improvements requires advances power system modeling and computation. This dissertation addresses a smart grid management procedure known as Optimal Transmission Switching.

6.1 Enabling Topological Flexibility

The potential for cost savings from the added flexibility of network topologies has long been highlighted in power systems literature. However, the paradigm shift to consider transmission assets as controllable has primarily been blocked by problems related to OTS tractability. This research improves OTS tractability by first highlighting the sources of the problem complexity and addressing each with solution methods that improve tractability without degrading solution quality. As a result, the primary concerns facing steady-state transmission topology reconfiguration have been addressed in this dissertation. Specifically, two critically important problems impeding the use of OTS in system operations have been addressed in this document.

6.1.1 The OTS problem is intractable on large power systems

As noted in previous literature (see Chapter 1), determining the optimal network topology for cost minimizing generation dispatch poses significant computational burden. Through decision variable screening and network partitioning methods developed here, the OTS problem complexity is reduced. The reduced OTS complexity enables significantly faster solution times and, for the first time, OTS is solved on a large power system model.

The OTS problem is most commonly formulated using a linearized DC power flow approximation. This simplification enables the solution of OTS problems on relatively small power systems. By examining various network and engineering properties of optimally switched networks, Chapter 2 demonstrates two useful properties for simplifying the OTS problem to obtain solutions faster and on larger networks. First, relatively few switches are required to generate the majority of OTS savings. And second, the effects of switching seem to be relatively localized. These two conclusions provide the basis for the heuristic solutions developed in Chapter 3 and Chapter 4.

The Mixed Integer Programming problem feasible solution space presented by OTS (formulated in the linearized DC power flow model) scales exponentially with the number of switchable transmission lines considered in the optimization. This property of the OTS problem combined with the conclusions of Chapter 2 informs the development of a switchable line limiting screen in Chapter 3. The results show that pre-screening for switchable lines significantly reduces the OTS computation time. Additionally, properly selecting switchable lines reduces computation times without degrading solution quality (savings). The ΔABC selection criterion outperforms (reduced computation time, increased savings) all other selection criteria. The improved tractability of the OTS problem achieved by pre-screening for switchable lines enables the solutions of OTS problems on significantly larger systems and the inclusion of

more stringent reliability constraints. Additionally, the observation from Chapter 2 that near optimal results are achieved by switching a small number of lines is confirmed through the progressive switching analysis. By limiting the number of switchable lines to only the top ranked by the ΔABC screening criterion, near optimal results are obtained in even less computation time. The ability to achieve near optimal results with just a few switchable lines demonstrates the diminishing returns to additional topological flexibility in the smart grid.

Despite the significant tractability improvements made by pre-screening the OTS problem, pre-screened OTS may still render impracticably large problems when applied to real world power systems. Drawing upon the second conclusion of Chapter 2, the partitioned switching in Chapter 4 further reduces problem complexity by defining boundaries that localize the effects of topology reconfigurations. This strategy employs the common practice of zonal power system analysis to solve the OTS problem on partitioned sub-networks in parallel. However, in most power system zones are defined arbitrary to system properties. Thus, the effects of control actions like transmission switching are not necessarily contained within a particular zone. By taking into account the properties of electrical networks, a partitioning method that clusters nodes based on a measure of electrical distance is developed. Electrical distance partitioning produces favorable partitioning results that reduce the occurrence of "transaction leakage". The concept of limiting transaction leakage is abstractly similar to localizing the effects of transmission switching. The results show that the partitioning methods that limit transaction leakage provide good results to limit the inter-zonal effects of transmission switching.

With zonal boundaries that limit the inter-zonal effects of transmission switching, OTS can be applied to mitigate transmission congestion within zones. This selective application of partitioned OTS allows the solution of several (significantly) smaller and independent OTS

problems that can be solved simultaneously. Solving partitioned OTS problems in parallel again reduces the problem complexity and enables OTS solutions on larger systems in reduced computation time. The combinatorial effects of search space reductions through switchable line screening and partitioning for parallel optimization vastly improves the OTS problem tractability. Ultimately, these complexity reducing methods enable solutions on larger systems in shorter computation times. Success is demonstrated in Chapter 4 where, for the first time, the generation dispatch and transmission topology co-optimization problem is solved on large power systems.

6.1.2 Topology modifications may cause constraint violations in the AC system

OTS solutions obtained in the linearized DC power flow model can produce network topologies that are infeasible in real electricity systems. Chapter 5 presents a method to correct OTS topologies to ensure feasible AC power flow solutions. In addition to feasibility, the method produces favorable cost savings results in the AC power flow model.

The AC power flow formulation provides a more realistic and significantly more complex model of power system behavior than the linearized DC power flow formulation. The additional complexity has, until now, prevented the simulation of OTS in an AC power flow model. The results presented in Chapter 5 confirm the cost savings potential of OTS solutions (obtained in the DC model) in the AC model. By determining which switchable lines cause AC feasibility problems, the developed methods serve to modify the switchable line screening presented in Chapter 3 to ensure AC feasible transmission switching results. The simulations, presented on the RTS-96 network, demonstrate the ability for screened OTS to produce reliable (in both AC and DC systems) and cost saving topology reconfigurations.

6.2 The Future of OTS

The additional control and flexibility offered by the smart grid brings relevance to many interesting research topics. Despite the potential improvements exhibited by flexible network topologies and OTS, system operators have been reluctant to exploit these enhanced control strategies. This dissertation addresses several of the issues associated with the optimal topology problem complexity; one class of problems associated with implementation of OTS. There are other classes of problems that represent fruitful areas for future research.

This dissertation focuses on steady state power system operations. However, electrical power systems are dynamical systems that balance continuously changing load and generation resources. As such, several issues related to the dynamic system and component response to topology reconfigurations must be addressed to enable widespread adoption of OTS procedures. Dynamic power system analysis is defined by three time horizons: short-term (*time scale of cycles to tens of seconds*), medium-term (*tens of seconds – several minutes*), and long-term (*>several minutes*). Each time scale focuses on the responses of particular system elements based upon the response time of such elements. The dynamic behavior of a system element is considered constant if its response time is well beyond the time scale of interest. Likewise, the dynamic behavior of a particular element is considered instantaneous if its response time is miniscule in comparison to the time scale of interest. An event, such as the act of switching on or off a transmission line, would create surges in voltages and currents that propagate throughout the network. The behavior of propagations determines the short term element response necessary to maintain stability. The new network topology created by transmission switching ultimately enables a long term response in the form of generator dispatch changes. In the medium term, system constraints must be respected while generators adjust to the new dispatch levels. Each model requires dynamic data on the particular elements of interest. In order to

completely characterize the system responses to transmission switching actions, several analyses with complete system data would be required.

The linearized DC approximation is the most common linearization of complex power flows through a network. The shortcomings of the DC model are addressed at length in Chapter 5. While a method is developed that achieves reliable OTS solutions in both the AC and linearized DC power flow models. Solving the complete topology and generation dispatch co-optimization in the AC power flow model remains intractable given the current state of optimization technology. However, recent developments in power systems research have produced a linear model of AC power flow that approximates both real and reactive power flows in addition to voltage magnitudes [**89**]. Incorporating OTS into such a model requires some significant reformulation to include integer breaker status variables on both ends of transmission lines. This formulation would allow switching actions on the 'to' end, 'from' end or both ends of transmission lines to allow lines to behave as capacitive elements while removed from service. The additional integer variables and the more realistic power flow model would add to OTS problem complexity but could provide solutions that are more representative of actual complex power flows.

Thus far in the evolution of optimal transmission switching the benefits of topology modifications have been relatively narrowly defined. The state of the art of OTS considers a system cost objective function. By relaxing this narrow benefit definition several interesting and open research questions arise; such as whether OTS implementation would increase emissions or energy losses through transmission lines. Additional market analyses of OTS could assess whether transmission switching can reduce instances of market power. Reliability and security improvements may also be possible through significant problem reformulation. These research

directions will undoubtedly benefit from the tractability improvements presented in this document.

Appendix

Appendix A Primer on Power System Analysis

Electricity is a common medium for the transportation of energy. Energy can be converted from mechanical or chemical energy to electrical energy and transmitted as a flow of electrons through wires to a destination where it can be converted back to a useful form of energy such as heat, light or motion. We typically refer to the process of converting some form of energy to electrical energy as generation, and the use or consumption of electrical energy as load. The rate at which electric energy is transferred from generation to load is known as electric power, or electric power flow. To maintain a reliable system, total system generation must be equal to load at all times. This energy balance requires that we generate and transport enough power to meet consumer demand at all times. The limited capacity of the transmission system provides a constraint that often limits the amount of power that can be generated at particular locations and injected into the transmission network. In order to solve the problem of meeting consumer demand under transmission constraints, we must first understand the effect of transmission capacity constraints on the utilization of generation sources. In other words, we need to perform "power flow" calculations that describe the electricity flow through each transmission line due to a pattern of injections by generators. This Appendix outlines the mathematical and physical foundations of power flow calculations. Since power flow is nonlinear, these calculations can be quite complex. This Appendix also outlines some simplified power flow models often used by power system engineers.[3] The following nomenclature is used throughout this Appendix:

[3] In the completion of this Appendix I have drawn broadly from three sources [**16**,**59**,**115**].

Variables		*Parameters*	
$v(t)$	*time varying voltage*	$\tilde{Z}$	*complex impedance*
$i(t)$	*time varying current*	X	*Reactance*
V	*peak voltage magnitude*	R	*Resistance*
I	*peak current magnitude*	Z	*impedance magnitude*
θ	*voltage phase angle*	Y	*Admittance*
φ	*current phase angle*	G	*Conductance*
t	*Time*	B	*Susceptance*
ω	*radial frequency*	j	$(\sqrt{-1})$ *imaginary number*
$p(t)$	*time varying power*		
P	*average power*		
Q	*reactive power*		
S	*complex power*		
F_{ik}	*power flow along line connecting nodes i and k*		
i,k,r	*bus indices*		

In the U.S., the vast majority of the electrical generation, transmission and distribution systems are alternating current (AC) systems. In AC systems, the voltage (v) and current (i) magnitudes are time-variant, usually in the form of a sine wave. In the U.S. the voltage and current waveforms alternate at a frequency (*f*) of 60 Hz. Voltage is a measure of electrical potential and is analogous to water pressure in a pipe. Similarly, current is a measure of the rate of flow of electric charge and is analogous to water flow in a pipe system.

$$v(t) = V\sin(\omega t - \theta) \qquad (84)$$

$$i(t) = I\sin(\omega t - \varphi) \qquad (85)$$

Equations (84) and (85) represent the time varying waveforms of voltage and current where $\omega=2\pi f$ is the radial frequency of the waveform, V and I are the magnitudes of the sinusoidal voltage and current respectively, θ is the phase angle by which the voltage waveform is shifted

from a reference value, and φ is the phase angle difference between the voltage and current waveforms. We often use the voltage waveform as a reference, setting $\theta=0$ and allowing us to write the voltage equation as:

$$v(t) = V\sin(\omega t) \tag{86}$$

The time varying value known as instantaneous power flow is calculated as the product of the voltage and current:

$$p(t) = v(t)i(t) = VI\sin(\omega t)\sin(\omega t - \varphi) \tag{87}$$

Using the product-to-sum trigonometric identity:

$$\sin u \sin v = \frac{1}{2}[\cos(u - v) - \cos(u + v)] \tag{88}$$

and the angle difference trigonometric identity:

$$\cos(u \pm v) = \cos u \cos v \mp \sin u \sin v \tag{89}$$

we can rewrite the instantaneous power equation as:

$$p(t) = \frac{VI}{2}\cos(\varphi)\left(1 - \cos(2\omega t)\right) - \frac{VI}{2}\sin(\varphi)\sin(2\omega t) \tag{90}$$

This power waveform oscillates around an average value known as the average power. The average power is often referred to as "real" power since it is the quantity that is measured for metering purposes. Integration with respect to time of the instantaneous power waveform over one complete cycle yields the average power equation:

$$P = \frac{VI}{2}\cos(\varphi) \tag{91}$$

Equation (89) shows that the average power is always positive and stems from the first term of equation (88). Since the real power flowing to a load is always positive, this is the quantity that is measured for metering purposes. Figure 30 represents the waveforms of an AC voltage, current and the resulting instantaneous and average power.

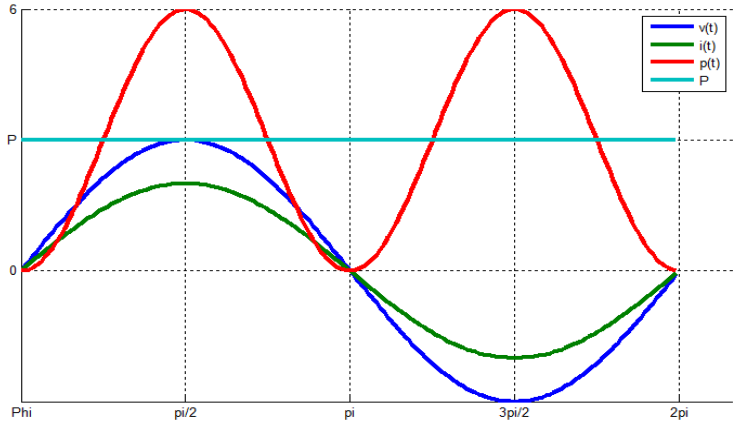

Figure 30: Voltage current and power waveforms (θ=0, φ=0)

When a phase difference exists between the voltage and current (i.e., when φ in equation (85) is nonzero), reactive power is generated. While real power represents a positive net energy flow from generation to load, reactive power flows equally in both directions and thus the net energy flow due to reactive power is zero. The second term of equation (90) represents the reactive power component of the instantaneous power and expresses the alternating flow of energy toward and away from the load. The magnitude of the reactive power (Q) is calculated as:

$$Q = \frac{VI}{2}\sin(\varphi) \qquad (92)$$

We can use Euler's Theorem to express the magnitudes of the terms of equation (90) by combining equations (91) and (92) into a complex number known as complex power (S). This transformation is often used in the simulation of large power systems (especially before the availability of modern, high-speed computing) since calculations involving complex numbers are computationally easier than calculations involving sine and cosine. Where $j = \sqrt{-1}$, the complex power is given by:

$$S = P + jQ \quad (93)$$

While the analogies for water flow and pressure in a plumbing system hold for voltage and current in a power system, the concept of complex power has no such direct analogy. There are several loose analogies for complex power. Perhaps the most accurate analogy is constructed by imagining filling a water tank by carrying buckets of water up a ladder and dumping them in the tank. Each time you climb a latter with a bucket full of water, you do work. If you come back down the ladder with that same bucket of water, work has been done on you and from an energy conservation standpoint; the net work exerted is zero. If you climb to the top of the ladder and dump the bucket of water into the tank and then return down the ladder with an empty bucket you have exerted a net positive amount of work. Climbing the ladder and dumping the water in the tank before returning with an empty bucket is analogous to real power flow. Similarly, climbing the ladder with a full bucket and returning down the ladder with a full bucket is analogous to reactive power.

The materials that make up electric transmission lines cannot transfer power with perfect efficiency; all transmission lines exhibit some resistance, or "impedance" to increased current flow. Transmission lines with higher impedance are more inefficient, losing more of the injected power in the form of heat. These losses are known as "resistive losses." The electrical impedance that characterizes transmission lines is governed by several physical characteristics of the transmission line including: length, height, diameter, line spacing, materials and other design parameters. The electrical property that describes the difficulty to transmit AC electricity across a transmission line is the complex impedance ($\tilde{Z}$) which is constructed with the real component expressing resistance (R) and the imaginary component expressing the reactance (X):

$$\tilde{Z} = R + jX \quad (94)$$

$$Z = \sqrt{R^2 + X^2} \qquad (95)$$

The resistance of the line determines the electrical losses incurred, and the reactance measures the strength of the line's magnetic field due to a current flow across the line. We also define several complementary measures of how easily current flows over a transmission line: the admittance of the line is $Y = Z^{-1}$, the conductance of the line is $G = R^{-1}$ and the susceptance of the line is $B = X^{-1}$.

The power flow across a transmission line in an AC power network is determined by Kirchhoff's Laws and Ohm's Laws. To describe these flows mathematically, we will need a concept known as the "power factor angle". The power factor angle (φ) is defined as the ratio of real power to complex power and is equivalent to the phase angle difference between the current and voltage waveforms defined in equation (85). The power factor angle induced by a current flowing across a transmission line is given by:

$$\varphi = \cos^{-1}\left(\frac{R}{Z}\right) = \sin^{-1}\left(\frac{X}{Z}\right) \qquad (96)$$

Using Ohm's Law ($I = V/\tilde{Z}$), we can write the real power flow across a transmission line connecting node *i* to node *k* as a function of the voltage phase angle difference between nodes *i* and *k*:[4][5]

$$F_{ik} = \frac{V_i V_k}{\tilde{Z}_{ik}}\left[\cos(\varphi_{ik}) - \cos\left(\varphi_{ik} - (\theta_i - \theta_k)\right)\right] \qquad (97)$$

[4] Double Subscript Notation: The order of subscripts represents the direction of flow of current between two nodes when the current is considered to be positive. When applied to voltages, this notation represents the voltage difference between the node identified by the first subscript and the voltage of the node identified by the second subscript. For instance, I_{ab} denotes a positive current flowing from node *a* to node *b*, and V_{ab} denotes the voltage of node *a* with respect to the voltage of node *b*, or $V_{ab}=V_a-V_b$. Similarly, Z_{ab} denotes the impedance between nodes *a* and *b*, and F_{ab} denotes the positive flow of power from node *a* to node *b*.

[5] Note that in equation (97) we are no longer assuming that $\vartheta=0$ as we were in equation (86).

The AC power flow equation in equation (97) is highly nonlinear, making fast power flow calculations difficult. Making the following assumptions, we can approximate the power flow across a transmission line so that we may study a grid of transmission lines more easily.

1. Nominal voltage assumption: The voltage is normalized to 1 per-unit[6] and thus there is no voltage drop across a transmission line.

   $V_i = V_k = 1$

2. Lossless flow assumption: We assume that transmission lines have a resistance of zero; thus, resistive losses are also zero. This assumption is justified by the fact that resistances of transmission lines are often orders of magnitude smaller than the reactances.

   $R \ll X \Rightarrow R \ll Z \Rightarrow \frac{R}{z} \approx 0 \Rightarrow \cos(\varphi) = 0$

3. Small angle assumption: The difference between voltage phase angles at nodes *i* and *j* is small.

   $\theta_i \approx \theta_k \Rightarrow \sin(\theta_i - \theta_k) \approx (\theta_i - \theta_k)$

By assumption 1, we can rewrite (97):

$$F_{ik} = \frac{1}{\tilde{Z}_{ik}}\left[\cos(\varphi_{ik}) - \cos\left(\varphi_{ik} - (\theta_i - \theta_k)\right)\right] \quad (98)$$

The angle difference trigonometric identity allows us to write:

$$F_{ik} = \frac{V_i V_k}{\tilde{Z}_{ik}}[\cos(\varphi_{ik}) - (\cos(\varphi_{ik})\cos(\theta_i - \theta_k) + \sin(\varphi_{ik})\sin(\theta_i - \theta_k))] \quad (99)$$

Invoking assumption 2 yields:

[6] Per-unit measurements refer to the expression of system voltages as a fraction of a defined base quantity. For example, if the base quantity in question were 110 kV, all voltages would be defined as $V_{pu}=V/110kV$.

$$F_{ik} = \frac{1}{X_{ik}} \sin(\theta_i - \theta_k) \qquad (100)$$

And finally, assumption 3 enables us to approximate the power flow along a line as:

$$F_{ik} = \frac{1}{X_{ik}} (\theta_i - \theta_k) = B_{ik}(\theta_i - \theta_k) \qquad (101)$$

These approximations are known as the linearized decoupled (DC) power flow approximations. The DC power flow enables a relatively fast solution for the flow across each transmission line in a complicated network with reasonable accuracy. Equation (97) shows that the power flow through a transmission line is a function of the voltage phase angles at the nodes connected by the line and the susceptance of the line. The larger the difference between nodal voltage angles, the greater potential for power flow along that line. In order to calculate the amount of power flowing through each transmission line in a network, we must first simultaneously calculate the voltage phase angles at each node in the network.

In the simplest form, power network models are made up of electrical busses (nodes) connected by transmission lines (branches). Busses simply represent the ends of a transmission line and can take the form of transmission line junctions, locations of electrical load, locations of electrical generation or some combination thereof. We model the network as a circuit where electricity is generated, flows through a network of transmission lines, and is consumed by electrical loads. Electricity flows through the network according to Kirchhoff's laws which state that the sum of all currents into and out of a bus must be equal to zero (*Kirchhoff's Current Law - KCL*) and the sum of all voltage differences around a closed loop in the circuit must be equal to zero (*Kirchhoff's Voltage Law - KVL*). When parallel paths exist for electricity flow, Kirchhoff's laws dictate that the flow along each path is determined by the relative impedance of the path. For example, suppose 2 parallel paths exist between nodes 1 and 2, path A and path B. Path A

has an impedance three times larger than the impedance of B. Any power injection at node 1 to serve a load at node 2 would result in a flow across the two parallel paths. The flow along path B will be three times larger than the flow along path A. In more complex and realistic networks, the existence of "loops" in the transmission topology means that we cannot use intuitive calculations to determine power flows. In order to solve for the power flow across each line in a complex network, we must solve equation (97) simultaneously for every node in the network. Additionally, Kirchhoff's laws dictate that that the net amount of power generated or consumed at a bus must flow through the transmission lines connected to that bus. This power balance requirement in conjunction with equation (97) results in the linearized DC power flow equation:

$$P_i = \sum_{k=1}^{N} B_{ik}\theta_{ik} = P_{Gi} - P_{Di} \quad \forall\, i \qquad (\ 102\ )$$

Where P_i denotes the net power generated (P_{Gi}) and consumed (P_{Di}) at bus i, and the susceptance of each line is represented in the B matrix. The entry B_{ik} corresponding to the i^{th} row and the k^{th} column in the B matrix represents the susceptance of the transmission line connecting bus i and bus k. The diagonal elements of the B matrix represent the self susceptances which are calculated as the negative sum of the susceptances of all of the lines connected to bus i. When there is no direct connection between bus i and bus k the corresponding B entry is equal to zero.

The power flow problem in a complex network (larger than 3 nodes, $n>3$) presents many challenges. The power generated at several different points in the network flows through all parallel paths to the loads. In order to solve for the flow across any transmission line in the network, we must also solve for the flow across all other transmission lines in the network. In a system with N busses, the system of equations given by equation (102) generates N equations with N unknown bus voltage angles (θ).

$$\begin{array}{rcl} P_1 & = & B_{11} + B_{12}\theta_{12} + \cdots + B_{1n}\theta_{1n} \\ P_2 & = & B_{21}\theta_{21} + B_{22} + \cdots + B_{2n}\theta_{2n} \\ \vdots & \vdots & \vdots \\ P_n & = & B_{n1}\theta_{n1} + \cdots + B_{n,n-1}\theta_{n,n-1} + B_{nn} \end{array} \quad (103)$$

However, the system of linear equations is not independent and thus any solution will render each θ_i as a function of all $\theta_{k\neq i}$. That is, the DC power flow equations are *underidentified.* Therefore, power systems analysis generally assumes that the voltage angle at one generator bus is controlled to a specified value. This bus is referred to as the "slack bus." By controlling the voltage angle at the slack bus to maintain a constant value (usually θ=0) one of the equations in the above system becomes unnecessary and we obtain an independent system of N-1 equations with N-1 unknowns.

Given the quantities of power generation and load at each point in the network, we are now able to solve for the power flow through each transmission line in the network. A useful tool in power system analysis, particularly in the linearized DC approximation of the power flow equations, is the sensitivity factors[7]. The sensitivity factors measure the change in power flows across each transmission line due to a change in a power injection at any bus in the network. The sensitivity factors depend only on the elements of the B matrix and thus are static (do not change with system state) in the DC approximation. Rearranging the system of equations given by equation (102) and substituting into equation (101) yields:

$$\theta = B^{-1}P \quad (104)$$

$$F_{ik} = B_{ik}(B_{ir}^{-1}P_r - B_{kr}^{-1}P_r) \quad (105)$$

[7] The sensitivity factors are also referred to as the power flow sensitivities, power transfer distribution factors (PTDF) and shift factors.

where $B_{ir}^{-1}$and B_{kr}^{-1} correspond to the $(i,r)^{th}$ and $(k,r)^{th}$ entries of the inverse of the B matrix, while B_{ik} represents the susceptance of the transmission line connecting bus *i* and bus *k.* Differentiating with respect to P_r we can solve for the line flow sensitivity factors:

$$\frac{\partial F_{ik}}{\partial P_r} = B_{ik}(B_{ir}^{-1} - B_{kr}^{-1}) \ \forall \ i,k,r \qquad (106)$$

With the line flow sensitivity factors, we can analyze the change in flow across a transmission line due to power injections anywhere in the network. This analysis proves useful when allocating generation to relieve transmission constraints.

The power system concepts, linearized DC power flow calculations and line flow sensitivity factors outlined in this document provide the reader with a basic foundation for the understanding of power systems analysis. The analysis that I have outlined here is commonly found in the power systems literature and is used in my candidacy proposal to demonstrate some relevant concepts on an example network.

Appendix B Electrical Distance Clustering

B.1 Electrical Distance Metric

The calculation of an electrical distance follows similarly to that of "resistance distance" in [**92**]. A network of resistors with current injections at each node can be described by a conductance matrix G, such that the current injection at node a is:

$$I_a = \sum_{b=1}^{n} g_{ab} V_b \qquad \textbf{(107)}$$

Similar to the system of equations in (103), the matrix G is underdefined. Again, we define a reference node, r to maintain a voltage $V_r = 0$. The sub-matrix of G associated with the non-reference nodes ($\bar{r}$), $G_{\bar{r}\bar{r}}^{-1}$, is full rank. Therefore we can compute the voltages associated with non-reference nodes:

$$V_{\bar{r}} = G_{\bar{r}\bar{r}}^{-1} I_{\bar{r}} \qquad \textbf{(108)}$$

$g_{a,a}^{-1}$ represents the diagonal element of $G_{\bar{r}\bar{r}}^{-1}$ associated with node a describing the change in voltage difference between nodes a and r due to a current injection at node a and a corresponding current removal at node r. Thus the electrical distance between a and r is $g_{a,a}^{-1} \forall a$. To measure the distance between nodes a and b, where $a \neq b \neq r$, one can evaluate:

$$e(a,b) = g_{a,a}^{-1} + g_{b,b}^{-1} - g_{b,a}^{-1} - g_{a,b}^{-1} \qquad (109)$$

which gives the voltage difference between a and b after unit injection at a and corresponding removal from b. In matrix from, where $diag(G_{\bar{r}\bar{r}}^{-1})$ represents a matrix with diagonal elements $g_{a,a}^{-1} \forall a \neq r$, and off-diagonal elements equal to zero, and [1] denotes a matrix where all elements are equal to one, the electrical distance matrix calculations follow:

$$E_{\bar{r}\bar{r}} = [1] diag(G_{\bar{r}\bar{r}}^{-1}) + diag(G_{\bar{r}\bar{r}}^{-1})[1] - G_{\bar{r}\bar{r}}^{-1} - [G_{\bar{r}\bar{r}}^{-1}]^T \qquad (110)$$

$$E_{r\bar{r}} = diag(G_{\bar{r}\bar{r}}^{-1}) \qquad (111)$$

$$E_{\bar{r}r} = diag(G_{\bar{r}\bar{r}}^{-1}) \quad (112)$$

where $E_{\bar{r}r}$ refers to vector of non-reference elements in the reference column of the distance matrix. As mentioned in Appendix A, the resistance term of the edge (transmission line) impedance in power networks is typically dominated by the reactance term. In AC power networks, this property allows us to approximate the sensitivity of nodal voltage phase angles (θ) to changes in real power injections (P):

$$\Delta P = \left[\frac{\partial P}{\partial \theta}\right] \Delta\theta. \quad (113)$$

By setting $G = [\partial P/\partial\theta]$ in (110), (111) and (112), the distance matrix (E) is similar to "resistance distance", but measures the incremental changes in phase angle differences due to power transactions rather than voltage magnitude changes resulting from current injections. In the dc power flow model [**93**], the quadrant of the Jacobian matrix that represents the sensitivity $[\partial P/\partial\theta]$ is simply equal to the system susceptance matrix B. Using the pseudo-inverse of $[\partial P/\partial\theta]$, we can write the electrical distance matrix in elementary form independent of reference bus definitions:

$$e(a,b) = B_{a,a}^{-1} + B_{b,b}^{-1} - B_{b,a}^{-1} - B_{a,b}^{-1} \quad (114)$$

Equations (109) - (113) describe a measure of electrical distance *e(a,b)*, given a sensitivity matrix G. This discussion describes the conditions under which *e(a,b)* qualifies as a proper distance metric in some metric space. Following [**94**], [**92**], a distance metric *e(·)* on an arbitrary metric space satisfies the following properties, for all *a*, *b*, *c*:

- Symmetry: $e(a,b) = e(b,a)$
- Identity: $e(a,b) = 0 \iff a = b$
- Non-Negativity: $e(a,b) \geq 0$

- Triangle Inequality: $e(a,b) + e(b,c) \geq e(a,c)$

The last of these properties, the triangle inequality, will be the main focus of this discussion. Lagonotte ([**78**]) found that an electrical distance measure related to voltages generally, but not always, obeyed the triangle inequality. Here a similar finding is demonstrated for an analogous distance measure which is based upon real power sensitivities. Building on [**78**], the conditions are characterized under which the triangle inequality will fail to hold for this electrical distance measure.

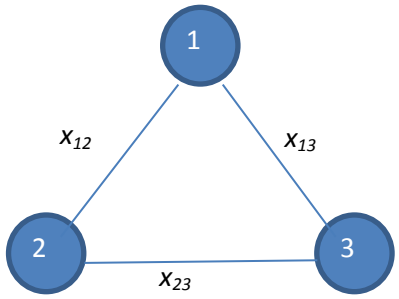

Figure 31: Connected 3 node with arbitrary branch reactances

For the connected network shown above we have line reactances x_{ij}. We can thus construct the full susceptance matrix *B:*

$$B = \begin{bmatrix} \frac{-1}{x_{12}} + \frac{-1}{x_{13}} & \frac{1}{x_{12}} & \frac{1}{x_{13}} \\ \frac{1}{x_{12}} & \frac{-1}{x_{12}} + \frac{-1}{x_{23}} & \frac{1}{x_{23}} \\ \frac{1}{x_{13}} & \frac{1}{x_{23}} & \frac{-1}{x_{13}} + \frac{-1}{x_{23}} \end{bmatrix}$$

In this example, we are ignoring line resistances, enabling us to write the sensitivities of bus voltage angle differences $(\theta_i - \theta_j)$ to a change in power flow as:

$$\frac{d(\theta_i - \theta_j)}{dP_{i \to j}} = B_{ij}^{-1}$$

Where the elements of B^{-1} are calculated by incrementally removing the i^{th} row and the i^{th} column from B to form $B_{\prime i}$. The diagonal elements of $B_{\prime i}^{-1}$ form the off diagonal elements of the column $B_{.i}^{-1}$.

$$B_{\prime 1} = \begin{bmatrix} -- & -- & -- \\ -- & \frac{-1}{x_{12}} + \frac{-1}{x_{23}} & \frac{1}{x_{23}} \\ -- & \frac{1}{x_{23}} & \frac{-1}{x_{13}} + \frac{-1}{x_{23}} \end{bmatrix}$$

$$B_{.1}^{-1} = \begin{bmatrix} 0 \\ \frac{\frac{-1}{x_{13}} + \frac{-1}{x_{23}}}{\left(\frac{-1}{x_{12}} + \frac{-1}{x_{23}}\right)\left(\frac{-1}{x_{13}} + \frac{-1}{x_{23}}\right) - \frac{1}{x_{23}}\frac{1}{x_{23}}} \\ \frac{\frac{-1}{x_{12}} + \frac{-1}{x_{23}}}{\left(\frac{-1}{x_{12}} + \frac{-1}{x_{23}}\right)\left(\frac{-1}{x_{13}} + \frac{-1}{x_{23}}\right) - \frac{1}{x_{23}}\frac{1}{x_{23}}} \end{bmatrix}$$

$$B_{.2}^{-1} = \begin{bmatrix} \frac{\frac{-1}{x_{13}} + \frac{-1}{x_{23}}}{\left(\frac{-1}{x_{12}} + \frac{-1}{x_{13}}\right)\left(\frac{-1}{x_{13}} + \frac{-1}{x_{23}}\right) - \frac{1}{x_{13}}\frac{1}{x_{13}}} \\ 0 \\ \frac{\frac{-1}{x_{12}} + \frac{-1}{x_{13}}}{\left(\frac{-1}{x_{12}} + \frac{-1}{x_{13}}\right)\left(\frac{-1}{x_{13}} + \frac{-1}{x_{23}}\right) - \frac{1}{x_{13}}\frac{1}{x_{13}}} \end{bmatrix}$$

$$B_{.3}^{-1} = \begin{bmatrix} \frac{\frac{-1}{x_{12}} + \frac{-1}{x_{23}}}{\left(\frac{-1}{x_{12}} + \frac{-1}{x_{13}}\right)\left(\frac{-1}{x_{12}} + \frac{-1}{x_{23}}\right) - \frac{1}{x_{12}}\frac{1}{x_{12}}} \\ \frac{\frac{-1}{x_{12}} + \frac{-1}{x_{13}}}{\left(\frac{-1}{x_{12}} + \frac{-1}{x_{13}}\right)\left(\frac{-1}{x_{12}} + \frac{-1}{x_{23}}\right) - \frac{1}{x_{12}}\frac{1}{x_{12}}} \\ 0 \end{bmatrix}$$

The resulting B^{-1} matrix:

$$B^{-1} = \begin{bmatrix} 0 & \frac{-x_{12}(x_{13}+x_{23})}{x_{12}+x_{13}+x_{23}} & \frac{-x_{13}(x_{12}+x_{23})}{x_{12}+x_{13}+x_{23}} \\ \frac{-x_{12}(x_{13}+x_{23})}{x_{12}+x_{13}+x_{23}} & 0 & \frac{-x_{23}(x_{12}+x_{13})}{x_{12}+x_{13}+x_{23}} \\ \frac{-x_{13}(x_{12}+x_{23})}{x_{12}+x_{13}+x_{23}} & \frac{-x_{23}(x_{12}+x_{13})}{x_{12}+x_{13}+x_{23}} & 0 \end{bmatrix}$$

$$e(a,b) = B_{a,a}^{-1} + B_{b,b}^{-1} - B_{b,a}^{-1} - B_{a,b}^{-1}$$

$$= \begin{bmatrix} 0 & \frac{x_{12}(x_{13}+x_{23})}{x_{12}+x_{13}+x_{23}} & \frac{x_{13}(x_{12}+x_{23})}{x_{12}+x_{13}+x_{23}} \\ \frac{x_{12}(x_{13}+x_{23})}{x_{12}+x_{13}+x_{23}} & 0 & \frac{x_{23}(x_{12}+x_{13})}{x_{12}+x_{13}+x_{23}} \\ \frac{x_{13}(x_{12}+x_{23})}{x_{12}+x_{13}+x_{23}} & \frac{x_{23}(x_{12}+x_{13})}{x_{12}+x_{13}+x_{23}} & 0 \end{bmatrix} \quad (115)$$

Applying the triangle inequality to (115), for each of the three triplets, leads to the following sufficient condition on the three reactances:

$$(x_{12}x_{23} \geq 0 \cap (x_{12}+x_{23}+x_{13}) > 0) \cup (x_{12}x_{23} < 0 \cap (x_{12}+x_{23}+x_{13}) < 0)$$

which is clearly satisfied for a strictly positive set of reactances. Figure 32 shows the surface in x_{12}, x_{13}, x_{23} space where violations of the triangle inequality are observed, for all combinations of $x_{ab} \in [-1, 1]$. Areas of the surface where $e(a,b) + e(b,c) - e(a,c) < 0$ were shaded, showing combinations of x_{12}, x_{13}, x_{23} that yielded triangle inequality violations. Otherwise, if one or more of the branch reactances is less than zero, a violation may occur. As in [**78**], we empirically find that E, thus defined, satisfies the properties of a distance matrix so long as all series branch reactances are non-negative, which would be the case with transmission lines with large series capacitors.

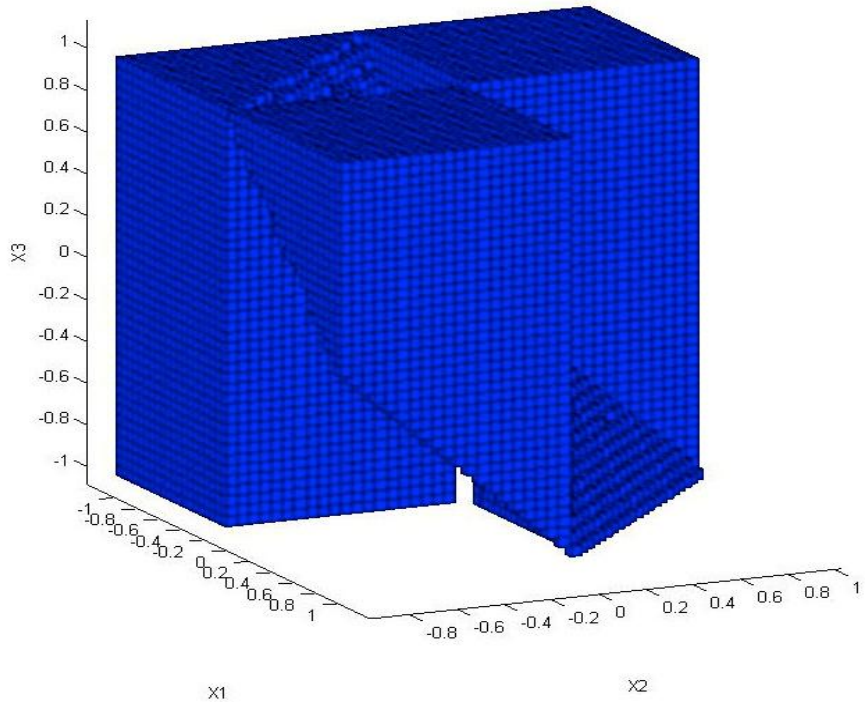

Figure 32: Illustration of the conditions under which three reactances x12, x23, x13 connecting a three bus network satisfy the triangle inequality. Combinations that result in a triangle inequality violation are shaded.

Using this metric we can define a measure that is roughly analogous to node degree, but for a fully connected network with continuous weights for each node pair. To do so we measure the average distance from each node *a* to other nodes in the system:

$$< e_a \geq \sum_{b=1}^{n} \frac{e_{ab}}{n-1} \qquad (116)$$

and to invert it to obtain a measure of electrical centrality (modified from [**95**]):

$$c_a = \frac{1}{< e_a >} \qquad (117)$$

B.2 Measures of Clustering Quality

In order to validate the clustering solutions obtained from a clustering algorithm, a measure of aggregate clustering quality is necessary. While quality measures will vary in importance

based on the application, the following measures are useful as a starting point. In this section we describe four measures of clustering quality, for a system of n nodes with p clusters. The first quality metric is based on the electrical cohesiveness (as discussed in section 4.1), the second and third measure the extent to which the clusters are appropriately sized, and the fourth index measures connectedness. For simplicity, each index is normalized to fit within the range [0,1] with 1 indicating the highest quality.

B.2.1 Electrical Cohesiveness Index (ECI)

The electrical cohesiveness index (ECI) measures the extent to which the buses within each cluster are electrically proximate to other cluster members, and thus measures the extent to which phase angles within a cluster will react in concert given a change in power injections in the network. The ECI measure is essentially a normalized version of (50). ECI evaluates to one when all nodes are in separate clusters ($p = n$), because every node is "perfectly" connected to every other node in each cluster. ECI evaluates to zero when all nodes are in one cluster, reflecting the fact that randomly chosen node pairs within very large clusters are, on average, very far electrically from one another. With these endpoints we define ECI as follows:

$$ECI = 1 - \frac{\hat{e}(C)}{\hat{e}_{max}} = 1 - \frac{\sum_{i=1}^{n} \sum_{j \in M_i} e_{ij}}{\sum_{i=1}^{n} \sum_{j=1}^{n} e_{ij}} \qquad (118)$$

In (118), the numerator is the sum of distances within each cluster, while the denominator is the sum of the pairwise distances between all buses in the network.

B.2.2 Between-Cluster Connectedness Index (BCCI)

The between-cluster connectedness index (BCCI) measures the extent to which buses in different clusters are loosely connected to one another. Unlike ECI, BCCI evaluates to one when all nodes are in the same cluster, because there are no cross-cluster connections. For an

atomistic solution (p = n), BCCI is zero because all nodes are strongly connected to nodes outside of their clusters. This bounded BCCI is defined as:

$$BCCI = 1 - \frac{h(C)}{h_{max}} = \frac{\sum_{i=1}^{n} \sum_{j \notin M_i} \frac{1}{e_{ij}}}{\sum_{i=1}^{n} \sum_{\substack{j=1 \\ j \neq i}}^{n} \frac{1}{e_{ij}}} \quad (119)$$

In (119), the numerator is the sum of connection strengths within each cluster, while the denominator is the maximum possible $h(C)$.

B.2.3 Cluster Count Index (CCI)

The cluster count index measures the proximity of the number of clusters in a given clustering solution, p, to a predetermined ideal number of clusters, p_*. p_* is a user-defined parameter exogenous to the method of defining clusters; here we assume that the user has some prior notion of the ideal number of clusters. We define CCI using the shape of the log- normal probability density function with its mode set at p_*, as follows:

$$CCI = e^{\frac{-(\ln\rho - \ln\rho_*)^2}{2\sigma^2}} \quad (120)$$

where $\sigma = \omega \ln(n)$. We choose the log-normal density function because it is a simple density function that has the desired properties for our application; the use of other density functions including flexible functions such as the Weibull function would certainly be possible. CCI thus has a support of [0, ∞] and evaluates to one when the number of clusters is equal to p_*. CCI approaches zero as the number of clusters approaches zero or infinity. ω is a parameter that sets the width of the fitness function relative to n; that is, ω is effectively a penalty factor for deviating from the ideal number of clusters.

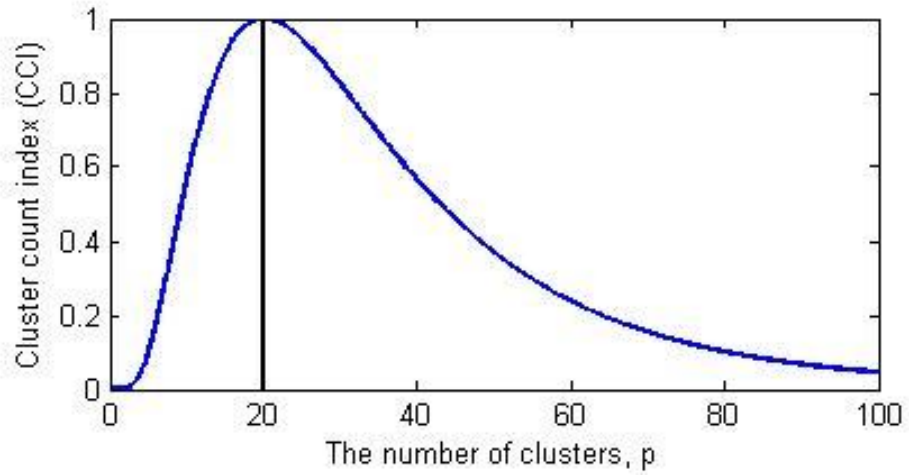

Figure 33: Illustration of the cluster count index, which is similar in shape to the cluster size index. Here ω =0.1 and n = 4458 (The size of the PJM system used)

A relatively large value for ω indicates a small penalty factor, while a small value for ω produces a larger penalty factor as shown in Figure 33. In the examples used in this Section we set ω to 0.05. Smaller values will effectively narrow the set of possible solutions to those that have almost exactly p_* clusters, which could lead to convergence problems for the Genetic Algorithm (Section B.3.4) by penalizing deviations from the optimal number of clusters too heavily. An extremely small value of ω is thus approximately equivalent to defining CCI as a binary variable, equal to one if $p = p_*$ and zero otherwise. Defining CCI in this way is certainly possible within the scope of our clustering method, but in the particular applications that follow we are interested in the impact of relaxing the constraint on CCI somewhat. Large values of ω, on the other hand, produce small penalties for deviating from the desired number of clusters. In this case, other quality metrics could dominate CCI (in a way that is not intended by the user), potentially leading to trivial solutions.

B.2.4 Cluster Size Index (CSI)

The Cluster Size Index (CSI) is similar to the Cluster Count Index in that it uses the shape of the log-normal distribution with its mode at the optimal value. CSI measures the deviation from

ideal cluster sizes. As with CCI, the ideal number of clusters is assumed to be a user-defined parameter. To obtain CSI we measure the size of each cluster, and then obtain a weighted average of cluster sizes:

$$\bar{s} = \sum_{i=1}^{n} s_i / n \qquad (121)$$

where s_i is the size of the cluster that node i resides in. The optimal cluster size is defined as $s_* = n/p_*$. We thus define CSI as:

$$CSI = e^{\frac{-(\ln s - \ln s_*)^2}{2\sigma^2}} \qquad (122)$$

B.2.5 Cluster Connectedness (CC)

By definition, a cluster is a set of nodes that are physically connected to one another by a network of links. A proper cluster, therefore, should not contain any islands. To enforce this definition we define Cluster Connectedness (CC) as a binary measure that evaluates to zero when any cluster is not fully connected, and one if all clusters are fully connected.

B.2.6 Aggregate clustering fitness

To evaluate the aggregate quality or fitness (f) of a given clustering solution, we use a multiplicative aggregate fitness function, calculated as the weighted product of the four quality measures above:

$$f = ECI^{\alpha} \cdot BCCI^{\beta} \cdot CCI^{\gamma} \cdot CSI^{\zeta} \cdot CC \qquad (123)$$

where $\alpha, \beta, \gamma, \zeta$ are user-defined scalars that define the relative importance of ECI, BCCI, CSI, CCI respectively. Our fitness function as defined in (123) uses the product of the four measures for two related reasons. First, we seek an aggregate fitness function satisfying "preferential independence" of the four individual quality metrics. Preferential independence is defined by the condition $\frac{\partial^2 f}{\partial a \partial b} \neq 0$ for any two values of distinct individual quality metrics a

and *b*; thus any multiplicative fitness function would satisfy preferential independence (additive fitness metrics, for example, will not satisfy preferential independence). Using a fitness function that does not satisfy preferential independence may produce clustering solutions with high fitness scores, but low scores for one or more quality metrics. Further, a multiplicative form of the fitness function will automatically produce a fitness score of zero whenever any cluster is not fully connected. Second, the interaction of the four individual clustering quality metrics prevents our algorithm from converging on trivial solutions. Since our four individual clustering quality metrics are defined on a [0,1] scale, our clustering algorithm (discussed in Section B.3.4) seeks to drive each individual measure of clustering quality towards a value equal to one. A score of one for an individual clustering measure, however, would in some cases yield a trivial solution. An example would be that when $ECI = 1$, we have the trivial case of $p=n$, where each individual node is its own cluster. The interaction of the four quality metrics in the aggregate fitness function removes the possibility of such trivial solutions, since $ECI = 1$ would necessarily imply that $BCCI = 0$, and the fitness function (123) would evaluate to zero. This underscores the strength of our method overcoming the classic problem of single member clusters [**96**], which usually have to be treated differently by the clustering algorithm or even removed. For instance, in [**74**], the authors remove buses that match generation and load from one of the test cases.

B.3 Clustering Methods

B.3.1 Hierarchical

Hierarchical clustering starts with individual nodes and uses a bottom-up, or agglomerate, technique to build clusters. The method uses an iterative approach that links the two clusters with the smallest distance. Starting with singleton clusters, each iteration yields one less cluster until the entire network is included within one cluster or some cutoff value is encountered.

Typical cutoffs could be a maximum number of clusters, maximum size of a cluster, or a minimum/maximum value of the distance metric.

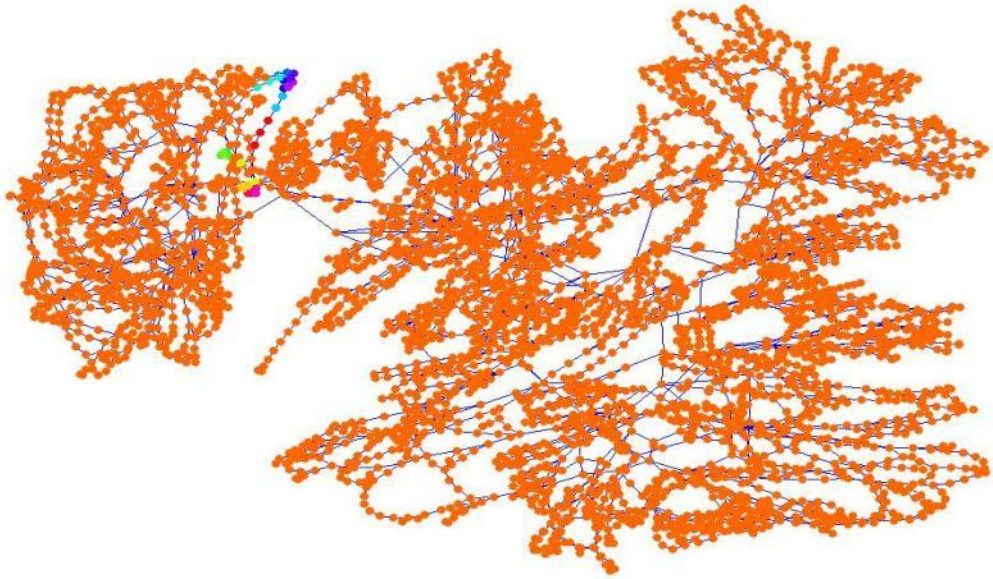

Figure 34: Hierarchical Clustering on PJM Network with 15 Clusters

Hierarchical clustering on the 4458 bus version of the PJM network was performed using average electrical distances. The results of the clustering depended primarily upon the threshold set for completion. When using a maximum number of clusters, the method produced one large cluster and several singleton clusters as shown in Figure 34. In an attempt to reduce the number of singleton clusters, several different cutoff methods were used. The use of an electrical distance value for the cutoff produced similar results that were dominated by one large cluster and the number of small or singleton clusters increased as the distance cutoff was lowered. Ultimately, we found that the sensitivity of the PJM system to the cutoff value was driven by the distribution of the electrical distances within the PJM network. When adjusting the cutoff value, we found that there were some electrical distance values that produced a dramatic change in the number of clusters. Figure 36 shows the plot of the number of clusters obtained on the PJM

network associated with distance cutoff values. The relatively fat tail of the CDF in Figure 35 shows that there is a large number of links with large electrical distances in the network. These large distance links tend to correspond to the edges of the network where the nodes are not highly connected and thus are limited to clusters with other nodes that usually have large electrical distances associated with them. Since hierarchical clustering uses an agglomerative approach, the nodes contained in the tail of the CDF will be absorbed into clusters in later iterations. Therefore, when setting a distance cutoff, clustering forms several small clusters and one large cluster. Figure 37 shows the resulting 2587 clusters obtained by hierarchical clustering with a distance cutoff value of 100. We have found that the irregularity of the CDF of electrical distances and the sparsity of the adjacency matrix in electrical networks fails to produce desirable results with hierarchical clustering. Hierarchical clustering has been used with some success on smaller test systems to determine price zone s [**73**], however when looking at electrical distance in large systems the method fails to produce desirable results. The overall fitness score for the hierarchical clustering method on the PJM network is 0.0012.

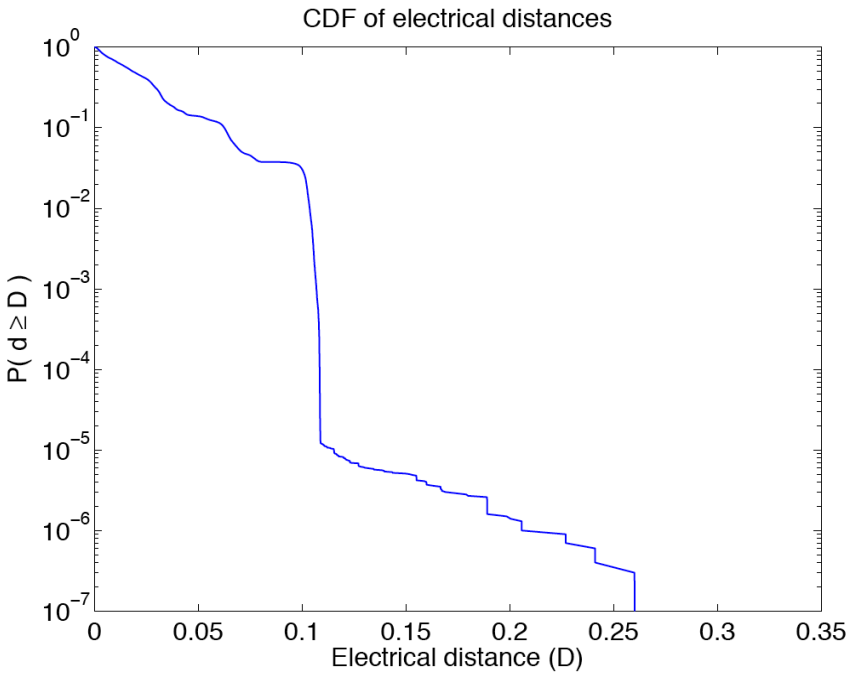

Figure 35: CDF of Electrical Distances in PJM Network

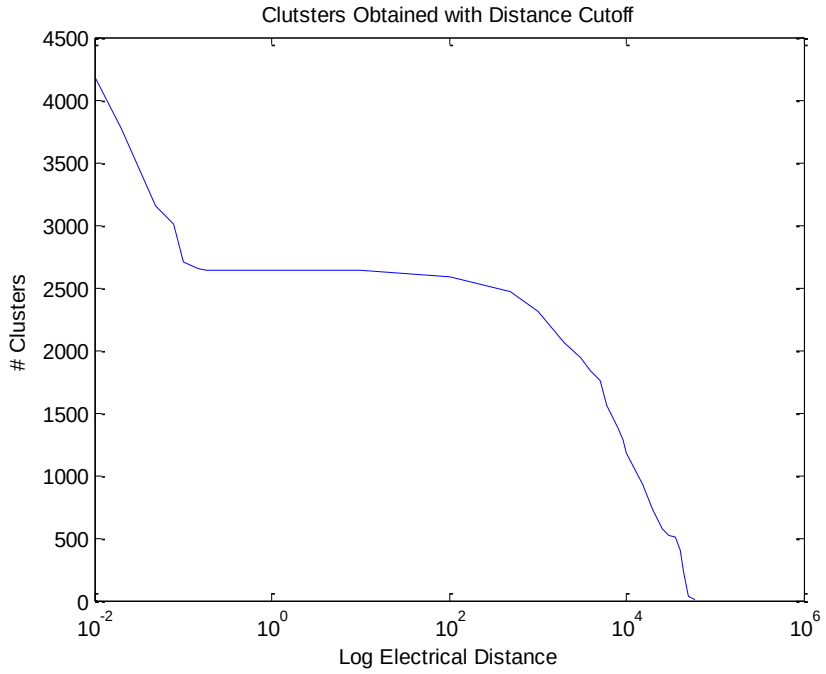

Figure 36: Distance Cutoff vs. Number of Clusters on PJM Network

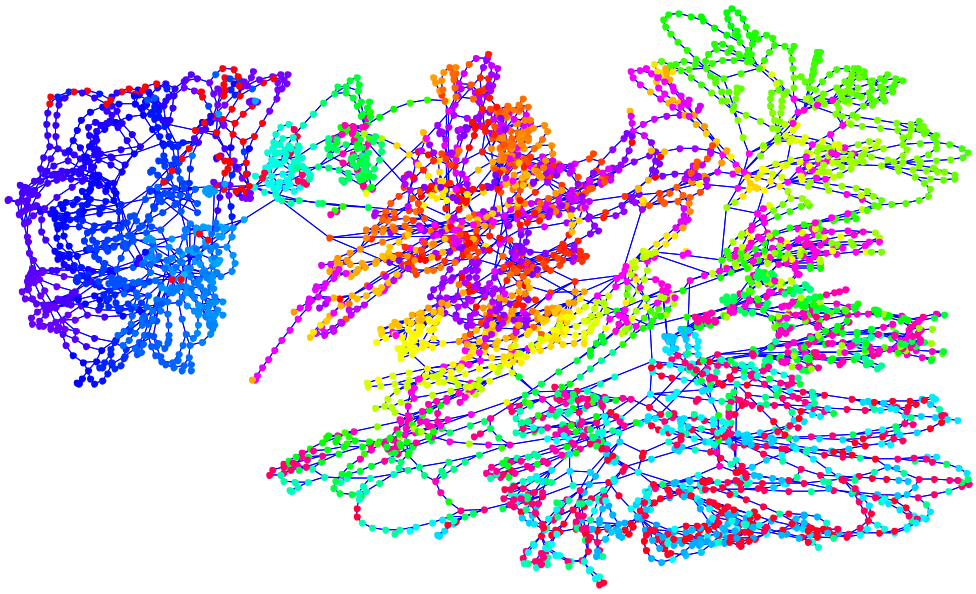

Figure 37: Hierarchical Clustering on PJM Network with a Distance Cutoff value of 100

B.3.2 K-Means

K-means clustering uses a top-down, or divisive, approach that begins with a complete network, and then divides the network into clusters and finally adjusts those clusters based upon some criteria. The aim of the K-means algorithm is to divide M points in N dimensions into K clusters so that the within-cluster sum of squares is minimized [**97**]. The method starts by assigning K random points within the network. Each node in the network is assigned to the closest of the K points to form initial clusters. The points are relocated to the centroid of each cluster. Each node is then reassigned to the nearest centroid. The method iterates until some minimum movement of centroids is encountered. One of the primary concerns is that k-means clustering can find local minima. That is, the algorithm can create multiple clusters out of closely connected nodes depending on the starting points. K-means clustering has been utilized

on electrical networks for the purpose of reducing a larger network into smaller sub-networks for static security analysis by [**98**].

K-means clustering on electrical networks using electrical distances abstracts the direct node-node connections. This topological abstraction is useful when describing the physics of electricity flow. However, the physical network topology plays a key role in several market and reliability calculations in power systems. Thus, for most applications in power systems, it is necessary to preserve the topological connectedness of clusters. To ensure connected clusters from k-means clustering, we add an additional step to the algorithm. After the centroid-node distance is minimized, the clusters are analyzed for topological connectedness. In the event that clusters are topologically disconnected, the disconnected nodes are transferred to the cluster of their nearest, connected, neighbor. In large networks, this additional step "fixes" the disconnected k-means clusters without imposing a significant change in the clustering fitness value.

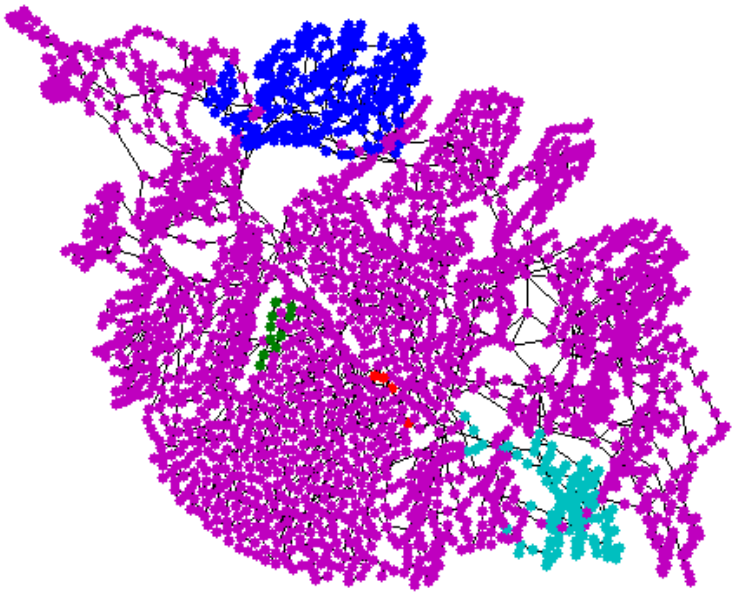

Figure 38: K-Means Clustering on the 2383 bus Polish Power Network with 5 Clusters

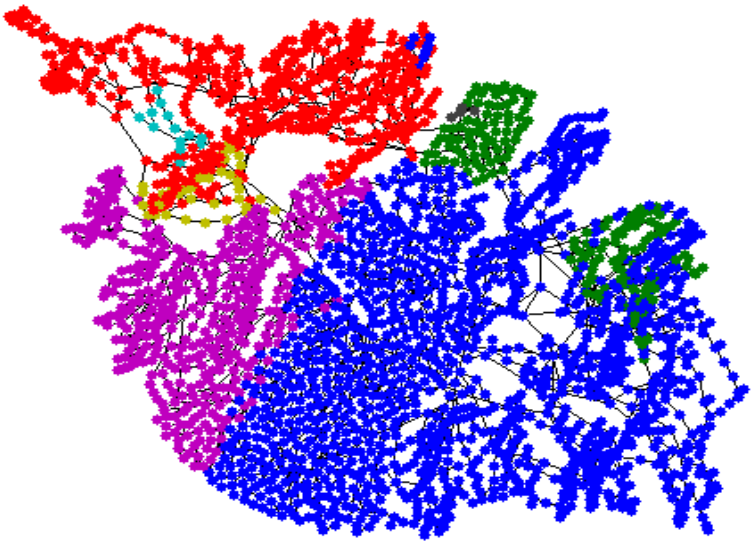

Figure 39: K-Means Clustering on the 2383 bus Polish Power Network with 10 Clusters

Figure 38 and Figure 39 show the results of k-means clustering on the 2383 bus Polish power network. The modified ("fixed") k-means clustering methods resulted in clustering solutions with fitness values of 0.0077 and 0.0018 for 5 and 10 clusters, respectively.

B.3.3 Spectral

We use a form of spectral clustering as an extension of k-means clustering that executes the k-means algorithm on the spectral representation of the network. An introduction to spectral clustering is given by [**99**] and a brief development of the methods used in this paper follows. Luxburg presents spectral clustering as an approximation of the RatioCut problem. When given an adjacency matrix *W*, the simplest way to construct a partition is to solve the mincut problem is by choosing partitions $A_1, \ldots, A_k$ which minimize

$$cut(A_1, \ldots, A_k) = \sum_{i=1}^{k} \sum_{i \in A_i, j \in \overline{A_i}} w_{ij}$$

Usually the mincut problem leads to solutions that consist of separating one node from the network. We witnessed similar solutions in the hierarchical clustering approach. One suggested solution to this problem is achieved by adjusting the objective function to form RatioCut

$$RatioCut(A_1, \ldots, A_k) = \sum_{i=1}^{k} \frac{cut(A_i, \overline{A_i})}{|A_i|}$$

The size of subset A is measured by the by its number of nodes $|A_i|$. Unnormalized spectral clustering introduces a method to solve a relaxation of the RatioCut problem. Solving for the Eigen vectors f_i of the unnormalized Laplacian matrix L allows us to perform clustering by the k-means algorithm using the spectral coordinates for each point given by the Eigen vectors, $f_1, \ldots, f_i$.

In the case of electrical distance clustering, the unnormalized graph Laplacian matrix corresponds to the Bbus matrix derived in Appendix A. The *n* largest Eigenvalues of the Bbus

form the spectral centroids for a k-means clustering routine, while the spectral centroid-node distances are contained in the corresponding Eigen vectors. By performing k-means clustering on the *n* largest Eigenvalues and the distances contained in the corresponding Eigenvectors, we again abstract the topological connectedness of the network. Thus, the same "fix" described in the previous section is used to ensure connected clusters. That is, in the event of disconnected clusters, the disconnected nodes are assigned to the cluster associated with their nearest (E-distance) topologically connected neighbor.

Figure 40 and Figure 41 show the results of spectral clustering on the 2383 bus Polish Power system with 5 and 10 clusters. The "fixed" solutions have fitness scores of 0.2537 and 0.1430 for the 5 and 10 cluster solutions, respectively.

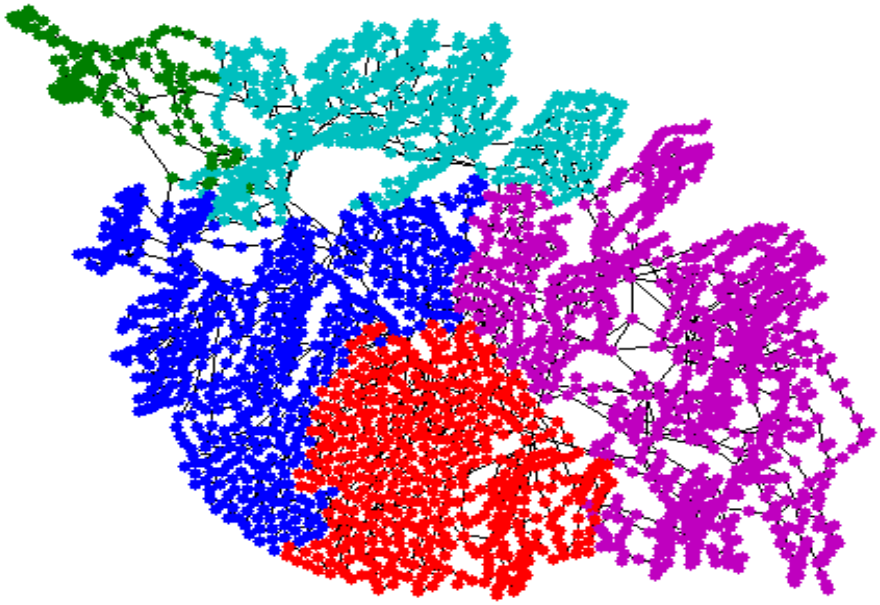

Figure 40: Spectral Clustering on the 2383 bus Polish Power Network with 5 Clusters

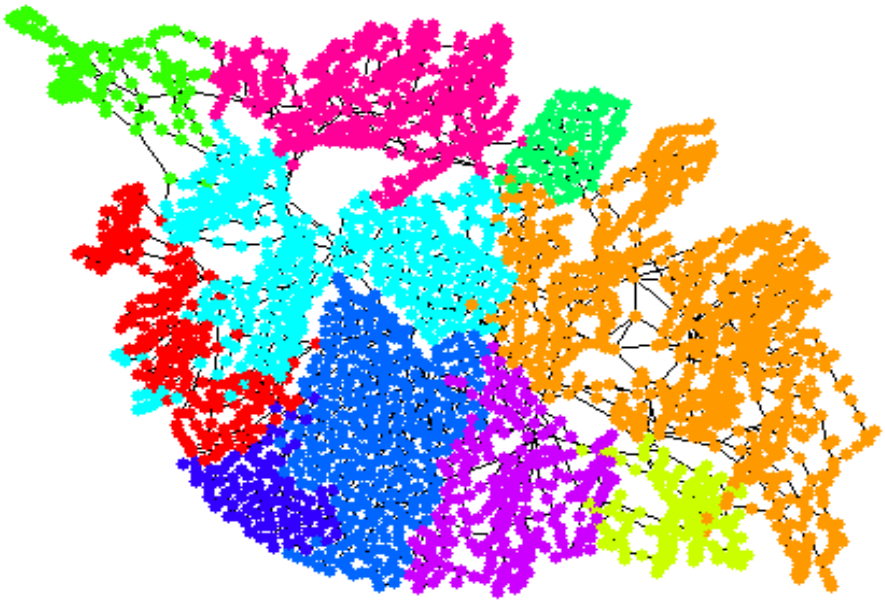

Figure 41: Spectral Clustering on the 2383 bus Polish Power Network with 10 Clusters

B.3.4 A Genetic Algorithm for Power Grid Clustering

Statistical clustering algorithms require a measure of similarity or distance that can be defined between individual data points and between clusters [**96**], [**100**]. A number of useful distance measures exist, but those used in existing clustering algorithms are well-defined distance metrics, defined on some Lp norm.

It is important to note that electrical distances differ substantially from topological distances (d_{ij} , the number of branches that must be utilized to travel a topological path between Bus *i* and Bus *j*) in power grids. The power systems literature contains a number of examples where statistical clustering has been employed using topological distance metrics (e.g., [**101**], [**102**], [**98**]), but these methods will generally not produce electrically cohesive clusters.

Genetic algorithms (GAs) can be very effective at solving non-convex optimization problems, particularly, when given an appropriate representation of possible solutions and an evaluation function that faithfully maps the real problem we want to solve. Our approach uses the clustering quality measure given in Eq. (123) as the fitness function for a genetic algorithm [**103**]. In this section we describe the method used to represent solutions in the GA, the methods used to generate the initial population of solutions, and the approach used for selection, crossover and mutation.

In any genetic algorithm GA, each clustering solution (phenotype) is represented as a string of n_g integers. In GA terminology [**103**] a string that represents a solution is known as a genotype, since it encodes the actual solution (the phenotype) into an abstract representation. In our clustering GA, each solution is represented as a string of $n_g = n$ integer bytes (g = [g_1 ... gn]), where n is the number of nodes in the network. In this representation, each g_i is an index between 0 and the number of topological neighbors for Node i (m_i, which is equivalent to the number of buses adjacent to Bus i). When $g_i = 1$, Node i is located in the same cluster as its first neighbor; when $g_i = 2$, it is located in the same cluster as its second topological neighbor; etc. When $g_i = 0$, Node i is not necessarily placed in the same cluster as any other node, however it may end up clustered with one or more of its neighbors (e.g., Node k with connection g_k) if g_k indicates a connection to Node i. Every solution within the bounds $0 \leq g_i \leq m_i$, $\forall\ i$ is a valid solution to the cluster problem. A change to a single byte can divide a cluster into two clusters, or merge it with a neighboring cluster. This flexibility increases the power of mutation and crossover operations, which are the primary methods for search in a genetic algorithm (see the end of this section).

To generate an initial population for the GA we produce random clusters by selecting random nodes as cluster centroids and iteratively expanding the clusters to encompass neighboring nodes until each node is assigned to exactly one cluster.

The selection of parents for crossover operations and for elitism occurs through the use of the fitness function in Eq. (123). Since every genotype within the feasible range is a valid clustering solution, CC evaluates to one for all genotypes.

Therefore we use the simplified fitness function $f = ECI \cdot BCCI \cdot C\,SI \cdot CCI$ (thus setting $\alpha = 1$, $\beta = 1$, $\gamma = 1$and $\zeta = 1$ in Eq. (123)) for selection. Parents for crossover operations are selected using the standard tournament without replacement selection method [**104**], [**105**], in which the selection of each individual depends upon a fitness comparison with a given number (tournament size) of other fitness scores from different individuals. In each generation the GA generates a set of new individuals equal to 80% of the population through crossover. The new individuals replace existing individuals probabilistically, using the roulette wheel method. The crossover process is summarized as follows:

1. Select two parents using a tournament algorithm without replacement that compares the fitness scores.
2. Choose a single random point of the genotype at which both parents are split (single point crossover).
3. Create a new individual with the vector head of one parent and the vector tail of the second.
4. Replace an individual in the population, with replacement probabilities proportional to fitness.

The top 3 individuals are retained without modification at each generation (elitism).

Mutation occurs at the end of each generation on all but the three highest fitness (most elite) individuals. When a byte mutates it is randomly reset to an integer in the feasible set $g_{i,new} \in \{0, 1,\cdots,m_i\}$. We use a mutation probability of $1/n$, so that we get approximately one mutation per individual per generation. The results of GA clustering one the 2383 bus Polish power network are shown in Figure 42 where the fitness score is 0.2694.

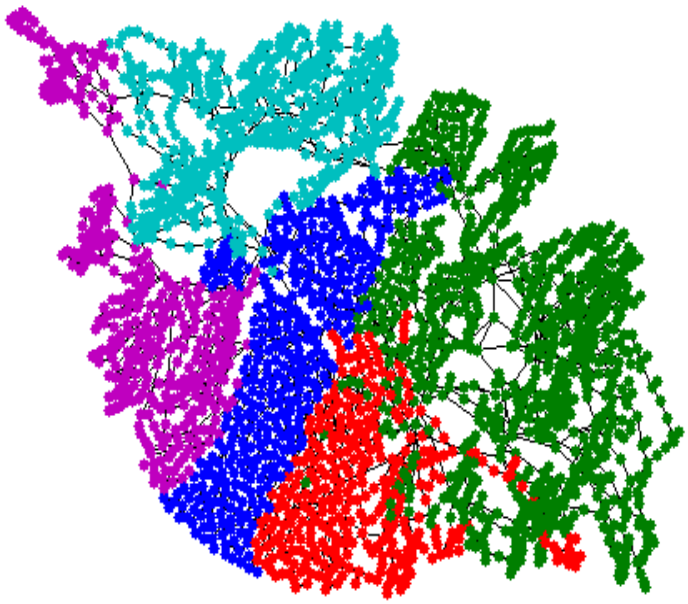

Figure 42: GA Clustering on the 2383 bus Polish Power Network with 5 Clusters

Appendix C System Data

C.1 IEEE Reliability Test System 1996 (RTS-96) Data

function mpc = case96_pwl

%% MATPOWER Case Format : Version 2

mpc.version = '2';

%%----- Power Flow Data -----%%

%% system MVA base

mpc.baseMVA = 100;

%Bus Data:

%bus_i	type	Pd	Qd	Gs	Bs	area	Vm	Va	Base KV	zone	Vmax	Vmin
mpc.bus = [												
101	2	108	22	0	0	1	1	0	138	1	1.06	0.94;
102	2	97	20	0	0	1	1	0	138	1	1.06	0.94;
103	1	180	37	0	0	1	1	0	138	1	1.06	0.94;
104	1	74	15	0	0	1	1	0	138	1	1.06	0.94;
105	1	71	14	0	0	1	1	0	138	1	1.06	0.94;
106	1	136	28	0	1	1	1	0	138	1	1.06	0.94;
107	2	125	25	0	0	1	1	0	138	1	1.06	0.94;
108	1	171	35	0	0	1	1	0	138	1	1.06	0.94;
109	1	175	36	0	0	1	1	0	138	1	1.06	0.94;
110	1	195	40	0	0	1	1	0	138	1	1.06	0.94;
111	1	0	0	0	0	1	1	0	230	1	1.06	0.94;
112	1	0	0	0	0	1	1	0	230	1	1.06	0.94;
113	3	745	54	0	0	1	1	0	230	1	1.06	0.94;
114	2	80	39	0	0	1	1	0	230	1	1.06	0.94;
115	2	132	64	0	0	1	1	0	230	1	1.06	0.94;
116	2	100	20	0	0	1	1	0	230	1	1.06	0.94;
117	1	0	0	0	0	1	1	0	230	1	1.06	0.94;
118	2	333	68	0	0	1	1	0	230	1	1.06	0.94;
119	1	75	37	0	0	1	1	0	230	1	1.06	0.94;
120	1	53	26	0	0	1	1	0	230	1	1.06	0.94;
121	2	0	0	0	0	1	1	0	230	1	1.06	0.94;
122	2	0	0	0	0	1	1	0	230	1	1.06	0.94;
123	2	0	0	0	0	1	1	0	230	1	1.06	0.94;
124	1	0	0	0	0	1	1	0	230	1	1.06	0.94;
201	2	108	22	0	0	2	1	0	138	1	1.06	0.94;
202	2	97	20	0	0	2	1	0	138	1	1.06	0.94;

203	1	180	37	0	0	2	1	0	138	1	1.06	0.94;
204	1	74	15	0	0	2	1	0	138	1	1.06	0.94;
205	1	71	14	0	0	2	1	0	138	1	1.06	0.94;
206	1	136	28	0	1	2	1	0	138	1	1.06	0.94;
207	2	125	25	0	0	2	1	0	138	1	1.06	0.94;
208	1	171	35	0	0	2	1	0	138	1	1.06	0.94;
209	1	175	36	0	0	2	1	0	138	1	1.06	0.94;
210	1	195	40	0	0	2	1	0	138	1	1.06	0.94;
211	1	0	0	0	0	2	1	0	230	1	1.06	0.94;
212	1	0	0	0	0	2	1	0	230	1	1.06	0.94;
213	2	745	54	0	0	2	1	0	230	1	1.06	0.94;
214	2	80	39	0	0	2	1	0	230	1	1.06	0.94;
215	2	132	64	0	0	2	1	0	230	1	1.06	0.94;
216	2	100	20	0	0	2	1	0	230	1	1.06	0.94;
217	1	0	0	0	0	2	1	0	230	1	1.06	0.94;
218	2	333	68	0	0	2	1	0	230	1	1.06	0.94;
219	1	75	37	0	0	2	1	0	230	1	1.06	0.94;
220	1	53	26	0	0	2	1	0	230	1	1.06	0.94;
221	2	0	0	0	0	2	1	0	230	1	1.06	0.94;
222	2	0	0	0	0	2	1	0	230	1	1.06	0.94;
223	2	0	0	0	0	2	1	0	230	1	1.06	0.94;
224	1	0	0	0	0	2	1	0	230	1	1.06	0.94;
301	2	108	22	0	0	3	1	0	138	1	1.06	0.94;
302	2	97	20	0	0	3	1	0	138	1	1.06	0.94;
303	1	180	37	0	0	3	1	0	138	1	1.06	0.94;
304	1	74	15	0	0	3	1	0	138	1	1.06	0.94;
305	1	71	14	0	0	3	1	0	138	1	1.06	0.94;
306	1	136	28	0	1	3	1	0	138	1	1.06	0.94;
307	2	125	25	0	0	3	1	0	138	1	1.06	0.94;
308	1	171	35	0	0	3	1	0	138	1	1.06	0.94;
309	1	175	36	0	0	3	1	0	138	1	1.06	0.94;
310	1	195	40	0	0	3	1	0	138	1	1.06	0.94;
311	1	0	0	0	0	3	1	0	230	1	1.06	0.94;
312	1	0	0	0	0	3	1	0	230	1	1.06	0.94;
313	2	745	54	0	0	3	1	0	230	1	1.06	0.94;
314	2	80	39	0	0	3	1	0	230	1	1.06	0.94;
315	2	132	64	0	0	3	1	0	230	1	1.06	0.94;
316	2	100	20	0	0	3	1	0	230	1	1.06	0.94;
317	1	0	0	0	0	3	1	0	230	1	1.06	0.94;
318	2	333	68	0	0	3	1	0	230	1	1.06	0.94;
319	1	75	37	0	0	3	1	0	230	1	1.06	0.94;
320	1	53	26	0	0	3	1	0	230	1	1.06	0.94;
321	2	0	0	0	0	3	1	0	230	1	1.06	0.94;

```
    322     2     0     0     0     0     3     1     0     230     1     1.06    0.94;
    323     2     0     0     0     0     3     1     0     230     1     1.06    0.94;
    324     1     0     0     0     0     3     1     0     230     1     1.06    0.94;
    325     1     0     0     0     0     3     1     0     230     1     1.06    0.94;
];
```

%Generator Data: Columns 1-10

```
%bus    Pg      Qg      Q max   Q min   Vg      M Base  status  P max   P min
mpc.gen = [
  101   10      0       10      0       1.035   100     1       20      15.8
  101   10      0       10      0       1.035   100     1       20      15.8
  101   76      14.1    30      -25     1.035   100     1       76      15.2
  101   76      14.1    30      -25     1.035   100     1       76      15.2
  102   10      0       10      0       1.035   100     1       20      15.8
  102   10      0       10      0       1.035   100     1       20      15.8
  102   76      7       30      -25     1.035   100     1       76      15.2
  102   76      7       30      -25     1.035   100     1       76      15.2
  107   80      17.2    60      0       1.025   100     1       100     25
  107   80      17.2    60      0       1.025   100     1       100     25
  107   80      17.2    60      0       1.025   100     1       100     25
  113   95.1    40.7    80      0       1.02    100     1       197     68.95
  113   95.1    40.7    80      0       1.02    100     1       197     68.95
  113   95.1    40.7    80      0       1.02    100     1       197     68.95
  114   0       13.7    200     -50     0.98    100     1       0       0
  115   12      0       6       0       1.014   100     1       12      2.4
  115   12      0       6       0       1.014   100     1       12      2.4
  115   12      0       6       0       1.014   100     1       12      2.4
  115   12      0       6       0       1.014   100     1       12      2.4
  115   12      0       6       0       1.014   100     1       12      2.4
  115   155     0.05    80      -50     1.014   100     1       155     54.25
  116   155     25.22   80      -50     1.017   100     1       155     54.25
  118   400     137.4   200     -50     1.05    100     1       400     100
  121   400     108.2   200     -50     1.05    100     1       400     100
  122   50      -4.96   16      -10     1.05    100     1       50      0
  122   50      -4.96   16      -10     1.05    100     1       50      0
  122   50      -4.96   16      -10     1.05    100     1       50      0
  122   50      -4.96   16      -10     1.05    100     1       50      0
  122   50      -4.96   16      -10     1.05    100     1       50      0
  122   50      -4.96   16      -10     1.05    100     1       50      0
  123   155     31.79   80      -50     1.05    100     1       155     54.25
  123   155     31.79   80      -50     1.05    100     1       155     54.25
```

123	350	71.78	150	-25	1.05	100	1	350	140
201	10	0	10	0	1.035	100	1	20	15.8
201	10	0	10	0	1.035	100	1	20	15.8
201	76	14.1	30	-25	1.035	100	1	76	15.2
201	76	14.1	30	-25	1.035	100	1	76	15.2
202	10	0	10	0	1.035	100	1	20	15.8
202	10	0	10	0	1.035	100	1	20	15.8
202	76	7	30	-25	1.035	100	1	76	15.2
202	76	7	30	-25	1.035	100	1	76	15.2
207	80	17.2	60	0	1.025	100	1	100	25
207	80	17.2	60	0	1.025	100	1	100	25
207	80	17.2	60	0	1.025	100	1	100	25
213	95.1	40.7	80	0	1.02	100	1	197	68.95
213	95.1	40.7	80	0	1.02	100	1	197	68.95
213	95.1	40.7	80	0	1.02	100	1	197	68.95
214	0	13.68	200	-50	0.98	100	1	0	0
215	12	0	6	0	1.014	100	1	12	2.4
215	12	0	6	0	1.014	100	1	12	2.4
215	12	0	6	0	1.014	100	1	12	2.4
215	12	0	6	0	1.014	100	1	12	2.4
215	12	0	6	0	1.014	100	1	12	2.4
215	155	0.048	80	-50	1.014	100	1	155	54.25
216	155	25.22	80	-50	1.017	100	1	155	54.25
218	400	137.4	200	-50	1.05	100	1	400	100
221	400	108.2	200	-50	1.05	100	1	400	100
222	50	-4.96	16	-10	1.05	100	1	50	0
222	50	-4.96	16	-10	1.05	100	1	50	0
222	50	-4.96	16	-10	1.05	100	1	50	0
222	50	-4.96	16	-10	1.05	100	1	50	0
222	50	-4.96	16	-10	1.05	100	1	50	0
222	50	-4.96	16	-10	1.05	100	1	50	0
223	155	31.79	80	-50	1.05	100	1	155	54.25
223	155	31.79	80	-50	1.05	100	1	155	54.25
223	350	71.78	150	-25	1.05	100	1	350	140
301	10	0	10	0	1.035	100	1	20	15.8
301	10	0	10	0	1.035	100	1	20	15.8
301	76	14.1	30	-25	1.035	100	1	76	15.2
301	76	14.1	30	-25	1.035	100	1	76	15.2
302	10	0	10	0	1.035	100	1	20	15.8
302	10	0	10	0	1.035	100	1	20	15.8
302	76	7	30	-25	1.035	100	1	76	15.2
302	76	7	30	-25	1.035	100	1	76	15.2
307	80	17.2	60	0	1.025	100	1	100	25

```
  307    80    17.2    60     0    1.025    100    1    100    25
  307    80    17.2    60     0    1.025    100    1    100    25
  313    95.1  40.7    80     0    1.02     100    1    197    68.95
  313    95.1  40.7    80     0    1.02     100    1    197    68.95
  313    95.1  40.7    80     0    1.02     100    1    197    68.95
  314    0     13.68   200    -50  0.98     100    1    0      0
  315    12    0       6      0    1.014    100    1    12     2.4
  315    12    0       6      0    1.014    100    1    12     2.4
  315    12    0       6      0    1.014    100    1    12     2.4
  315    12    0       6      0    1.014    100    1    12     2.4
  315    12    0       6      0    1.014    100    1    12     2.4
  315    155   0.048   80     -50  1.014    100    1    155    54.25
  316    155   25.22   80     -50  1.017    100    1    155    54.25
  318    400   137.4   200    -50  1.05     100    1    400    100
  321    400   108.2   200    -50  1.05     100    1    400    100
  322    50    -4.96   16     -10  1.05     100    1    50     0
  322    50    -4.96   16     -10  1.05     100    1    50     0
  322    50    -4.96   16     -10  1.05     100    1    50     0
  322    50    -4.96   16     -10  1.05     100    1    50     0
  322    50    -4.96   16     -10  1.05     100    1    50     0
  322    50    -4.96   16     -10  1.05     100    1    50     0
  323    155   31.79   80     -50  1.05     100    1    155    54.25
  323    155   31.79   80     -50  1.05     100    1    155    54.25
  323    350   71.78   150    -25  1.05     100    1    350    140
];
%Generator Data Continued: Columns 11-21

 %Pc1   Pc2   Qc1 min   Qc1 max   Qc2 min   Qc2 max   Ramp agc   Ramp 10   Ramp 30   Ramp q   apf
[
    0     0        0         0         0         0          0         0         0        0    0;
    0     0        0         0         0         0          0         0         0        0    0;
    0     0        0         0         0         0          0         0         0        0    0;
    0     0        0         0         0         0          0         0         0        0    0;
    0     0        0         0         0         0          0         0         0        0    0;
    0     0        0         0         0         0          0         0         0        0    0;
    0     0        0         0         0         0          0         0         0        0    0;
    0     0        0         0         0         0          0         0         0        0    0;
    0     0        0         0         0         0          0         0         0        0    0;
    0     0        0         0         0         0          0         0         0        0    0;
    0     0        0         0         0         0          0         0         0        0    0;
    0     0        0         0         0         0          0         0         0        0    0;
    0     0        0         0         0         0          0         0         0        0    0;
    0     0        0         0         0         0          0         0         0        0    0;
    0     0        0         0         0         0          0         0         0        0    0;
    0     0        0         0         0         0          0         0         0        0    0;
```

0	0	0	0	0	0	0	0	0	0	0;
0	0	0	0	0	0	0	0	0	0	0;
0	0	0	0	0	0	0	0	0	0	0;
0	0	0	0	0	0	0	0	0	0	0;
0	0	0	0	0	0	0	0	0	0	0;
0	0	0	0	0	0	0	0	0	0	0;
0	0	0	0	0	0	0	0	0	0	0;
0	0	0	0	0	0	0	0	0	0	0;
0	0	0	0	0	0	0	0	0	0	0;
0	0	0	0	0	0	0	0	0	0	0;
0	0	0	0	0	0	0	0	0	0	0;
0	0	0	0	0	0	0	0	0	0	0;
0	0	0	0	0	0	0	0	0	0	0;
0	0	0	0	0	0	0	0	0	0	0;
0	0	0	0	0	0	0	0	0	0	0;
0	0	0	0	0	0	0	0	0	0	0;
0	0	0	0	0	0	0	0	0	0	0;
0	0	0	0	0	0	0	0	0	0	0;
0	0	0	0	0	0	0	0	0	0	0;
0	0	0	0	0	0	0	0	0	0	0;
0	0	0	0	0	0	0	0	0	0	0;
0	0	0	0	0	0	0	0	0	0	0;
0	0	0	0	0	0	0	0	0	0	0;
0	0	0	0	0	0	0	0	0	0	0;
0	0	0	0	0	0	0	0	0	0	0;
0	0	0	0	0	0	0	0	0	0	0;
0	0	0	0	0	0	0	0	0	0	0;
0	0	0	0	0	0	0	0	0	0	0;
0	0	0	0	0	0	0	0	0	0	0;
0	0	0	0	0	0	0	0	0	0	0;
0	0	0	0	0	0	0	0	0	0	0;
0	0	0	0	0	0	0	0	0	0	0;
0	0	0	0	0	0	0	0	0	0	0;
0	0	0	0	0	0	0	0	0	0	0;
0	0	0	0	0	0	0	0	0	0	0;
0	0	0	0	0	0	0	0	0	0	0;
0	0	0	0	0	0	0	0	0	0	0;
0	0	0	0	0	0	0	0	0	0	0;
0	0	0	0	0	0	0	0	0	0	0;
0	0	0	0	0	0	0	0	0	0	0;
0	0	0	0	0	0	0	0	0	0	0;
0	0	0	0	0	0	0	0	0	0	0;
0	0	0	0	0	0	0	0	0	0	0;

```
0 0 0 0 0 0 0 0 0 0 0;
0 0 0 0 0 0 0 0 0 0 0;
0 0 0 0 0 0 0 0 0 0 0;
0 0 0 0 0 0 0 0 0 0 0;
0 0 0 0 0 0 0 0 0 0 0;
0 0 0 0 0 0 0 0 0 0 0;
0 0 0 0 0 0 0 0 0 0 0;
0 0 0 0 0 0 0 0 0 0 0;
0 0 0 0 0 0 0 0 0 0 0;
0 0 0 0 0 0 0 0 0 0 0;
0 0 0 0 0 0 0 0 0 0 0;
0 0 0 0 0 0 0 0 0 0 0;
0 0 0 0 0 0 0 0 0 0 0;
0 0 0 0 0 0 0 0 0 0 0;
0 0 0 0 0 0 0 0 0 0 0;
0 0 0 0 0 0 0 0 0 0 0;
0 0 0 0 0 0 0 0 0 0 0;
0 0 0 0 0 0 0 0 0 0 0;
0 0 0 0 0 0 0 0 0 0 0;
0 0 0 0 0 0 0 0 0 0 0;
0 0 0 0 0 0 0 0 0 0 0;
0 0 0 0 0 0 0 0 0 0 0;
0 0 0 0 0 0 0 0 0 0 0;
0 0 0 0 0 0 0 0 0 0 0;
0 0 0 0 0 0 0 0 0 0 0;
0 0 0 0 0 0 0 0 0 0 0;
0 0 0 0 0 0 0 0 0 0 0;
0 0 0 0 0 0 0 0 0 0 0;
0 0 0 0 0 0 0 0 0 0 0;
0 0 0 0 0 0 0 0 0 0 0;
0 0 0 0 0 0 0 0 0 0 0;
0 0 0 0 0 0 0 0 0 0 0;
0 0 0 0 0 0 0 0 0 0 0;
0 0 0 0 0 0 0 0 0 0 0;
0 0 0 0 0 0 0 0 0 0 0;
0 0 0 0 0 0 0 0 0 0 0;
0 0 0 0 0 0 0 0 0 0 0;
0 0 0 0 0 0 0 0 0 0 0;
0 0 0 0 0 0 0 0 0 0 0;
0 0 0 0 0 0 0 0 0 0 0;
0 0 0 0 0 0 0 0 0 0 0;
0 0 0 0 0 0 0 0 0 0 0;
];
```

% Branch Data:

%f bus	T bus	r	x	b	rateA	rateB	rateC	ratio	angle	status	angmin	angmax
mpc.branch = [												
101	102	0.003	0.014	0.461	175	193	200	1	0	1	-360	360;
101	103	0.055	0.211	0.057	175	208	220	1	0	1	-360	360;
101	105	0.022	0.085	0.023	175	208	220	1	0	1	-360	360;
102	104	0.033	0.127	0.034	175	208	220	1	0	1	-360	360;
102	106	0.05	0.192	0.052	175	208	220	1	0	1	-360	360;
103	109	0.031	0.119	0.032	175	208	220	1	0	1	-360	360;
103	124	0.002	0.084	0	400	510	600	1.115	0	1	-360	360;
104	109	0.027	0.104	0.028	175	208	220	1	0	1	-360	360;
105	110	0.023	0.088	0.024	175	208	220	1	0	1	-360	360;
106	110	0.014	0.061	2.459	175	193	200	1	0	1	-360	360;
107	108	0.016	0.061	0.017	175	208	220	1	0	1	-360	360;
107	203	0.042	0.161	0.044	175	208	220	1	0	1	-360	360;
108	109	0.043	0.165	0.045	175	208	220	1	0	1	-360	360;
108	110	0.043	0.165	0.045	175	208	220	1	0	1	-360	360;
109	111	0.002	0.084	0	400	510	600	1.13	0	1	-360	360;
109	112	0.002	0.084	0	400	510	600	1.13	0	1	-360	360;
110	111	0.002	0.084	0	400	510	600	1.115	0	1	-360	360;
110	112	0.002	0.084	0	400	510	600	1.115	0	1	-360	360;
111	114	0.005	0.042	0.088	500	600	625	1	0	1	-360	360;
112	113	0.006	0.048	0.1	500	600	625	1	0	1	-360	360;
112	123	0.012	0.097	0.203	500	600	625	1	0	1	-360	360;
113	123	0.011	0.087	0.182	500	600	625	1	0	1	-360	360;
113	215	0.01	0.075	0.158	500	600	625	1	0	1	-360	360;
114	116	0.005	0.059	0.082	350	600	625	1	0	1	-360	360;
115	116	0.002	0.017	0.036	500	600	625	1	0	1	-360	360;
115	121	0.006	0.049	0.103	500	600	625	1	0	1	-360	360;
115	121	0.006	0.049	0.103	500	600	625	1	0	1	-360	360;
115	124	0.007	0.052	0.109	500	600	625	1	0	1	-360	360;
116	117	0.003	0.026	0.055	500	600	625	1	0	1	-360	360;
116	119	0.003	0.023	0.049	500	600	625	1	0	1	-360	360;
117	118	0.002	0.014	0.03	500	600	625	1	0	1	-360	360;
117	122	0.014	0.105	0.221	500	600	625	1	0	1	-360	360;
118	121	0.003	0.026	0.055	500	600	625	1	0	1	-360	360;
118	121	0.003	0.026	0.055	500	600	625	1	0	1	-360	360;
119	120	0.005	0.04	0.083	500	600	625	1	0	1	-360	360;
119	120	0.005	0.04	0.083	500	600	625	1	0	1	-360	360;
120	123	0.003	0.022	0.046	500	600	625	1	0	1	-360	360;

120	123	0.003	0.022	0.046	500	600	625	1	0	1	-360	360;
121	122	0.009	0.068	0.142	500	600	625	1	0	1	-360	360;
123	217	0.01	0.074	0.155	500	600	625	1	0	1	-360	360;
201	202	0.003	0.014	0.461	175	193	200	1	0	1	-360	360;
201	203	0.055	0.211	0.057	175	208	220	1	0	1	-360	360;
201	205	0.022	0.085	0.023	175	208	220	1	0	1	-360	360;
202	204	0.033	0.127	0.034	175	208	220	1	0	1	-360	360;
202	206	0.05	0.192	0.052	175	208	220	1	0	1	-360	360;
203	209	0.031	0.119	0.032	175	208	220	1	0	1	-360	360;
203	224	0.002	0.084	0	400	510	600	1.115	0	1	-360	360;
204	209	0.027	0.104	0.028	175	208	220	1	0	1	-360	360;
205	210	0.023	0.088	0.024	175	208	220	1	0	1	-360	360;
206	210	0.014	0.061	2.459	175	193	200	1	0	1	-360	360;
207	208	0.016	0.061	0.017	175	208	220	1	0	1	-360	360;
208	209	0.043	0.165	0.045	175	208	220	1	0	1	-360	360;
208	210	0.043	0.165	0.045	175	208	220	1	0	1	-360	360;
209	211	0.002	0.084	0	400	510	600	1.13	0	1	-360	360;
209	212	0.002	0.084	0	400	510	600	1.13	0	1	-360	360;
210	211	0.002	0.084	0	400	510	600	1.115	0	1	-360	360;
210	212	0.002	0.084	0	400	510	600	1.115	0	1	-360	360;
211	214	0.005	0.042	0.088	500	600	625	1	0	1	-360	360;
212	213	0.006	0.048	0.1	500	600	625	1	0	1	-360	360;
212	223	0.012	0.097	0.203	500	600	625	1	0	1	-360	360;
213	223	0.011	0.087	0.182	500	600	625	1	0	1	-360	360;
214	216	0.005	0.059	0.082	350	600	625	1	0	1	-360	360;
215	216	0.002	0.017	0.036	500	600	625	1	0	1	-360	360;
215	221	0.006	0.049	0.103	500	600	625	1	0	1	-360	360;
215	221	0.006	0.049	0.103	500	600	625	1	0	1	-360	360;
215	224	0.007	0.052	0.109	500	600	625	1	0	1	-360	360;
216	217	0.003	0.026	0.055	500	600	625	1	0	1	-360	360;
216	219	0.003	0.023	0.049	500	600	625	1	0	1	-360	360;
217	218	0.002	0.014	0.03	500	600	625	1	0	1	-360	360;
217	222	0.014	0.105	0.221	500	600	625	1	0	1	-360	360;
218	221	0.003	0.026	0.055	500	600	625	1	0	1	-360	360;
218	221	0.003	0.026	0.055	500	600	625	1	0	1	-360	360;
219	220	0.005	0.04	0.083	500	600	625	1	0	1	-360	360;
219	220	0.005	0.04	0.083	500	600	625	1	0	1	-360	360;
220	223	0.003	0.022	0.046	500	600	625	1	0	1	-360	360;
220	223	0.003	0.022	0.046	500	600	625	1	0	1	-360	360;
221	222	0.009	0.068	0.142	500	600	625	1	0	1	-360	360;
301	302	0.003	0.014	0.461	175	193	200	1	0	1	-360	360;
301	303	0.055	0.211	0.057	175	208	220	1	0	1	-360	360;
301	305	0.022	0.085	0.023	175	208	220	1	0	1	-360	360;

```
    302    304   0.033   0.127   0.034   175   208   220     1     0     1    -360   360;
    302    306    0.05   0.192   0.052   175   208   220     1     0     1    -360   360;
    303    309   0.031   0.119   0.032   175   208   220     1     0     1    -360   360;
    303    324   0.002   0.084       0   400   510   600 1.115     0     1    -360   360;
    304    309   0.027   0.104   0.028   175   208   220     1     0     1    -360   360;
    305    310   0.023   0.088   0.024   175   208   220     1     0     1    -360   360;
    306    310   0.014   0.061   2.459   175   193   200     1     0     1    -360   360;
    307    308   0.016   0.061   0.017   175   208   220     1     0     1    -360   360;
    308    309   0.043   0.165   0.045   175   208   220     1     0     1    -360   360;
    308    310   0.043   0.165   0.045   175   208   220     1     0     1    -360   360;
    309    311   0.002   0.084       0   400   510   600  1.13     0     1    -360   360;
    309    312   0.002   0.084       0   400   510   600  1.13     0     1    -360   360;
    310    311   0.002   0.084       0   400   510   600 1.115     0     1    -360   360;
    310    312   0.002   0.084       0   400   510   600 1.115     0     1    -360   360;
    311    314   0.005   0.042   0.088   500   600   625     1     0     1    -360   360;
    312    313   0.006   0.048     0.1   500   600   625     1     0     1    -360   360;
    312    323   0.012   0.097   0.203   500   600   625     1     0     1    -360   360;
    313    323   0.011   0.087   0.182   500   600   625     1     0     1    -360   360;
    314    316   0.005   0.059   0.082   350   600   625     1     0     1    -360   360;
    315    316   0.002   0.017   0.036   500   600   625     1     0     1    -360   360;
    315    321   0.006   0.049   0.103   500   600   625     1     0     1    -360   360;
    315    321   0.006   0.049   0.103   500   600   625     1     0     1    -360   360;
    315    324   0.007   0.052   0.109   500   600   625     1     0     1    -360   360;
    316    317   0.003   0.026   0.055   500   600   625     1     0     1    -360   360;
    316    319   0.003   0.023   0.049   500   600   625     1     0     1    -360   360;
    317    318   0.002   0.014    0.03   500   600   625     1     0     1    -360   360;
    317    322   0.014   0.105   0.221   500   600   625     1     0     1    -360   360;
    318    321   0.003   0.026   0.055   500   600   625     1     0     1    -360   360;
    318    321   0.003   0.026   0.055   500   600   625     1     0     1    -360   360;
    319    320   0.005    0.04   0.083   500   600   625     1     0     1    -360   360;
    319    320   0.005    0.04   0.083   500   600   625     1     0     1    -360   360;
    320    323   0.003   0.022   0.046   500   600   625     1     0     1    -360   360;
    320    323   0.003   0.022   0.046   500   600   625     1     0     1    -360   360;
    321    322   0.009   0.068   0.142   500   600   625     1     0     1    -360   360;
    325    121   0.012   0.097   0.203   500   600   625     1     0     1    -360   360;
    318    223   0.013   0.104   0.218   500   600   625     1     0     1    -360   360;
    323    325       0   0.009       0   722   893   893     1     0     1    -360   360;
];

%Generator Cost Data

 %1   startup      shutdown    n   x1       y1       ...       xn       yn
```

```
mpc.gencost = [
	1	7.59E-05	0	4	15.8	2363	16	2461	19.8	4287	20	4377.15;
	1	7.59E-05	0	4	15.8	2363	16	2461	19.8	4287	20	4377.15;
	1	0.00106	0	4	15.2	258.3	38	674	60.8	1253	76	1800.71;
	1	0.00106	0	4	15.2	258.3	38	674	60.8	1253	76	1800.71;
	1	7.59E-05	0	4	15.8	2363	16	2461	19.8	4287	20	4377.15;
	1	7.59E-05	0	4	15.8	2363	16	2461	19.8	4287	20	4377.15;
	1	0.00106	0	4	15.2	258.3	38	674	60.8	1253	76	1800.71;
	1	0.00106	0	4	15.2	258.3	38	674	60.8	1253	76	1800.71;
	1	0.00475	0	4	25	1699	50	3657	80	6330	100	8296.68;
	1	0.00475	0	4	25	1699	50	3657	80	6330	100	8296.68;
	1	0.00475	0	4	25	1699	50	3657	80	6330	100	8296.68;
	1	0.01176	0	4	68.95	4835	118.2	8770	157.6	12212	197	15919.2;
	1	0.01176	0	4	68.95	4835	118.2	8770	157.6	12212	197	15919.2;
	1	0.01176	0	4	68.95	4835	118.2	8770	157.6	12212	197	15919.2;
	1	0	0	4	0	0	0.3	1000	0.6	2005	0.9	3010;
	1	0.00057	0	4	2.4	205.2	6	521	9.6	940.9	12	1332.48;
	1	0.00057	0	4	2.4	205.2	6	521	9.6	940.9	12	1332.48;
	1	0.00057	0	4	2.4	205.2	6	521	9.6	940.9	12	1332.48;
	1	0.00057	0	4	2.4	205.2	6	521	9.6	940.9	12	1332.48;
	1	0.00057	0	4	2.4	205.2	6	521	9.6	940.9	12	1332.48;
	1	0.0017	0	4	54.25	798.1	93	1414	124	1964	155	2588.22;
	1	0.0017	0	4	54.25	798.1	93	1414	124	1964	155	2588.22;
	1	0	0	4	100	2200	200	4400	320	7040	400	8800;
	1	0	0	4	100	2200	200	4400	320	7040	400	8800;
	1	0	0	4	0	0	49	4.9	49.5	4.95	50	5;
	1	0	0	4	0	0	49	4.9	49.5	4.95	50	5;
	1	0	0	4	0	0	49	4.9	49.5	4.95	50	5;
	1	0	0	4	0	0	49	4.9	49.5	4.95	50	5;
	1	0	0	4	0	0	49	4.9	49.5	4.95	50	5;
	1	0	0	4	0	0	49	4.9	49.5	4.95	50	5;
	1	0.0017	0	4	54.25	798.1	93	1414	124	1964	155	2588.22;
	1	0.0017	0	4	54.25	798.1	93	1414	124	1964	155	2588.22;
	1	0.00795	0	4	140	2094	227.5	3602	280	4607	350	6085.46;
	1	7.59E-05	0	4	15.8	2363	16	2461	19.8	4287	20	4377.15;
	1	7.59E-05	0	4	15.8	2363	16	2461	19.8	4287	20	4377.15;
	1	0.00106	0	4	15.2	258.3	38	674	60.8	1253	76	1800.71;
	1	0.00106	0	4	15.2	258.3	38	674	60.8	1253	76	1800.71;
	1	7.59E-05	0	4	15.8	2363	16	2461	19.8	4287	20	4377.15;
	1	7.59E-05	0	4	15.8	2363	16	2461	19.8	4287	20	4377.15;
	1	0.00106	0	4	15.2	258.3	38	674	60.8	1253	76	1800.71;
	1	0.00106	0	4	15.2	258.3	38	674	60.8	1253	76	1800.71;
	1	0.00475	0	4	25	1699	50	3657	80	6330	100	8296.68;
```

```
1   0.00475    0  4     25    1699     50   3657     80    6330   100  8296.68;
1   0.00475    0  4     25    1699     50   3657     80    6330   100  8296.68;
1   0.01176    0  4  68.95    4835  118.2   8770  157.6   12212   197  15919.2;
1   0.01176    0  4  68.95    4835  118.2   8770  157.6   12212   197  15919.2;
1   0.01176    0  4  68.95    4835  118.2   8770  157.6   12212   197  15919.2;
1         0    0  4      0       0    0.3   1000    0.6    2005   0.9  3010;
1   0.00057    0  4    2.4   205.2      6    521    9.6   940.9    12  1332.48;
1   0.00057    0  4    2.4   205.2      6    521    9.6   940.9    12  1332.48;
1   0.00057    0  4    2.4   205.2      6    521    9.6   940.9    12  1332.48;
1   0.00057    0  4    2.4   205.2      6    521    9.6   940.9    12  1332.48;
1   0.00057    0  4    2.4   205.2      6    521    9.6   940.9    12  1332.48;
1    0.0017    0  4  54.25   798.1     93   1414    124    1964   155  2588.22;
1    0.0017    0  4  54.25   798.1     93   1414    124    1964   155  2588.22;
1         0    0  4    100    2200    200   4400    320    7040   400  8800;
1         0    0  4    100    2200    200   4400    320    7040   400  8800;
1         0    0  4      0       0     49    4.9   49.5    4.95    50  5;
1         0    0  4      0       0     49    4.9   49.5    4.95    50  5;
1         0    0  4      0       0     49    4.9   49.5    4.95    50  5;
1         0    0  4      0       0     49    4.9   49.5    4.95    50  5;
1         0    0  4      0       0     49    4.9   49.5    4.95    50  5;
1         0    0  4      0       0     49    4.9   49.5    4.95    50  5;
1    0.0017    0  4  54.25   798.1     93   1414    124    1964   155  2588.22;
1    0.0017    0  4  54.25   798.1     93   1414    124    1964   155  2588.22;
1   0.00795    0  4    140    2094  227.5   3602    280    4607   350  6085.46;
1  7.59E-05    0  4   15.8    2363     16   2461   19.8    4287    20  4377.15;
1  7.59E-05    0  4   15.8    2363     16   2461   19.8    4287    20  4377.15;
1   0.00106    0  4   15.2   258.3     38    674   60.8    1253    76  1800.71;
1   0.00106    0  4   15.2   258.3     38    674   60.8    1253    76  1800.71;
1  7.59E-05    0  4   15.8    2363     16   2461   19.8    4287    20  4377.15;
1  7.59E-05    0  4   15.8    2363     16   2461   19.8    4287    20  4377.15;
1   0.00106    0  4   15.2   258.3     38    674   60.8    1253    76  1800.71;
1   0.00106    0  4   15.2   258.3     38    674   60.8    1253    76  1800.71;
1   0.00475    0  4     25    1699     50   3657     80    6330   100  8296.68;
1   0.00475    0  4     25    1699     50   3657     80    6330   100  8296.68;
1   0.00475    0  4     25    1699     50   3657     80    6330   100  8296.68;
1   0.01176    0  4  68.95    4835  118.2   8770  157.6   12212   197  15919.2;
1   0.01176    0  4  68.95    4835  118.2   8770  157.6   12212   197  15919.2;
1   0.01176    0  4  68.95    4835  118.2   8770  157.6   12212   197  15919.2;
1         0    0  4      0       0    0.3   1000    0.6    2005   0.9  3010;
1   0.00057    0  4    2.4   205.2      6    521    9.6   940.9    12  1332.48;
1   0.00057    0  4    2.4   205.2      6    521    9.6   940.9    12  1332.48;
1   0.00057    0  4    2.4   205.2      6    521    9.6   940.9    12  1332.48;
1   0.00057    0  4    2.4   205.2      6    521    9.6   940.9    12  1332.48;
```

```
  1   0.00057        0   4    2.4   205.2    6    521    9.6   940.9   12   1332.48;
  1    0.0017        0   4   54.25  798.1    93   1414   124   1964    155  2588.22;
  1    0.0017        0   4   54.25  798.1    93   1414   124   1964    155  2588.22;
  1         0        0   4   100    2200     200  4400   320   7040    400  8800;
  1         0        0   4   100    2200     200  4400   320   7040    400  8800;
  1         0        0   4   0      0        49   4.9    49.5  4.95    50   5;
  1         0        0   4   0      0        49   4.9    49.5  4.95    50   5;
  1         0        0   4   0      0        49   4.9    49.5  4.95    50   5;
  1         0        0   4   0      0        49   4.9    49.5  4.95    50   5;
  1         0        0   4   0      0        49   4.9    49.5  4.95    50   5;
  1         0        0   4   0      0        49   4.9    49.5  4.95    50   5;
  1    0.0017        0   4   54.25  798.1    93   1414   124   1964    155  2588.22;
  1    0.0017        0   4   54.25  798.1    93   1414   124   1964    155  2588.22;
  1   0.00795        0   4   140    2094     227.5 3602   280   4607    350  6085.46;
];
```

Load Scaling Data:

Area/Bus number			% of System Load	Load	
1	2	3		MW	MVar
101	201	301	3.8	108	22
102	202	302	3.4	97	20
103	203	303	6.3	180	37
104	204	304	2.6	74	15
105	205	305	2.5	71	14
106	206	306	4.8	136	28
107	207	307	4.4	125	25
108	208	308	6	171	35
109	209	309	6.1	175	36
110	210	310	6.8	195	40
113	213	313	9.3	265	54
114	214	314	6.8	194	39
115	215	315	11.1	317	64
116	216	316	3.5	100	20
118	218	318	11.7	333	68
119	219	319	6.4	181	37
120	220	320	4.5	128	26
Total			100	2850	580

Hour	Summer Weekdays % of peak load
12:00 - 1:00AM	64
1:00-2:00	60
2:00-3:00	58
3:00-4:00	56
4:00-5:00	56
5:00-6:00	58
6:00-7:00	64
7:00-8:00	76
8:00-9:00	87
9:00-10:00	95
10:00-11:00	99
11:00-12:00PM	100
12:00-1:00	99
1:00-2:00	100
2:00-3:00	100
3:00-4:00	97
4:00-5:00	96
5:00-6:00	96
6:00-7:00	93
7:00-8:00	92
8:00-9:00	92
9:00-10:00	93
10:00-11:00	87
11:00-12:00	72

C.2 IEEE 118-Bus System Data

```
%% MATPOWER Case Format : Version 2

mpc.version = '2';

 %%-----  Power Flow Data  -----%%

%% system MVA base

mpc.baseMVA = 100;

 %bus_i  type   Pd     Qd     Gs     Bs     area          Vm        Va      baseKV     zone     Vmax
 mpc.bus = [
        1        2     51     27      0      0      1        0.955     10.983     138           1     1.06     0.94;
```

2	1	20	9	0	0	1	0.97139	11.523	138	1	1.06	0.94;
3	1	39	10	0	0	1	0.96769	11.866	138	1	1.06	0.94;
4	2	39	12	0	0	1	0.998	15.583	138	1	1.06	0.94;
5	1	0	0	0	-40	1	1.00198	16.028	138	1	1.06	0.94;
6	2	52	22	0	0	1	0.99	13.302	138	1	1.06	0.94;
7	1	19	2	0	0	1	0.98933	12.857	138	1	1.06	0.94;
8	2	28	0	0	0	1	1.015	21.049	345	1	1.06	0.94;
9	1	0	0	0	0	1	1.04292	28.303	345	1	1.06	0.94;
10	2	0	0	0	0	1	1.05	35.884	345	1	1.06	0.94;
11	1	70	23	0	0	1	0.98509	13.016	138	1	1.06	0.94;
12	2	47	10	0	0	1	0.99	12.499	138	1	1.06	0.94;
13	1	34	16	0	0	1	0.9683	11.641	138	1	1.06	0.94;
14	1	14	1	0	0	1	0.98359	11.783	138	1	1.06	0.94;
15	2	90	30	0	0	1	0.97	11.489	138	1	1.06	0.94;
16	1	25	10	0	0	1	0.98391	12.198	138	1	1.06	0.94;
17	1	11	3	0	0	1	0.99513	14.006	138	1	1.06	0.94;
18	2	60	34	0	0	1	0.973	11.793	138	1	1.06	0.94;
19	2	45	25	0	0	1	0.963	11.314	138	1	1.06	0.94;
20	1	18	3	0	0	1	0.95776	12.192	138	1	1.06	0.94;
21	1	14	8	0	0	1	0.95841	13.779	138	1	1.06	0.94;
22	1	10	5	0	0	1	0.96954	16.332	138	1	1.06	0.94;
23	1	7	3	0	0	1	0.99972	21.249	138	1	1.06	0.94;
24	2	13	0	0	0	1	0.992	21.118	138	1	1.06	0.94;
25	2	0	0	0	0	1	1.05	28.184	138	1	1.06	0.94;
26	2	0	0	0	0	1	1.015	29.965	345	1	1.06	0.94;
27	2	71	13	0	0	1	0.968	15.613	138	1	1.06	0.94;
28	1	17	7	0	0	1	0.96157	13.889	138	1	1.06	0.94;
29	1	24	4	0	0	1	0.96322	12.897	138	1	1.06	0.94;
30	1	0	0	0	0	1	0.98553	19.04	345	1	1.06	0.94;
31	2	43	27	0	0	1	0.967	13.014	138	1	1.06	0.94;
32	2	59	23	0	0	1	0.964	15.054	138	1	1.06	0.94;
33	1	23	9	0	0	1	0.97161	10.864	138	1	1.06	0.94;
34	2	59	26	0	14	1	0.986	11.505	138	1	1.06	0.94;
35	1	33	9	0	0	1	0.9807	11.08	138	1	1.06	0.94;
36	2	31	17	0	0	1	0.98	11.085	138	1	1.06	0.94;
37	1	0	0	0	-25	1	0.99208	11.969	138	1	1.06	0.94;
38	1	0	0	0	0	1	0.96204	17.106	345	1	1.06	0.94;
39	1	27	11	0	0	1	0.97049	8.598	138	1	1.06	0.94;
40	2	66	23	0	0	1	0.97	7.525	138	1	1.06	0.94;
41	1	37	10	0	0	1	0.96683	7.079	138	1	1.06	0.94;
42	2	96	23	0	0	1	0.985	8.674	138	1	1.06	0.94;
43	1	18	7	0	0	1	0.97858	11.459	138	1	1.06	0.94;
44	1	16	8	0	10	1	0.98505	13.945	138	1	1.06	0.94;

45	1	53	22	0	10	1	0.98667	15.776	138	1	1.06	0.94;
46	2	28	10	0	10	1	1.005	18.582	138	1	1.06	0.94;
47	1	34	0	0	0	1	1.01705	20.805	138	1	1.06	0.94;
48	1	20	11	0	15	1	1.02063	20.025	138	1	1.06	0.94;
49	2	87	30	0	0	1	1.025	21.028	138	1	1.06	0.94;
50	1	17	4	0	0	1	1.00108	18.989	138	1	1.06	0.94;
51	1	17	8	0	0	1	0.96688	16.37	138	1	1.06	0.94;
52	1	18	5	0	0	1	0.95682	15.417	138	1	1.06	0.94;
53	1	23	11	0	0	1	0.94598	14.442	138	1	1.06	0.94;
54	2	113	32	0	0	1	0.955	15.353	138	1	1.06	0.94;
55	2	63	22	0	0	1	0.952	15.063	138	1	1.06	0.94;
56	2	84	18	0	0	1	0.954	15.25	138	1	1.06	0.94;
57	1	12	3	0	0	1	0.97058	16.455	138	1	1.06	0.94;
58	1	12	3	0	0	1	0.95904	15.598	138	1	1.06	0.94;
59	2	277	113	0	0	1	0.985	19.452	138	1	1.06	0.94;
60	1	78	3	0	0	1	0.99316	23.234	138	1	1.06	0.94;
61	2	0	0	0	0	1	0.995	24.125	138	1	1.06	0.94;
62	2	77	14	0	0	1	0.998	23.509	138	1	1.06	0.94;
63	1	0	0	0	0	1	0.96874	22.831	345	1	1.06	0.94;
64	1	0	0	0	0	1	0.98374	24.597	345	1	1.06	0.94;
65	2	0	0	0	0	1	1.005	27.722	345	1	1.06	0.94;
66	2	39	18	0	0	1	1.05	27.563	138	1	1.06	0.94;
67	1	28	7	0	0	1	1.01968	24.923	138	1	1.06	0.94;
68	1	0	0	0	0	1	1.00325	27.601	345	1	1.06	0.94;
69	3	0	0	0	0	1	1.035	30	138	1	1.06	0.94;
70	2	66	20	0	0	1	0.984	22.62	138	1	1.06	0.94;
71	1	0	0	0	0	1	0.98684	22.209	138	1	1.06	0.94;
72	2	12	0	0	0	1	0.98	21.112	138	1	1.06	0.94;
73	2	6	0	0	0	1	0.991	21.998	138	1	1.06	0.94;
74	2	68	27	0	12	1	0.958	21.671	138	1	1.06	0.94;
75	1	47	11	0	0	1	0.96733	22.933	138	1	1.06	0.94;
76	2	68	36	0	0	1	0.943	21.803	138	1	1.06	0.94;
77	2	61	28	0	0	1	1.006	26.757	138	1	1.06	0.94;
78	1	71	26	0	0	1	1.00342	26.453	138	1	1.06	0.94;
79	1	39	32	0	20	1	1.00922	26.752	138	1	1.06	0.94;
80	2	130	26	0	0	1	1.04	28.998	138	1	1.06	0.94;
81	1	0	0	0	0	1	0.99681	28.149	345	1	1.06	0.94;
82	1	54	27	0	20	1	0.98881	27.276	138	1	1.06	0.94;
83	1	20	10	0	10	1	0.98457	28.465	138	1	1.06	0.94;
84	1	11	7	0	0	1	0.97977	30.997	138	1	1.06	0.94;
85	2	24	15	0	0	1	0.985	32.55	138	1	1.06	0.94;
86	1	21	10	0	0	1	0.98669	31.181	138	1	1.06	0.94;
87	2	0	0	0	0	1	1.015	31.44	161	1	1.06	0.94;

```
    88     1    48    10     0     0     1    0.98746    35.68    138          1    1.06    0.94;
    89     2     0     0     0     0     1      1.005    39.734    138          1    1.06    0.94;
    90     2   440    42     0     0     1      0.985    33.331    138          1    1.06    0.94;
    91     2    10     0     0     0     1       0.98    33.352    138          1    1.06    0.94;
    92     2    65    10     0     0     1      0.993    33.841    138          1    1.06    0.94;
    93     1    12     7     0     0     1    0.98737    30.837    138          1    1.06    0.94;
    94     1    30    16     0     0     1    0.99081    28.687    138          1    1.06    0.94;
    95     1    42    31     0     0     1    0.98111    27.716    138          1    1.06    0.94;
    96     1    38    15     0     0     1     0.9928    27.549    138          1    1.06    0.94;
    97     1    15     9     0     0     1    1.01143    27.923    138          1    1.06    0.94;
    98     1    34     8     0     0     1    1.02351    27.446    138          1    1.06    0.94;
    99     2    42     0     0     0     1       1.01    27.085    138          1    1.06    0.94;
   100     2    37    18     0     0     1      1.017    28.081    138          1    1.06    0.94;
   101     1    22    15     0     0     1    0.99276    29.649    138          1    1.06    0.94;
   102     1     5     3     0     0     1    0.99159    32.341    138          1    1.06    0.94;
   103     2    23    16     0     0     1      1.001     24.48    138          1    1.06    0.94;
   104     2    38    25     0     0     1      0.971    21.742    138          1    1.06    0.94;
   105     2    31    26     0    20     1      0.965    20.634    138          1    1.06    0.94;
   106     1    43    16     0     0     1    0.96114    20.379    138          1    1.06    0.94;
   107     2    50    12     0     6     1      0.952    17.576    138          1    1.06    0.94;
   108     1     2     1     0     0     1    0.96621    19.434    138          1    1.06    0.94;
   109     1     8     3     0     0     1    0.96703    18.982    138          1    1.06    0.94;
   110     2    39    30     0     6     1      0.973    18.135    138          1    1.06    0.94;
   111     2     0     0     0     0     1       0.98     19.78    138          1    1.06    0.94;
   112     2    68    13     0     0     1      0.975    15.036    138          1    1.06    0.94;
   113     2     6     0     0     0     1      0.993    14.004    138          1    1.06    0.94;
   114     1     8     3     0     0     1    0.96068    14.727    138          1    1.06    0.94;
   115     1    22     7     0     0     1    0.96053     14.72    138          1    1.06    0.94;
   116     2   184     0     0     0     1      1.005    27.166    138          1    1.06    0.94;
   117     1    20     8     0     0     1    0.97382    10.958    138          1    1.06    0.94;
   118     1    33    15     0     0     1    0.94944    21.945    138          1    1.06    0.94;
];
```

%Generator Data : Columns 1:10

```
%bus    Pg       Qg          Qmax    Qmin    Vg       mBase    status    Pmax    Pmin
mpc.gen = [
    10     450    -51.04     200     -147    1.05     100        1      550       0
    12      85    91.27      120      -35    0.99     100        1      185       0
    25     220    49.72      140      -47    1.05     100        1      320       0
    26     314     9.89      1000    -1000   1.015    100        1      414       0
    31       7    31.57      300     -300    0.967    100        1      107       0
```

```
    46      19    -5.25     100   -100  1.005     100     1     119     0
    49     204   115.63     210    -85  1.025     100     1     304     0
    54      48      3.9     300   -300  0.955     100     1     148     0
    59     155    76.83     180    -60  0.985     100     1     255     0
    61     160   -40.39     300   -100  0.995     100     1     260     0
    65     391    80.76     200    -67  1.005     100     1     491     0
    66     392    -1.95     200    -67   1.05     100     1     492     0
    69  513.48   -82.39     300   -300  1.035     100     1   805.2     0
    80     477    104.9     280   -165   1.04     100     1     577     0
    87       4    11.02    1000   -100  1.015     100     1     104     0
    92     607     0.49       9     -3   0.99     100     1     100     0
   100     252   108.87     155    -50  1.017     100     1     352     0
   103      40    41.69      40    -15   1.01     100     1     140     0
   111      36    -1.84    1000   -100   0.98     100     1     136     0
];
```

%Generator Data Continued: Columns 11:21

```
Pc1  Pc2  Qc1min  Qc1max  Qc2min  Qc2max  ramp_agc  ramp_10  ramp_30  ramp_q  apf
[
  0    0       0       0       0       0         0        0        0       0  0;
  0    0       0       0       0       0         0        0        0       0  0;
  0    0       0       0       0       0         0        0        0       0  0;
  0    0       0       0       0       0         0        0        0       0  0;
  0    0       0       0       0       0         0        0        0       0  0;
  0    0       0       0       0       0         0        0        0       0  0;
  0    0       0       0       0       0         0        0        0       0  0;
  0    0       0       0       0       0         0        0        0       0  0;
  0    0       0       0       0       0         0        0        0       0  0;
  0    0       0       0       0       0         0        0        0       0  0;
  0    0       0       0       0       0         0        0        0       0  0;
  0    0       0       0       0       0         0        0        0       0  0;
  0    0       0       0       0       0         0        0        0       0  0;
  0    0       0       0       0       0         0        0        0       0  0;
  0    0       0       0       0       0         0        0        0       0  0;
  0    0       0       0       0       0         0        0        0       0  0;
  0    0       0       0       0       0         0        0        0       0  0;
  0    0       0       0       0       0         0        0        0       0  0;
  0    0       0       0       0       0         0        0        0       0  0;
];
```

%Branch Data

```
%fbus tbus r x b rate A rate B rate C ratio angle status angmin angmax
mpc.branch = [
    1    2  0.0303  0.0999  0.0254  220  230  250  0  0  1  -360  360;
    1    3  0.0129  0.0424  0.01082  220  230  250  0  0  1  -360  360;
    2   12  0.0187  0.0616  0.01572  220  230  250  0  0  1  -360  360;
    3    5  0.0241   0.108  0.0284  220  230  250  0  0  1  -360  360;
    3   12  0.0484    0.16  0.0406  220  230  250  0  0  1  -360  360;
    4    5  0.00176  0.00798  0.0021  440  460  500  0  0  1  -360  360;
    4   11  0.0209  0.0688  0.01748  220  230  250  0  0  1  -360  360;
    5    6  0.0119   0.054  0.01426  220  230  250  0  0  1  -360  360;
    5   11  0.0203  0.0682  0.01738  220  230  250  0  0  1  -360  360;
    6    7  0.00459  0.0208  0.0055  220  230  250  0  0  1  -360  360;
    7   12  0.00862   0.034  0.00874  220  230  250  0  0  1  -360  360;
    8    9  0.00244  0.0305   1.162  1100  1150  1250  0  0  1  -360  360;
    8    5  0  0.0267  0  880  920  1000  0  0  1  -360  360;
    8   30  0.00431  0.0504  0.514  220  230  250  0  0  1  -360  360;
    9   10  0.00258  0.0322   1.23  1100  1150  1250  0  0  1  -360  360;
   11   12  0.00595  0.0196  0.00502  220  230  250  0  0  1  -360  360;
   11   13  0.02225  0.0731  0.01876  220  230  250  0  0  1  -360  360;
   12   15  0.0215  0.0707  0.01816  220  230  250  0  0  1  -360  360;
   12   17  0.0212  0.0834  0.0214  220  230  250  0  0  1  -360  360;
   12  117  0.0329   0.14  0.0358  220  230  250  0  0  1  -360  360;
   13   15  0.0744  0.2444  0.06268  220  230  250  0  0  1  -360  360;
   14   15  0.0595   0.195  0.0502  220  230  250  0  0  1  -360  360;
   15   17  0.0132  0.0437  0.0444  440  460  500  0  0  1  -360  360;
   15   19   0.012  0.0394  0.0101  220  230  250  0  0  1  -360  360;
   15   33   0.038  0.1244  0.03194  220  230  250  0  0  1  -360  360;
   16   17  0.0454  0.1801  0.0466  220  230  250  0  0  1  -360  360;
   17   19  0.0123  0.0505  0.01298  220  230  250  0  0  1  -360  360;
   17   31  0.0474  0.1563  0.0399  220  230  250  0  0  1  -360  360;
   17  113  0.00913  0.0301  0.00768  220  230  250  0  0  1  -360  360;
   18   19  0.01119  0.0493  0.01142  220  230  250  0  0  1  -360  360;
   19   20  0.0252   0.117  0.0298  220  230  250  0  0  1  -360  360;
   19   34  0.0752   0.247  0.0632  220  230  250  0  0  1  -360  360;
   20   21  0.0183  0.0849  0.0216  220  230  250  0  0  1  -360  360;
   21   22  0.0209   0.097  0.0246  220  230  250  0  0  1  -360  360;
```

22	23	0.0342	0.159	0.0404	220	230	250	0	0	1	-360	360;
23	24	0.0135	0.0492	0.0498	220	230	250	0	0	1	-360	360;
23	25	0.0156	0.08	0.0864	440	460	500	0	0	1	-360	360;
23	32	0.0317	0.1153	0.1173	220	230	250	0	0	1	-360	360;
24	70	0.00221	0.4115	0.10198	220	230	250	0	0	1	-360	360;
24	72	0.0488	0.196	0.0488	220	230	250	0	0	1	-360	360;
25	27	0.0318	0.163	0.1764	440	460	500	0	0	1	-360	360;
26	25	0	0.0382	0	220	230	250	0	0	1	-360	360;
26	30	0.00799	0.086	0.908	660	690	750	0	0	1	-360	360;
27	28	0.01913	0.0855	0.0216	220	230	250	0	0	1	-360	360;
27	32	0.0229	0.0755	0.01926	220	230	250	0	0	1	-360	360;
27	115	0.0164	0.0741	0.01972	220	230	250	0	0	1	-360	360;
28	31	0.0237	0.0943	0.0238	220	230	250	0	0	1	-360	360;
29	31	0.0108	0.0331	0.0083	220	230	250	0	0	1	-360	360;
30	17	0	0.0388	0	660	690	750	0	0	1	-360	360;
30	38	0.00464	0.054	0.422	220	230	250	0	0	1	-360	360;
31	32	0.0298	0.0985	0.0251	220	230	250	0	0	1	-360	360;
32	113	0.0615	0.203	0.0518	220	230	250	0	0	1	-360	360;
32	114	0.0135	0.0612	0.01628	220	230	250	0	0	1	-360	360;
33	37	0.0415	0.142	0.0366	220	230	250	0	0	1	-360	360;
34	36	0.00871	0.0268	0.00568	220	230	250	0	0	1	-360	360;
34	37	0.00256	0.0094	0.00984	440	460	500	0	0	1	-360	360;
34	43	0.0413	0.1681	0.04226	220	230	250	0	0	1	-360	360;
35	36	0.00224	0.0102	0.00268	220	230	250	0	0	1	-360	360;
35	37	0.011	0.0497	0.01318	220	230	250	0	0	1	-360	360;
37	39	0.0321	0.106	0.027	220	230	250	0	0	1	-360	360;
37	40	0.0593	0.168	0.042	220	230	250	0	0	1	-360	360;
38	37	0	0.0375	0	660	690	750	0	0	1	-360	360;
38	65	0.00901	0.0986	1.046	440	460	500	0	0	1	-360	360;
39	40	0.0184	0.0605	0.01552	220	230	250	0	0	1	-360	360;
40	41	0.0145	0.0487	0.01222	220	230	250	0	0	1	-360	360;
40	42	0.0555	0.183	0.0466	220	230	250	0	0	1	-360	360;
41	42	0.041	0.135	0.0344	220	230	250	0	0	1	-360	360;
42	49	0.0715	0.323	0.086	220	230	250	0	0	1	-360	360;
42	49	0.0715	0.323	0.086	220	230	250	0	0	1	-360	360;
43	44	0.0608	0.2454	0.06068	220	230	250	0	0	1	-360	360;
44	45	0.0224	0.0901	0.0224	220	230	250	0	0	1	-360	360;
45	46	0.04	0.1356	0.0332	220	230	250	0	0	1	-360	360;

45	49	0.0684	0.186	0.0444	220	230	250	0	0	1	-360	360;
46	47	0.038	0.127	0.0316	220	230	250	0	0	1	-360	360;
46	48	0.0601	0.189	0.0472	220	230	250	0	0	1	-360	360;
47	49	0.0191	0.0625	0.01604	220	230	250	0	0	1	-360	360;
47	69	0.0844	0.2778	0.07092	220	230	250	0	0	1	-360	360;
48	49	0.0179	0.0505	0.01258	220	230	250	0	0	1	-360	360;
49	50	0.0267	0.0752	0.01874	220	230	250	0	0	1	-360	360;
49	51	0.0486	0.137	0.0342	220	230	250	0	0	1	-360	360;
49	54	0.073	0.289	0.0738	220	230	250	0	0	1	-360	360;
49	54	0.0869	0.291	0.073	220	230	250	0	0	1	-360	360;
49	66	0.018	0.0919	0.0248	440	460	500	0	0	1	-360	360;
49	66	0.018	0.0919	0.0248	440	460	500	0	0	1	-360	360;
49	69	0.0985	0.324	0.0828	220	230	250	0	0	1	-360	360;
50	57	0.0474	0.134	0.0332	220	230	250	0	0	1	-360	360;
51	52	0.0203	0.0588	0.01396	220	230	250	0	0	1	-360	360;
51	58	0.0255	0.0719	0.01788	220	230	250	0	0	1	-360	360;
52	53	0.0405	0.1635	0.04058	220	230	250	0	0	1	-360	360;
53	54	0.0263	0.122	0.031	220	230	250	0	0	1	-360	360;
54	55	0.0169	0.0707	0.0202	220	230	250	0	0	1	-360	360;
54	56	0.00275	0.00955	0.00732	220	230	250	0	0	1	-360	360;
54	59	0.0503	0.2293	0.0598	220	230	250	0	0	1	-360	360;
55	56	0.00488	0.0151	0.00374	220	230	250	0	0	1	-360	360;
55	59	0.04739	0.2158	0.05646	220	230	250	0	0	1	-360	360;
56	57	0.0343	0.0966	0.0242	220	230	250	0	0	1	-360	360;
56	58	0.0343	0.0966	0.0242	220	230	250	0	0	1	-360	360;
56	59	0.0825	0.251	0.0569	220	230	250	0	0	1	-360	360;
56	59	0.0803	0.239	0.0536	220	230	250	0	0	1	-360	360;
59	60	0.0317	0.145	0.0376	220	230	250	0	0	1	-360	360;
59	61	0.0328	0.15	0.0388	220	230	250	0	0	1	-360	360;
60	61	0.00264	0.0135	0.01456	440	460	500	0	0	1	-360	360;
60	62	0.0123	0.0561	0.01468	220	230	250	0	0	1	-360	360;
61	62	0.00824	0.0376	0.0098	220	230	250	0	0	1	-360	360;
62	66	0.0482	0.218	0.0578	220	230	250	0	0	1	-360	360;
62	67	0.0258	0.117	0.031	220	230	250	0	0	1	-360	360;
63	59	0	0.0386	0	440	460	500	0	0	1	-360	360;
63	64	0.00172	0.02	0.216	440	460	500	0	0	1	-360	360;
64	61	0	0.0268	0	220	230	250	0	0	1	-360	360;
64	65	0.00269	0.0302	0.38	440	460	500	0	0	1	-360	360;
65	66	0	0.037	0	220	230	250	0	0	1	-360	360;

65	68	0.00138	0.016	0.638	220	230	250	0	0	1	-360	360;
66	67	0.0224	0.1015	0.02682	220	230	250	0	0	1	-360	360;
68	69	0	0.037	0	440	460	500	0	0	1	-360	360;
68	81	0.00175	0.0202	0.808	220	230	250	0	0	1	-360	360;
68	116	0.00034	0.00405	0.164	440	460	500	0	0	1	-360	360;
69	70	0.03	0.127	0.122	440	460	500	0	0	1	-360	360;
69	75	0.0405	0.122	0.124	440	460	500	0	0	1	-360	360;
69	77	0.0309	0.101	0.1038	220	230	250	0	0	1	-360	360;
70	71	0.00882	0.0355	0.00878	220	230	250	0	0	1	-360	360;
70	74	0.0401	0.1323	0.03368	220	230	250	0	0	1	-360	360;
70	75	0.0428	0.141	0.036	220	230	250	0	0	1	-360	360;
71	72	0.0446	0.18	0.04444	220	230	250	0	0	1	-360	360;
71	73	0.00866	0.0454	0.01178	220	230	250	0	0	1	-360	360;
74	75	0.0123	0.0406	0.01034	220	230	250	0	0	1	-360	360;
75	77	0.0601	0.1999	0.04978	220	230	250	0	0	1	-360	360;
75	118	0.0145	0.0481	0.01198	220	230	250	0	0	1	-360	360;
76	77	0.0444	0.148	0.0368	220	230	250	0	0	1	-360	360;
76	118	0.0164	0.0544	0.01356	220	230	250	0	0	1	-360	360;
77	78	0.00376	0.0124	0.01264	220	230	250	0	0	1	-360	360;
77	80	0.017	0.0485	0.0472	440	460	500	0	0	1	-360	360;
77	80	0.0294	0.105	0.0228	220	230	250	0	0	1	-360	360;
77	82	0.0298	0.0853	0.08174	220	230	250	0	0	1	-360	360;
78	79	0.00546	0.0244	0.00648	220	230	250	0	0	1	-360	360;
79	80	0.0156	0.0704	0.0187	220	230	250	0	0	1	-360	360;
80	96	0.0356	0.182	0.0494	220	230	250	0	0	1	-360	360;
80	97	0.0183	0.0934	0.0254	220	230	250	0	0	1	-360	360;
80	98	0.0238	0.108	0.0286	220	230	250	0	0	1	-360	360;
80	99	0.0454	0.206	0.0546	220	230	250	0	0	1	-360	360;
81	80	0	0.037	0	220	230	250	0	0	1	-360	360;
82	83	0.0112	0.03665	0.03796	220	230	250	0	0	1	-360	360;
82	96	0.0162	0.053	0.0544	220	230	250	0	0	1	-360	360;
83	84	0.0625	0.132	0.0258	220	230	250	0	0	1	-360	360;
83	85	0.043	0.148	0.0348	220	230	250	0	0	1	-360	360;
84	85	0.0302	0.0641	0.01234	220	230	250	0	0	1	-360	360;
85	86	0.035	0.123	0.0276	220	230	250	0	0	1	-360	360;
85	88	0.02	0.102	0.0276	220	230	250	0	0	1	-360	360;
85	89	0.0239	0.173	0.047	220	230	250	0	0	1	-360	360;
86	87	0.02828	0.2074	0.0445	220	230	250	0	0	1	-360	360;

```
    88     89   0.0139    0.0712    0.01934   440   460   500   0   0   1   -360   360;
    89     90   0.0518     0.032      0.032   660   230   250   0   0   1   -360   360;
    89     91   0.0099     0.032      0.065   220   220   220   0   0   1   -360   360;
    89     92   0.0099    0.0505      0.065   220   690   750   0   0   1   -360   360;
    90     91   0.0254    0.0505      0.065   660   230   250   0   0   1   -360   360;
    91     92   0.0387    0.1272      0.032   220   230   250   0   0   1   -360   360;
    92     93   0.0258     0.032     0.0218   220   230   250   0   0   1   -360   360;
    92     94   0.0481     0.158     0.0406   220   230   250   0   0   1   -360   360;
    92    100   0.0648     0.295     0.0472   220   230   250   0   0   1   -360   360;
    92    102   0.0123    0.0559    0.01464   220   230   250   0   0   1   -360   360;
    93     94   0.0223    0.0732    0.01876   220   230   250   0   0   1   -360   360;
    94     95   0.0132    0.0434     0.0111   220   230   250   0   0   1   -360   360;
    94     96   0.0269    0.0869      0.023   220   230   250   0   0   1   -360   360;
    94    100   0.0178     0.058     0.0604   220   230   250   0   0   1   -360   360;
    95     96   0.0171    0.0547    0.01474   220   230   250   0   0   1   -360   360;
    96     97   0.0173    0.0885      0.024   220   230   250   0   0   1   -360   360;
    98    100   0.0397     0.179     0.0476   220   230   250   0   0   1   -360   360;
    99    100    0.018    0.0813     0.0216   220   230   250   0   0   1   -360   360;
   100    101   0.0277    0.1262     0.0328   220   230   250   0   0   1   -360   360;
   100    103    0.016    0.0525     0.0536   440   460   500   0   0   1   -360   360;
   100    104   0.0451     0.204     0.0541   220   230   250   0   0   1   -360   360;
   100    106   0.0605     0.229      0.062   220   230   250   0   0   1   -360   360;
   101    102   0.0246     0.112     0.0294   220   230   250   0   0   1   -360   360;
   103    104   0.0466    0.1584     0.0407   220   230   250   0   0   1   -360   360;
   103    105   0.0535    0.1625     0.0408   220   230   250   0   0   1   -360   360;
   103    110   0.03906   0.1813     0.0461   220   230   250   0   0   1   -360   360;
   104    105   0.00994   0.0378    0.00986   220   230   250   0   0   1   -360   360;
   105    106    0.014    0.0547    0.01434   220   230   250   0   0   1   -360   360;
   105    107    0.053     0.183     0.0472   220   230   250   0   0   1   -360   360;
   105    108   0.0261    0.0703    0.01844   220   230   250   0   0   1   -360   360;
   106    107    0.053     0.183     0.0472   220   230   250   0   0   1   -360   360;
   108    109   0.0105    0.0288     0.0076   220   230   250   0   0   1   -360   360;
   109    110   0.0278    0.0762     0.0202   220   230   250   0   0   1   -360   360;
   110    111    0.022    0.0755       0.02   220   230   250   0   0   1   -360   360;
   110    112   0.0247     0.064      0.062   220   230   250   0   0   1   -360   360;
   114    115   0.0023    0.0104    0.00276   220   230   250   0   0   1   -360   360;
];

%Generator Cost Data:

  %1   startup      shutdown    n    x1    y1    ...        xn           yn
```

```
mpc.gencost = [
    1    0    0    2    0    0    550    119.35;
    1    0    0    2    0    0    185    194.62;
    1    0    0    2    0    0    320    138.88;
    1    0    0    2    0    0    414    127.512;
    1    0    0    2    0    0    107    629.374;
    1    0    0    2    0    0    119    410.312;
    1    0    0    2    0    0    304    141.968;
    1    0    0    2    0    0    148    255.152;
    1    0    0    2    0    0    255    154.53;
    1    0    0    2    0    0    260    152.88;
    1    0    0    2    0    0    491    122.406;
    1    0    0    2    0    0    492    122.36;
    1    0    0    2    0    0    805.2  152.746;
    1    0    0    2    0    0    577    118.285;
    1    0    0    2    0    0    104    742.768;
    1    0    0    2    0    0    100    1000;
    1    0    0    2    0    0    352    134.112;
    1    0    0    2    0    0    140    280;
    1    0    0    2    0    0    136    295.528;
];
```

Works Cited

[1] Joseph Graves and John Clapp, "The Future of Electric Transmission," *The Energy Journal*, vol. 14, no. 10, pp. 11-21, December 2001.

[2] DOE ARPA-E, "Green Electricity Network Integration ," DOE-ARPA-E, Funding Opportunity FOA-0000473, 2011.

[3] S. Blumsack, "Network Topologies and Transmission investment Under Electric-Industry Restructuring," Pittsburgh, Pennsylvania, PhD Thesis 2006.

[4] A. Ipakchi and F. Albuyeh, "Grid of the Future," *IEEE Power and Energy Magazine*, pp. 52-62, February 2009.

[5] Paul L. Joskow, "Restructuring, Competition and Regulatory Reform in the U.S. Electricity Sector," in *Desigining Competitive Electricity Markets*.: INTERNATIONAL SERIES IN OPERATIONS RESEARCH & MANAGEMENT SCIENCE, 1998, ch. 2.

[6] Lauritz R. Christensen and William H. Greene, "Economies of Scale in U.S. Electric Power Generation," *The Journal of Political Economy*, vol. 84, no. 4, pp. 655-676, August 1976.

[7] Richard Sedano and Matthew Brown, "Electricity Transmission: A Primer," National Council on Electric Policy, 2004.

[8] Marc Nerlove, "Returns to Scale in Electricity Supply," *Mesurement in Economics - Studies in Mathematical Economics and Econometrics in Memory of Yehuda Grunfeld*, 1963.

[9] John F. Stewart, "Plant size, plant factor, and the shape of the average cost function in electric power generation: a nonhomogeneous capital approach," *The Bell Journal of Economics*, vol. 10, no. 2, pp. 549-565, Autumn 1979.

[10] William W. Hogan. (2002) Electricity Market Design and Structure: Working Paper on Standardized Transmission Service and Wholesale Electric Market Design. [Online]. www.whogan.com

[11] E. B. Fisher, R. P. O'Neill, and M. C. Ferris, "Optimal Transmission Swtiching," *IEEE Transactions on Power Systems*, vol. 23, no. 3, pp. 1346-1355, August 2008.

[12] Federal Energy Regulatory Comission. (2007, February) Preventing Undue Discrimination and Preference in Transmission Service. Order 890.

[13] Federal Energy Regulatory Comission. (2011, June) Transmission Planning and Cost Allocation by Transmission Owning and Operating Public Utilities. Order1000.

[14] Federal Energy Regulatory Comission. (2012, October) Docket No. RM10-23-002. Order 1000-B. [Online]. http://www.ferc.gov/whats-new/comm-meet/2012/101812/E-1.pdf

[15] U.S. Government Printing Office. (2005) 109th Congress Public Law 58. [Online]. http://www.gpo.gov/fdsys/pkg/PLAW-109publ58/html/PLAW-109publ58.htm

[16] Federal Energy Regulatory Comission. (2011, June) Increasing Efficiency Through Improved Software. [Online]. http://www.ferc.gov/industries/electric/indus-act/market-planning/2011-conference.asp

[17] Dietrich Braess, "Über ein Paradoxon aus der Verkehrsplanung," *Untemehmensforschung*, vol. 12, pp. 258-268, 1969.

[18] John J. Grainger and William D. Stevenson, *Power System Analysis*. New York, United States: McGraw-Hill Inc., 1994.

[19] Kory W. Hedman, Shmuel S. Oren, and Richard P. O'Neill, "A Review of Transmission Switching and Network Topology Optimization," in *IEEE PES General Meeting*, Detroit, MI, 2011.

[20] B. Hobbs, "Optimizaton methods for elecric utility resource planning," *European Journal of Operational Research*, vol. 83, pp. 1-20, 1995.

[21] K. Nara, "State of the arts of the modern heuristics application to power systems," in *IEEE Power Engineering Society Winter Meeting,2000*, 2000, pp. 1279-1283.

[22] G. Latore, R. D. Cruz, J. M. Areiza, and A. Villegas, "Classification of publications and models on transmission expansion planning," *IEEE Transactions on Power Systems*, vol. 18, no. 2, pp. 938-946, 2003.

[23] J. McCalley et al., "Models for transmission expansion planning based on reconfigurable capacitor switching," in *Economic Market Design and Planning for Electric Power systems*, J. Momoh and L. Mili, Eds.: John Wiley and Sons, 2006.

[24] R. Bent and W. Daniel, "Randomized Discrepancy Bounded Local Search for Transmission Expansion Planning," in *IEEE Power and Energy Society General Meeting*, Detroit, MI, 2011.

[25] H. J. Koglin and H. Muller, "Overload Reduction Through Corrective Switching Actions," in

International Conference on Power System Montoring and Control, 1980, pp. 159-164.

[26] H. Glavitsh, "Switching as Means of Control in the Power System," *International Journal of Electrical Power Energy Systems*, vol. 7, no. 2, pp. 92-100, April 1985.

[27] J G Rolim, "A Study of the Use of Corrective Switching in Transmission Systems," *IEEE Transactions on Power Systems*, vol. 14, no. 1, pp. 336-341, February 1999.

[28] R. Van Amerongen and H. P. Van Meeteren, "Security Control by Real Power Rescheduling Network Switching and Load Shedding," CIGRE, France, 32-02, 1980.

[29] J. C. Dodu, A. Merlin, and J. M. David, "On the Search of Optimal Switching Configurations in Power Transmission Systems Studies," in *Power System Computation Conference (PSCC)*, Lausanne, 1981, pp. 282-292.

[30] H. J. Koglin and M. F. Medeiros, "Further Developments in Corrective Switching," in *CIGRE/IFAC Symposium on Control Applications for Power System Security*, Florence, 1983.

[31] C. A. Rossier and A. Germond, "Network Topology Optimization for Power System Security Enhancement," in *CIGRE/IFAC Symposium on Control Applications for Power System Security*, Florence, 1983.

[32] H. J. Koglin and M. F. Medeiros, "Corrective Switching by Means of Optimal Strategy," in *CIGRE/IFAC Symposium on Planning and Operation of Electric Energy Systems*, Rio de Janeiro, 1985, pp. 804-809.

[33] R. Bacher and H. Glavitsch, "Network Topology Optimization with Security Constraints," *IEEE*

Transactions on Power Systems, vol. PWRS-1, no. 4, pp. 103-111, November 1986.

[34] A. A. Mazi, B. F. Wollenberg, and M. H. Hesse, "Corrective Control of Power Systems Flows by Line and Bus-Bar Switching," *IEEE Transactions on Power Systems*, vol. PWRS-1, no. 3, pp. 258-265, August 1986.

[35] A. G. Bakirtzis and A. P. Melioppoulos, "Incorporation of Switching Operations in Power System Corrective Control Computations," *IEEE Transactions on Power Systems*, vol. PWRS-2, no. 3, pp. 669-676, August 1987.

[36] B. G. Gorenstin, L. A. Terry, M. V.F. Pereira, and L.M. V.G. Pinto, "A Framework for Integration of Network Topology Optimization and Generation Rescheduling in Power System Security Applications," in *Power System Computation Conference*, Lisbon, 1987, pp. 124-130.

[37] E. B. Makram, K. P. Thornton, and H. E. Brown, "Selection of Lines to be Switched to Eleiminate Overloaded Lines Using a Z-Matrix Method," *IEEE Transactions on Power Systems*, vol. 4, no. 2, pp. 653-661, May 1989.

[38] O. Paillet and L. Dubost, "AMPERE - A Knowledge-based System for Network Reconfiguration," in *Symposium on Expert Systems Application to Power Systems*, Stockholm-Helsinki, 1988.

[39] G. Schnyder and H. Glavitsch, "Security Enhancement Using an Optimal Switching Power Flow," *IEEE Transactions on Power Systems*, vol. 5, no. 2, pp. 674-681, May 1990.

[40] V. H. Quintana and N. Muller, "Overload and Voltage Control of Power Systems by Line Switching and Generation Rescheduling," *Canadian Journal of Electrical and Computer Engineering*, vol. 15, no. 4, pp. 167-173, 1990.

[41] T. J. Bertram, K. D. Demaree, and L. C. Dangelmaier, "An Integrated Package for Real-Time Security Enhancement," *IEEE Transactions on Power Systems*, vol. 5, no. 2, pp. 592-600, May 1990.

[42] J. I. Sancha, J. L. Fernandez, and J. Hebero, "SEGRE, An Expert System for Reactive Power Management in Electric Power Systems," in *Intelligent Systems Applications to Power Systems*, Montpellier, 1994, pp. 389-395.

[43] J. G. Rolim, M. R. Irving, and L.J.B. Machado, "SECTE - An Expert System for Voltage Control, Including Topological Changes," in *IFAC Symposium on Control of Power Plants and Power Systems*, Cancun, 1995, pp. 65-70.

[44] J. N. Wrubel, P. S. Rapeienski, K. L. Lee, B. S. Gisin, and G. W. Woodzel, "Practical Experience With Corrective Switching Algorithm for On-Line Applications," *IEEE Transactions on Power Systems*, vol. 11, no. 1, pp. 415-421, February 1996.

[45] J. O. Freitas e Silva and L J.B. Machado, "Switching Lines Selection to Integrate the Network Optimization with the Ususal Overload Control Actions of Electric Power Systems," in *11th Power Systems Computation Conference*, 1993, pp. 233-239.

[46] H. Glavitsch, H. Kronig, and R. Bacher, "Combined Use of Linear Programming and Load Flow Techniques in Determining Optimal Switching Sequences," in *8th Power Systems and Computation Conference*, Helsinki, 1984, pp. 627-637.

[47] W. Shao and V. Vittal, "Corrective Switching Algorithm for Relieving Overloads and Voltage Violations," *IEEE Transactions on Power Systems*, vol. 20, no. 4, pp. 1877-1885, Nov 2005.

[48] K. W. Hedman, R. P. O'Neill, E. B. Fisher, and S. S. Oren, "Optimal Transmission Switching - Sensitivity Analysis and Extensions," *IEEE Transactioins on Power Systems*, vol. 23, no. 3, pp. 1469-1479, August 2008.

[49] K. W. Hedman, R. P. O'Neill, E. B. Fisher, and S. S. Oren, "Optimal Transmission Switching With Contingency Analysis," *IEEE Transactions on Power Systems*, vol. 24, no. 3, pp. 1577-1586, August 2009.

[50] M. Doll and J. F. Verstege, "Congestion Management in a Deregulated Environment Using Corrective Measures," in *IEEE Power and Energy Society Winter Meeting*, Columbus, OH, 2001, pp. 393-398.

[51] R. P. O'Neill, R. Baldick, U. Helman, M. H. Rothkopf, and W. Stewart, "Dispatchable Transmission in RTO Markets," *IEEE Transactions on PowerSystems*, vol. 20, no. 1, pp. 171-179, February 2005.

[52] K. W. Hedman, M. C. Ferris, R. P. O'Neill, E. B. Fisher, and S. S. Oren, "Co-Optimization of Generation Unit Commitment and Transmission Switching With N-1 Reliability," *IEEE Transactions on Power Systems*, vol. 25, no. 2, pp. 1052-1063, May 2010.

[53] R. P. O'Neill, K. W. Hedman, E. Krall, A. Papavasiliou, and S. Oren, "Economic analysis of the N-1 reliable unit commitment and transmission switching problem using duality concepts," *Energy Systems*, vol. 1, no. 2, pp. 165-195, May 2010.

[54] Karen Lyons, Hamish Fraser, and Hethie Parmesano, "An Introduction to Financial Transmission Rights," *The Electricity Journal*, vol. 13, no. 10, pp. 31-37, December 2000.

[55] Richard P. O'Neill, Emily Bartholomew Fisher, Benjamin F. Hobbs, and Ross Baldick, "Towards a

Complete Real-Time Electricity Market Design," *Journal of Regulatory Economics*, vol. 34, no. 3, pp. 220-250, December 2008.

[56] Kory Hedman, Shmuel Oren, and Richard O'Neil, "Optimal Transmission Switching: Economic Efficiency and Market Implications," *Journal of Regulatory Economics*, 2012.

[57] Reliability Test System Task Force of the Application of Probability Methods Subcommittee, "The IEEE Reliability Test System - 1996," *IEEE Transactions on Power Systems*, vol. 14, no. 3, pp. 1010-1020, August 1999.

[58] J. Duncan Glover and Mulukutla S. Sarma, *Power System Analysis And Design*, 3rd ed.: Wadsworth Group, 2002.

[59] Dynadec Decision Technologies. (2011) [Online]. www.dynadec.com

[60] Mokhtar S. Bazaraa, John J. Jarvis, and Hanif D. Sherali, *Linear Programming and Network Flows*, 3rd ed. Hoboken, New Jersey: John Wiley and Sons Inc., 2005.

[61] University of Washington Department of Electrical Engineering. (1993, August) Power Systems Test Case Archive. [Online]. http://www.ee.washington.edu/research/pstca/

[62] C. Barrows and S. Blumsack, "Transmission Switching in the RTS-96 Test System," *IEEE Transactions on Power Systems*, vol. PP, no. 99, November 2011.

[63] Javad Lavaei and Steven Low, "Zero Duality Gap in Optimal Power Flow Problem," *IEEE Transactions on Power Systems*, vol. 27, no. 1, February 2012.

[64] R. Johnson and D. Wichern, *Applied multivariate statistical analysis*. Upper Saddle River, NJ:

Prentice Hall, 2002, vol. 5.

[65] J. Vesanto and E. Alhoniemi, "Clustering of the self-organizing map," *IEEE Transactions on Neural Networks*, vol. 11, no. 3, pp. 586-600, 2002.

[66] Russell Bent and Pascal Van Hentenryck, "Spatial, Temporal, and Hybrid Decompositions for Large-Scale Vehicle Routing with Time Windows," in *Principles and Practice of Constraint Programming*, 2010, pp. 99-113.

[67] G. Kron, "A set of principles to interconnect the solutions of physical systems," *Journal of Applied Physics*, vol. 24, no. 8, pp. 965-980, 1953.

[68] H. Happ, "The operation and control of large interconnected power systems," *IEEE Transactions on Circuit Theory*, vol. 20, no. 3, pp. 212-222, 1973.

[69] H. Happ, "Diakoptics, the solution of system problems by tearing," *Proceedings of the IEEE*, vol. 62, no. 7, pp. 930-940, 1974.

[70] L. Hang, A. Bose, and V. Venkatasubramanian, "A fast voltage security assessment method using adaptive bounding," *IEEE Transactions on Power Systems*, vol. 15, pp. 1137-1141, Aug 2000.

[71] J. Zhong, E. Nobile, A. Bose, and K. Bhattacharya, "Localized reactive power markets using the concept of voltage control areas," *IEEE Transactions on Power Systems*, vol. 19, pp. 1555-1561, Aug 2004.

[72] S. Tiptipakorn, "A spectrical bisection partitioning method for electric power network applications," Department of Electrical and Computer Engineering, University of Wisconsin,

Madison, Master's Report 2001.

[73] Hongming Yang, Renjun Zhou, and Jianhua Liu, "A RBFN Hierarchical Clustering Based Network Partitioning Method for Zonal Pricing," in *2nd International Confrence on Electrical and Electronics Engineering (ICEEE) and XI Conference on Electrical engineering (CIE 2005)*, Mexico city, Mexico, 2005.

[74] I. Kamwa, A. Pradhan, and G. Joos, "Automatic segmentation of large power systems into fuzzy coherent areas for dynamic vulnerability assessment," *IEEE Transactions on Power Systems*, vol. 22, no. 4, pp. 1974-1985, 2007.

[75] I. Kamwa, A. Pradhan, G. Joss, and S. Samantaray, "Fuzzy partitioning of a real power system for dynamic vulnerability assessment," *IEEE Transactions on Power Systems*, vol. 24, no. 3, pp. 1356-1365, 2009.

[76] H. You, V. Vittal, and X. Wawng, "Slow coherency-based islanding," *IEEE Transactions on Power Systems*, vol. 19, no. 1, pp. 483-491, 2004.

[77] M. Wang and H. Chang, "Novel clustering method for coherency identification using an artificial neural network," *IEEE Transactions on Power Systems*, vol. 9, no. 4, pp. 2056-2062, 1994.

[78] P. Lagonotte, J. Sabonnadiere, J Y Leost, and J P Paul, "Structural analysis of the electrical system: application to secondary voltage control in france," *IEEE Transactions on Power Systems*, vol. 4, pp. 479-486, May 1989.

[79] Q. Lu and S. Brammer, "A new formulation of generator penalty factors," *IEEE Transactions on Power Systems*, vol. 10, pp. 990-994, May 1995.

[80] I. Dobson, M. Parashar, and C. Carter, "Combining phasor measurements to monitor cutset angles," in *Proceedings of the 2010 43rd Hawaii International Conference on System Sciences*, 2010, pp. 1-9.

[81] S. Blumsack, P. Hines, M. Patel, C. Barrows, and E. Cotilla-Sanchez, "Network Clustering for Load Deliverabiliity Assessments in PJM," Prepared for the PJM Interconnection, LLC., 2008.

[82] S. Arianos, E. Bompard, A. Carbone, and F. Xue, "Power grids vulnerability: a complex network approach," *Chaos*, vol. 19, 2009.

[83] V. Latora and M. Marchiori, "Efficient behaviour of small-world networks," *Physical Review Letters*, vol. 87, no. 19, p. 198701, 2001.

[84] R. D. Zimmerman, C. E. Murillo-Sanchez, and R. J. Thomas, "Matpower: Steady-state operation, planning and analysis tools for power systems research and education," *IEEE Transactions on Power Systems*, vol. 26, pp. 12-19, Feb 2011.

[85] Seth Adam Blumsack, Paul Hines, Mahendra Patel, Clayton Barrows, and Eduardo Cotilla Sanchez, "Defining Power Network Zones from Measures of Electrical Distance," in *IEEE Power and Energy Society General Meeting*, Calgary, 2009.

[86] Emil Iggland and Goran Anderson, "On Using Reduced Networks for Distributed DC Power Flow," in *IEEE PES General Meeting*, San Diego, CA, 2012.

[87] John J. Grainger and William D. Stevenson, *Power Syste Analysis*.: McGraw-Hill, 1994.

[88] Thomas J. Overbye, Xu Cheng, and Yan Sun, "A Comparison of the AC and DC Power Flow Models for LMP Calculation," in *Proceedings of the 37th Hawaii International Conference on*

System Sciences (HICSS), 2004.

[89] Carleton Coffrin, Pascal Van Hentenryck, and Russell Bent, "A Linear-Programming Approximation of AC Power Flows," *arXiv preprint*, vol. 1206.3614, 2012.

[90] A. Ipakchi, "Grid of the Future," *IEEE Power and Energy Magazine*, vol. 7, no. 2, pp. 52-62, March 2009.

[91] (2012) The Recovery Act. [Online]. www.recovery.gov

[92] D. Klein and M. Randic, "Resistance Distance," *Journal of Mathematical Chemistry*, vol. 12, pp. 81-95, 1993.

[93] B Stott, J. Jardim, and O. Alsac, "DC power flow revisited," *IEEE Transactions on Power Systems*, vol. 24, no. 3, pp. 1290-1300, 2009.

[94] W. Rudin, *Principles of Mathematical Analysis*, 1976th ed. New York: McGraw-Hill, 1964.

[95] Seth Blumsack and Paul Hines, "A Centrality Measure for Electrical Networks," in *proceedings of the 41st Hawaii international conference on system sciences*, Hawaii, 2008.

[96] D. Davies and D. Bouldin, "A cluster seperation measure," *IEEE Transactions on Pattern Analysis and Machine Intelligence*, no. 2, pp. 224-227, 1979.

[97] J. A. Hartigan and M. A. Wong, "A K-Means Clustering Algorithm," *Applied Statistics Vol.28, No.1*, pp. 100-108, 1979.

[98] Yu Jiaxi, Lin Yang, Liu Ruiye, and Guo Zhizhong, "Research on the time process-oriented power system static security analysis," in *Third International Confrence on Electrical Utility Deregulation*

and Restructuring and Power Technologies, 2008, DRPT 2008, Nanjuing, 2008, pp. 1516-1521.

[99] Ulrike von Luxburg, "A Tutorial on Spectral Clustering," 2006.

[100] J. Bezdek and N. Pal, "Some new indexes of cluster validity," *IEEE Transactions on Systems Management and Cybernetics, Part B: Cybernetics*, vol. 28, no. 3, pp. 301-315, 2002.

[101] A. O. M. Saleh and M. A. Laughton, "Cluster analysis of power system networks for array porcessing solutions," *IEEE Proceedings C: Generation, Transmission and Distribution*, vol. 132, no. 4, pp. 172-178, 1985.

[102] V. H. Quintana and N. Muller, "Partitioning of power networks and applications to security control," *IEEE Proceedings C: Generation, Transmission and Distribution*, vol. 138, no. 6, pp. 535-545, 1991.

[103] A. Eiben and J. Smith, *Intorduction to evolutionary computing*. Verlag: Springer, 2003.

[104] D. Goldberg, "A note on the boltzmann tournament selection for genetic algorithms and population-oriented simulated annealing," *Complex Systems*, vol. 4, no. 4, pp. 445-460, 1990.

[105] D. Goldberg, K. Deb, and J. Clark, "Genetic algorithms, noise, and the sizing of populations," *Urbana*, vol. 51, p. 61801, 1991.

[106] Peter W. Sauer. (2003, September) Power Systems Engineering Research Center. [Online]. http://www.pserc.wisc.edu/Sauer_Reactive%20Power_Sep%202003.pdf

[107] Clayton Barrows and Seth Blumsack, "Transmission Switching in the RTS-96 Test System," *IEEE PES Letters*, vol. 27, no. 2, p. 1134, May 2012.

[108] Eduardo Cotilla-Sanchez, Paul Hines, Clayton Barrows, and Seth Blumsack, "Multi-Objective Partitioning of Power Networks Based on Electrical Distance," *IEEE Transactions on Power Systems*, p. submitted for review, 2012.

Vita
Clayton Paul Barrows

EDUCATION

2007-2013 The Pennsylvania State University

Ph.D. Energy and Mineral Engineering
Energy Management and Policy Option

- Research Assistant 2007 – 2013, Teaching Assistant 2010 – 2011
- Graduate Student Intern, Los Alamos National Lab 2011
- PSU Energy & Environmental Economics Policy Initiative Research Travel Award Recipient 2012
- EME Department Outstanding Graduate Teaching Assistant Award Recipient 2011
- EMS College - Schenck Outstanding Teaching Assistant Award Recipient 2011
- Network Science Exploration Research Grant Recipient 2010

2001-2005 University of Wyoming

Bachelor of Science in Electrical Engineering

PUBLICATIONS AND RESEARCH

Journals, Books, and Conference Proceedings

- Barrows, C., Blumsack, S. & Bent, R. (2012). Computationally Efficient Transmission Switching: Solution Space Reduction. *IEEE Power and Energy Society General Meeting.*
- Cotilla-Sanchez, E., Hines, P., Barrows, C., & Blumsack, S. (2012). Comparing the Topological and Electrical Strucuture of the North American Electric Power Infrastructure. *IEEE Systems Journal*.
- Blumsack, S., Hines, P., Patel, M., Barrows, C., & Sanchez, E. (2013). Partitioning Methods for Electrical Networks. Currently under review at *IEEE Transactions on Power Systems* .
- Barrows, C., & Blumsack, S. (2011). Transmission Switching in the RTS-96 Test System. *IEEE Transactions on Power Systems*.
- Barrows, C., & Blumsack, S. A. (2011). Optimal Transmission Switching Analysis and Marginal Switching Results. *IEEE Power and Energy Society General Meeting.* Detroit.
- Hines, P., Blumsack, S., Sanchez, E. C., & Barrows, C. (2010). The Topological and Electrical Structure of Power Networks, *Proc. 43rd Hawaii International Conference on System Science.* Kauai, HI.
- Blumsack, S. A., Hines, P., Patel, M., Barrows, C., & Sanchez, E. C. (2009). Defining Power Network Zones from Measures of Electrical Distance. *IEEE Power and Energy Society General Meeting.* Calgary.
- Barrows, C. (2009). Reducing the Costs of Maintaining Electric Reliability through Electrical-Distance Network Partitioning. *Technology Management and Policy Graduate Consortium*.

Working Papers and Technical Reports

- Barrows, C. P., Fernandez, A., Marpoe, B., & Witmer, L. (2009). "Assessing the Costs of Dispatchable Wind Energy: An Integrated Wind-Turbine and Energy Storage System," The Pennsylvaina State University, Department of Energy and Minearal Engineering.
- Blumsack, S., Hines, P., Barrows, C., & Sanchez, E. (2008). "Network Clustering for Load Deliverability Assessments in PJM," For the PJM Interconnection, LLC.